

Mathematical Modeling and Optimal Control: Maximizing Yield in Submerged Alcoholic Fermentation

By
KNUST

NEBA FABRICE ABUNDE

B.Sc. (Hons) Biochemistry

A Thesis Submitted to the Department of Agricultural Engineering,

Kwame Nkrumah University of Science and Technology, Kumasi In

partial fulfillment of the requirements for the degree of

MASTER OF PHILOSOPHY

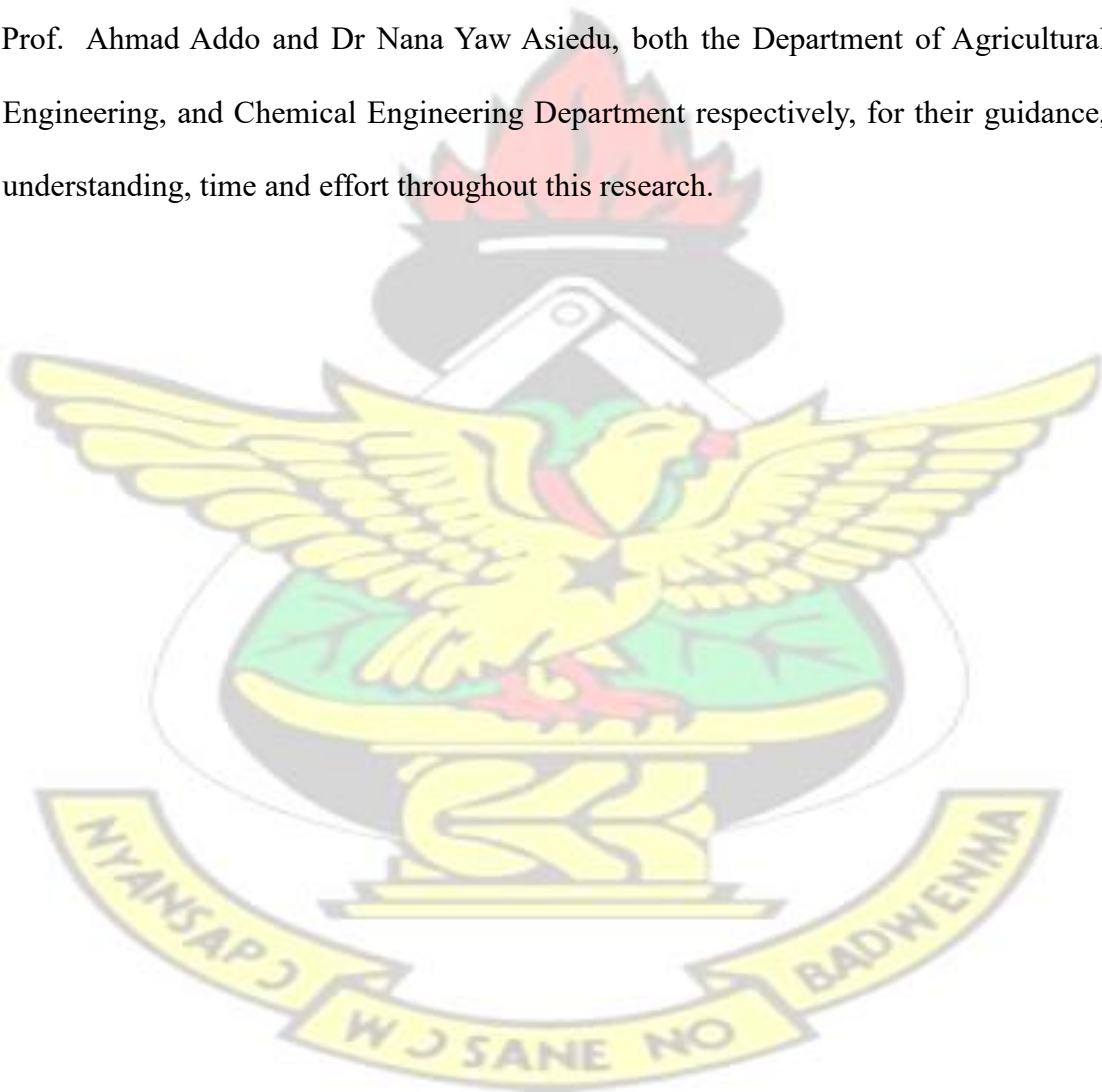
(Bioengineering)

College of Engineering

21 MAY, 2016

ACKNOWLEDGEMENT

Special thanks to the almighty God who provided me with the strength and wisdom that was required to carry this project. My supervisors and I express our sincere thanks to the Intra-ACP under the project “Strengthening African Higher Education through Academic Mobility”, STREAM for the scholarship awarded me. My appreciation also goes to Guinness Ghana Breweries Limited for the provision of industrial data for model validation in this study. I am very grateful to my supervisor, Prof. Ahmad Addo and Dr Nana Yaw Asiedu, both the Department of Agricultural Engineering, and Chemical Engineering Department respectively, for their guidance, understanding, time and effort throughout this research.



ABSTRACT

Advances in research into alternative starch sources for industrial production of alcoholic beverages, sorghum, cassava and maize are now being used as cheaper alternatives to imported barley in the brewery industry. In brewing, though involves several unit operations, the fermentation step is regarded as the heart of the entire production where a near optimal environment is desired for microorganisms to grow and produce ethanol. However, the use of fermenters is usually hampered by suboptimal conditions in terms of yield and productivity, along with the low tolerance of strains to process stresses such as substrate and product toxicity. Attempts to improve the industrial efficacy of fermenters have been in the areas of genetic engineering to improve strain tolerance, but usually involves detailed and unfeasible mechanistic studies. Statistical design of experiments which has also been used often results in local optima due to the relatively small dimensional space covered by the experiments. Mathematical techniques have recorded great successes but proposed solutions however did not consider all degrees of freedom of the problem simultaneously (Inhibition kinetics, temperature and pH). This thesis presents the modeling of substrate and/or product inhibition in three different fermentation substrates: sorghum, maize and cassava extracts. At a 99% confidence interval, the pattern of these inhibitions can be described as being a linear or an exponential decrease in ethanol concentration in the case of sorghum, linear and sudden growth stop in the case of maize, linear substrate exponential product, and exponential substrate exponential product in the case of cassava. Optimal control was applied to minimize the effects of such inhibition in sorghum extracts. Calculus of variation was introduced as a valuable tool to derive and solve the necessary conditions for optimality (optimal temperature and pH profiles). A Simulink model, developed and used for control validation shows an increase in ethanol yield by 14.18%, cell growth by 71.96% and a decrease in the residual substrate by 84.77%. Since the model was developed using industrial scale fermentation data, the results obtained in the simulations can satisfactorily represent a real operation unit. From the comparative results presented in the simulations, it is concluded that the proposed strategy can be used in practice to improve the performance of industrial scale alcoholic fermentation.

TABLE OF CONTENTS

DECLARATION	ii
ACKNOWLEDGEMENT	iii
ABSTRACT	iv
TABLE OF CONTENTS	v
LIST OF FIGURES	ix
LIST OF TABLES	xii
ABBREVIATIONS	xii
CHAPTER ONE: INTRODUCTION	1
1.1 Background of the Study	1
1.2 Statement of the Problem	3
1.3 Objectives	4
1.3.1 Main Objective	4
1.3.2 Specific Objectives	4
1.4 Justification of the Study	5
1.5 Significance of the Study	5
1.6 Scope and Limitations of the Study	6
1.7 Conceptual Framework	7
1.8 Organization of the Study	7
CHAPTER TWO: REVIEW OF PREVIOUS WORK ON MODELING AND OPTIMAL CONTROL OF FERMENTATION	8
2.1 Principles and Techniques in Industrial Fermentation	8
2.1.1 General Aspects of Fermentation Processes	8
2.1.2 Submerged Vs Solid State Fermentation	8
2.1.3 General Overview of Industrial Fermentation Process	9
2.2 Selection, Scale-Up, Operation and Control of Fermenters	10
2.2.1 Fermenter Design and Operation Modes	10
2.2.2 Considerations in Fermenter Design.....	11
2.2.2.1 Economic Aspects in Fermenter Design	11
2.2.2.2 Biological Aspects in Fermenter Design	12
2.2.3 Types of Fermenters Used in Alcoholic Fermentation	12
2.2.4 Process Scale up and Scale down in Alcohol Fermentation	13
2.2.5 Key Factors of Control in Submerged Fermentation	14
2.3 Biochemical and Microbial Aspects of Submerged Fermentation	15

2.3.1 Microorganisms and Fermentation Conditions in Brewing	15
2.3.2 Biochemical Pathways in Yeast Fermentation	16
2.4 Industrial Applications of Alcoholic Fermentation	17
2.4.1 Production of Alcoholic Beverages and Bakeries	17
2.4.3 Production of Biofuels	18
2.5 Kinetic and Dynamic Modelling of Fermentation Processes	19
2.5.1 The benefits of Modelling in Industrial Fermentation	19
2.5.2 General Characteristics of Dynamic Models	20
2.5.3 Modeling methods in Bioprocess Engineering	21
2.5.3.1 Traditional modeling procedure	21
2.5.3.2 Innovative artificial neural network modeling	22
2.5.4 Kinetic Models for Cell Growth Kinetics	23
2.5.4.1 Growth limitation through substrate concentration	24
2.5.4.2 Growth limitation through substrate and cell concentration	24
2.5.4.3 Growth kinetics with substrate inhibition	25
2.5.4.4 Growth Kinetics with Product Inhibition	25
2.5.4.5 Unstructured kinetic models for product formation	26
2.5.5 Reaction Schemes in Biochemical Process Modeling	26
2.6 Parameter Estimation in Bioprocess Modeling	27
2.6.1 Parameter Estimation Methods.....	28
2.7 Theory of Optimal Control in Submerged Fermentation	28
2.7.1 Performance Criteria of an Optimal Control Problem	29
2.7.2 Solution Methods for Optimal Control	30
2.7.2.1 Indirect Methods of Solving Optimal Control Problems	30
2.7.2.2 Direct Methods for Solving Optimal Control Problems	30
2.7.3 Numerical Methods in Optimal Control	31
2.8 Perspective and Motivation	31

CHAPTER THREE: MATHEMATICAL MODELING, AND PARAMETER ESTIMATION 32

3.1 Introduction and Chapter Overview	32
3.2 Experimental Methods and Data Collection	32
3.3 Model Development and Validation Methodology.....	33
3.4 Kinetic Modeling	36
3.4.1 Modeling of Growth Kinetics and Product Inhibition	36

3.4.2 Modeling Substrate Inhibition	37
3.5 Dynamic Balances and Governing Differential Equations.....	39
3.5.1 Systems Dynamics with Product Inhibition	40
3.5.2 Systems Dynamics with Substrate and Product Inhibition	41
3.6 Parameter Estimation and Model Statistical Validity	42
CHAPTER FOUR: RESULTS AND DISCUSSIONS: MODEL SIMULATION AND PARAMETER ESTIMATION	44
4.1 Overview of Chapter	44
4.2 Alcohol Fermentation with Sorghum Extracts	44
4.3 Alcohol Fermentation with Maize Extracts	52
4.4 Alcohol Fermentation with Cassava Extracts	57
4.4.1 Product Inhibition	58
4.4.2 Substrate and Product Inhibitor	61
4.5 Conclusion	66
CHAPTER FIVE: OPTIMAL CONTROL PROBLEM FORMULATION AND SOLUTION TECHNIQUE	67
5.1 Introduction and Overview	67
5.2 Objectives of the Optimal Control Strategy	68
5.3 Control Assumptions and Approximations	68
5.4 Modeling Temperature and pH dependence	68
5.5 Modeling the Effect of Controls on State Equations.....	69
5.6 Optimal Control Problem Formulation	71
5.7 Optimal Control Using the Linear Product Inhibition Model	72
5.8 Solution Technique by Calculus of Variations	76
5.8.1 State Equations	77
5.8.2 Costate Equations	77
5.8.3 Optimal Control Equations.....	78
5.8.4 Numerical Simulations and Control Validation	79
5.8.5 Results and Discussion.....	79
CHAPTER SIX: CONCLUSION AND RECOMMENDATIONS FOR FUTURE	
WORK	85
6.1 Conclusions	85
6.2 Recommendations	86

6.2.1 Optimal Control and Dynamic Stability Using the Other Inhibition Models	86
6.2.2 Model Based Control of CO ₂ during Alcohol Fermentation	86
6.2.3 Modeling the Effect of Temperature and pH on Cell Growth	87
6.2.4 Development of and Optimal Simulator for Alcohol fermentation	87
REFERENCES	88
APPENDIX	96
Appendix 1. Matlab codes for Parameter Estimation	96
Appendix 1a sample of code used for Product inhibition	96
Appendix 2. Matlab code for Optimality Conditions (Calculus of Variations)	101
Appendix 3: Matlab Code to Simulate the Hamiltonian Boundary Value Problem	102
Appendix 4: Simulink S-function used to Design Fermenter	104
Appendix 5: Tables for Model Statistical Validity for Cassava and Maize Extracts	112



LIST OF FIGURES

Figure 1.0: Impact logic representation of the study showing the problems, intervention, implementation and outcomes of the study.	7
Figure 2.1: Process flow diagram for bioprocess manufacturing	10
Figure 2.2: Environmental stresses exerted on <i>S. cerevisiae</i> during ethanol fermentation (Ingledew, 1999)	16
Figure 2.3: Simplified glycolytic scheme (Embden–Meyerhof–Parnas) in <i>S. cerevisiae</i> Abbreviations: HK: hexokinase, PGI: phosphoglucoisomerase, PFK: phosphofructokinase, FBPA: fructose bisphosphate aldolase, TPI: triose phosphate isomerase, GAPDH: glyceraldehydes-3-phosphate dehydrogenase, PGK: phosphoglycerate kinase, PGM: phosphoglyceromutase, ENO: enolase, PYK: pyruvate kinase, PDC: pyruvate decarboxylase, ADH: alcohol dehydrogenase (Fengwu, 2007).	17
Figure 3.1: procedure used for model development and validation	35
Figure 4.21: Experimental results and model fitting of no inhibition (Monod-model)	45
Figure 4.22: Experimental results and model fitting, case of linear inhibition model	46
Figure 4.23: Experimental results and model fitting of Sudden Growth Stop inhibition	46
Figure 4.24: Experimental results and model fitting of Exponential inhibition model	47
Figure 4.25: Simulation of substrate and Product variation as a function of biomass during fermentation using Linear Inhibition kinetics.	49
Figure 4.26: Simulation of substrate and product as a function of biomass during fermentation using Exponential Inhibition kinetics.	50
Figure 4.27 3D proximal interpolant simulation of product variation as a function of substrate and biomass using linear Inhibition Kinetic Model	51
Figure 4.28: 3D proximal interpolant simulation of product variation as a function of substrate and biomass using Exponential Inhibition Kinetic Model.	51
Figure 4.31: Experimental results and model fitting of no inhibition (Monod-model).	52
Figure 4.32: Experimental results and model fitting of linear inhibition model.	53
Figure 4.33: Experimental results and model fitting of Sudden Growth Stop inhibition	

model.	53
Figure 4.34: Experimental results and model fitting of Exponential Inhibition Model.	54
Figure 4.35: Simulation of substrate and Product variation as a function of biomass during fermentation of maize extracts using Linear Inhibition kinetic model.	56
Figure 4.36: Simulation of substrate and Product as a function biomass during fermentation, using Sudden Growth Stop Inhibition kinetic.	56
Figure 4.37 3D proximal interpolant simulation of product dynamics during fermentation using linear inhibition kinetic Model. -	57
Figure 4.38: 3D proximal interpolant simulation of biomass variation during fermentation using Sudden Growth Stop inhibition kinetic Model.	57
Figure 4.41: Experimental results and model fitting, case of no inhibition (Monod-Model).	58
Figure 4.42: Experimental results and model fitting, case of linear inhibition model	59
Figure 4.43: Experimental results and model fitting, case of Sudden Growth Stop inhibition model.	59
Figure 4.4 4: Experimental results and model fitting, case of Exponential inhibition model	60
Figure 4.45: Experimental results and model fitting (LS-EP model).	63
Figure 4.47: Experimental results and model fitting (ES-LP).	63
Figure 4.46: Experimental results and model fitting (LS-LP model).	64
Figure 4.48: Experimental results and model fitting (ES-EP model).	64
Figure 4.49: product dynamics as against substrate utilization and time ES-EP Inhibition Model.	65
Figure 4.5: Dynamics of product formation as against substrate utilization and cell growth (ES-EP Inhibition Model)	66
Figure 5.83: Optimal temperature profile obtained from numerical simulation of the necessary optimality conditions	80
Figure 5.82: optimal pH profile obtained from numerical simulation of the necessary optimality conditions	81
Figure 5.83: Simulink Model designed for the alcoholic fermentation of sorghum extracts.	81
Figure 5.84: Experimental results and model fitting	82
Figure 5.85: Dynamics of cell growth with optimal and conventional controls	83
Figure 5.86: Dynamics of product formation with optimal and conventional controls	

..... 83

Figure 5.87: Dynamics of substrate utilization with optimal and conventional controls

..... 84

KNUST



LIST OF TABLES

Table 2.1: kinetic models with growth limitation through substrate concentration	24
Table 2.2: Kinetic models with growth limitation through substrate and cell concentration	24
Table 2.3: Kinetic models with substrate inhibitions	25
Table 2.4: Models showing growth kinetics with product inhibition	25
Table 3.1: Mathematical expressions used in modeling product Inhibiton	36
Table 3.2: Mathematical expressions for the substrate and product inhibition factors	38
Table 4.21: Model Parameters for beer fermentation using Sorghum Extracts	47
Table 4.22: Model Statistical Validity with kinetics of linear inhibition, two sample F- test for variance (Biomass)	48
Table 4.23: Model Statistical Validity with kinetics of Exponential inhibition, two sample F-test for variance	48
Table 4.31: Model Parameters for beer fermentation using Maize Extracts	54
Table 4.41: Model Parameters for beer fermentation using Cassava Extracts, case of product inhibition	60
Table 4.42: Model Parameters for beer fermentation using Cassava Extracts, case of substrate and product inhibition	62
Table 5.81: Estimated Parameters for dynamic model used in optimal control, equation 3	80
Table 5.82: Obtainable concentrations for both the optimal and conventional operating conditions	81

ABBREVIATIONS

SmF:	Submerged fermentation
SSF:	Solid state fermentation
GRAS:	Generally Regarded as Safe
FBB:	Fluidized bed bioreactors
QbD:	Quality by Design
PAT:	Process Analytical Technology
ODEs:	Ordinary Differential Equations
GO:	Global Optimization
HBVP:	Hamiltonian Boundary Value Problem
GREA:	Ghana Renewable Energy Act
μ_{max}	Maximum specific growth rate (h^{-1})
q_{pmax}	Maximum rate of product formation (h^{-1})
P_{xmax}	Product concentration when product formation ceases ($g/100g$)
P_{pmax}	Product concentration when cell growth ceases ($g/100g$)
K_{ix}	Product inhibition coefficient on cell growth
K_{ip}	Product inhibition coefficient on product formation
K_{isx}	Substrate inhibition coefficient on cell growth
K_{isp}	Substrate inhibition coefficient on product formation
K_{sx}	Substrate saturation (Monod) constant for cell growth ($g/100g$)
K_{sp}	Substrate saturation (Monod) constant for product formation ($g/100g$)
Y_x	Yield coefficient of cell based on substrate utilization (g/g)
Y_p	Yield coefficient of product based on substrate utilization (g/g)
G_s	Growth coefficient of cell based on substrate utilization ($g/g \cdot h$)
M_s	Cell growth coefficient on substrate ($g/g \cdot h$)

CHAPTER ONE INTRODUCTION

1.1 Background of the Study

Concerns about large emissions from chemicals, lengthy chemical processes with high energy input, shortage of fossil fuels, increasing crude oil price and accelerated global warming have led to growing worldwide interests and significant transformation in biotechnology, not only in biological areas involving genomics, cell and protein engineering, but also in the engineering field of bioprocess manufacturing, such as large-scale fermentation and downstream optimization for the production value added products (Titchener-Hooker et al., 2008). In a generalized view of bioprocess manufacturing, though involves several unit operations the bioreactor is the crux, regarded as the heart of the entire production, where a near optimal environment is desired for microorganisms to grow, multiply and produce the desired product (Alford, 2006). However, the use of bioreactors at large-scale level is usually hampered by sub-optimal conditions in terms of yield and productivity, along with the low tolerance of strains to process stresses, such as substrate and product toxicity, and other fermentation inhibitors (Fischer et al., 2008; Parcunev et al., 2012; Naydenova et al., 2013).

In several attempts to improve the industrial efficacy of bioreactors, a variety of approaches have been proposed. Metabolic engineering and synthetic biology have been used to determine the optimal pathway configurations through the use of gene combinatorial methods to construct and consequently evaluate several metabolic pathways, combining genes from different sources to make the strain resistant to environmental stresses during fermentation. However, with the field of bioprocess engineering shifting from method development to application development (Palsson and Papin, 2009), these approaches involving detailed mechanistic studies of metabolic pathways becomes problematic, inherently involving inverse problem that cannot be

understood with certainty (Brenner, 2010). The implementation of microbial production on an industrial scale should focus towards process engineering strategies, which can ultimately enable control and optimization at the bioprocess level (Thilakavathi et al., 2007). But still at this level, the identification of optimal operation parameters in fermentation processes have been done empirically through statistical design of experiments to scale up bioreactor facilities and determine the optimal operating conditions (Alford, 2006). However, these empirical methods required construction of expensive prototype systems, time-consuming studies and most often lead to local optima due to the relatively small dimensional space covered by experiments (Alford, 2006; Yu *et al.*, 2013).

Alternatively, design and optimization of bioreactors can be enhanced via validated mathematical models developed from mechanistic studies that lead to a more in depth understanding of the very complex transport phenomena, microbial biochemical kinetics, and stoichiometric relationships associated with the process (Yu *et al.*, 2013). Furthermore, literature have shown that many university process control and modelling courses focus on theoretical aspects of continuous “ steady-state” types of processes and in contrast to this, a large percentage of today’s industrial bioprocesses are batch non-steady state processes (Alford, 2006). There appears to be a need for more focus in dealing with process transients and other nonlinear control dynamics of batch processing.

Considering a case study in alcoholic fermentation in brewing, barley grain has been the most common grain used in these factories since unlike other grains it provides additional advantages such as characteristic colour of beer, malty sweet flavor and dextrins to give the beer body, protein to form a good head, and perhaps most important,

the natural sugars needed for fermentation (Willaert, 2007). In the development of industrial tools for such fermentation many mathematical models were developed to describe the dynamics of ethanol fermentation from malted barley derived wort extract. These included the growth kinetic model of Engasser et al., (1981), the beer flavor model of Gee and Ramirez (1988), fusel alcohol model (Garcia et al., 1994), a neural network model for ethyl caproate (Garcia et al., 1995), a kinetic model of temperature effect on cell growth (Ramirez and Maciejowski, 2007), etc. Today with advances in research alternative starch sources, ranging from rice to sorghum, to wheat to cassava to corn are now being used for alcoholic fermentation. As a result some of the industrial simulators and control policies based on models calibrated with malted barley might no longer be reliable for process decisions. Therefore, a systematic process dynamic modeling and control is extremely necessary to investigate and control the kinetics of the alcoholic fermentation in different starch sources.

1.2 Statement of the Problem

In several studies regarding the dynamics of bioreactors, instability, in the form of oscillations have been observed and reported in both aerobic and anaerobic cultures of *Saccharomyces cerevisiae* (Chen and McDonald, 1990a, b; Beuse *et al.*, 1998; Fengwu, 2007). Biomass, glucose, ethanol, dissolved oxygen, pH, and some intracellular storage materials have shown sustainable oscillations, being more complicated in ethanol fermentation systems, due to ethanol inhibition and the lag response of yeast cells to this inhibition (Fengwu, 2007). This inhibition increase in residual sugar at the end of the fermentation, which decreases raw material consumption and correspondingly, decreases the ethanol yield if no economically acceptable attenuation strategies are developed (Fengwu, 2007). During the modeling of alcohol fermentation if inhibition

is considered, it is often conventional to predefine the inhibition pattern and this practice increases uncertainties in the model since ethanol inhibition pattern varies depending on the type of microorganism, and on the type and strength of fermentation wort (Russell, 2003).

1.3 Objectives

1.3.1 Main Objective

The main objective of this study is to investigate the dynamics of ethanol fermentation in three different fermentation works and maximize ethanol yield through the application of mathematical modeling and optimal control.

1.3.2 Specific Objectives

- a) To formulate systems of differential equations that describe the dynamics of cell growth, substrate utilization, ethanol formation.
- b) To develop a Matlab code that simultaneously simulates the model equations and estimate parameters with respect to experimental data.
- c) To determine the mathematical pattern of substrate and/or product inhibition on cell growth during ethanol fermentation.
- d) To formulate and solve an optimal control problem that determines the optimum temperature and pH profiles to maximize ethanol yield.

1.4 Justification of the Study

The fermentation of sugars by *Saccharomyces cerevisiae* and *S. carlsbergensis* is a process in which the formation of product is associated with cell growth. The yeast cells are subjected to stresses inherent to the process, that are caused by environmental conditions and physico-chemical factors such as high temperature, salinity, pH and high

concentrations of ethanol and sugar. Several papers have been published analyzing various aspects of the modeling and optimal control fermentation processes. Atala *et al.* (2001) presented a methodology for obtaining the optimum process temperature for the maintenance of cell viability, reducing glycerol production and increasing efficiency. An analysis of how to minimize the time of fermentation required in obtaining the desired product specifications is found in Cacik *et al.* (2001). Also, Wang *et al.* (2001) reported that an absorption chiller was used to estimate the kinetic parameters of the ethanol fermentation model. Furthermore, an on-off control strategy based on the solution of the initial value equations, defined by phase, is presented in Santos *et al.* (2006). However, proposed solutions did not consider all the degrees of freedom of the problem. In order to maximize ethanol yield, all the main aspects (ethanol inhibition kinetics, temperature and pH) should be considered simultaneously. There is therefore the need to model ethanol inhibition kinetics in different fermentation words and control such inhibitions through the application of optimal control.

1.5 Significance of the Study

Many researchers, factory type breweries and bioethanol plants in Ghana and the world at large are involved in research regarding the utilization of various local starch sources for ethanol fermentation (Mishra, *et al.*, 2011). In this effect, efficient and optimal fermenter performance is extremely important in maintaining beer production specifications and also to promote commercial bioethanol production from these sources, while meeting Ghana's energy targets (GREAA, 2011). Modeling the dynamics of ethanol fermentation will reveal possible underlying mechanisms involved in the inhibition of cell growth by high ethanol concentrations which will permit the development of more reliable process controllers and simulators for ethanol fermentation in brewing (Carrillo-Ureta, 2002; Alford, 2006).

1.6 Scope and Limitations of the Study

Starting with biomass harvesting, there are a number of steps to follow until the final product, ethanol, is obtained and of these processes. This study focuses on alcoholic fermentation of glucose to ethanol. The scope of the modelling will be unstructured and unsegregated dynamic first principle models, where kinetic and dynamic models will be developed to describe the fermentation process. From inoculation until the time when fermentation is terminated, many generations of the yeast cells produce the ethanol and it is conceivable that genetic mutations are introduced over several generations that can alter the metabolism of the cells. The kinetic and dynamic models assume that number of cells with such mutations is very small to have any material effect on the behaviour of the bulk of the bioreactor. Likewise, the modeling approach utilized in this study ignores the effects of microgravity (Anderson, 2004) and various mechanical and environmental factors on cell behaviour and gene expression. Bubble dynamics play an important role in gas transport and cell viability during fermentation. However, effects of bubbles that are produced as a result of CO₂ and O₂ sparging are not considered in the modeling (Meier et al., 1999; Ma et al., 2006). Finally, coupling reactions, in which cells require co-substrates or co-factors recycled by another companion reactions is ignored as well.

1.7 Conceptual Framework

Figure 1.0 presents an impact logic diagram which shows the relationship between the problem, intervention, implementation and outcome.

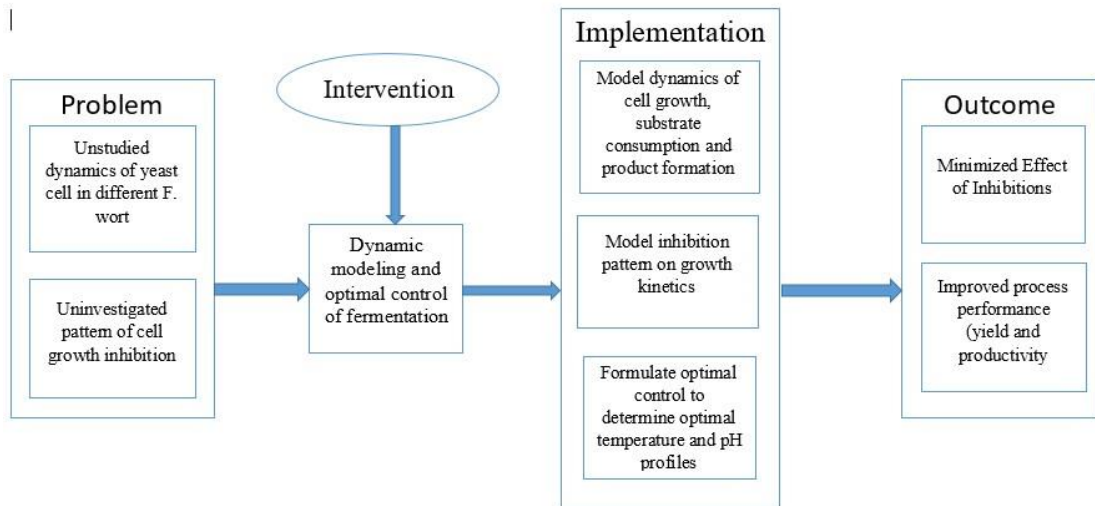


Figure 1.0: Impact logic representation of the study showing the problems, intervention, implementation and outcomes of the study.

1.8 Organization of the Study

The research work is organized into six chapters. Chapter one provides an introductory background, rationale for the mathematical approach utilized in the study and finally the scope and limitations to the study. Chapter two reviews related literature on modeling simulation and dynamic optimization of ethanol fermentation. Chapter three describes the detailed methodology utilized for the model development and validation. This considers the dynamic modeling, underlying model assumptions and approximations finite difference simulation, parameter estimation and model statistical validity. Chapter four presents the results for the model fitting and the model parameters with experimental data for the different substrates considered. Chapter five focuses on optimal control problem formulation and application of calculus of variation to determine necessary conditions for optimality. Chapter six presents a summary of the findings, conclusions of the study, recommendations made and some considerations for future research.

CHAPTER TWO REVIEW OF PREVIOUS WORK ON MODELING AND OPTIMAL CONTROL OF FERMENTATION

2.1 Principles and Techniques in Industrial Fermentation

2.1.1 General Aspects of Fermentation Processes

The term “fermentation”, as originally defined by Pasteur means “life without air”, anaerobe redox reactions in organisms describing the appearance of the action of yeast on extracts of fruit or malted grain (Stanbury *et al.*, 1995). Fermentation has come to have different meanings to biochemists and bioprocess engineers. Its biochemical meaning relates to the generation of energy by the catabolism of organic compounds, whereas, its meaning in industrial bioprocessing tends to be much broader, relating to techniques for large-scale production of microbial products (Carrillo-Ureta, 2002).

2.1.2 Submerged Versus Solid State Fermentation

Fermentation has been widely used for the production of a wide variety of value-added products. Over the years, fermentation techniques have gained immense importance due to their economic and environmental advantages over conventional chemical processes (Subramaniyam and Vimala 2012). Microbial fermentation techniques are classified under two categories: Submerged Fermentation, involving cultivation of microbes on solid substrate and Solid State Fermentation, in which microbes grow in a liquid medium (Renge *et al.*, 2012). Submerged fermentation is technically easier than SSF and is a well-developed system for industrial scale production of microbial metabolites (Vidyalakshmi *et al.*, 2009). On the other hand, even though SmF offers numerous advantages over SSF including its high amenability to process regulation, easy scale-up, feasible biomass determination, satisfactory reproducibility and relatively easy product purification, its industrial application faces numerous challenges including low volumetric productivity, relatively lower concentration of products, complex fermenter design and higher effluent generation (Subramaniyam and

Vimala, 2012). Researchers therefore seek means of optimizing productivity in SmF for economic production of biobased products and other specialty chemicals.

2.1.3 General Overview of Industrial Fermentation Process

Although the central unit operation in bioprocess manufacturing is the fermentation step, the upstream and downstream processes also play vital roles in obtaining and maintaining the quality of and specifications of the final product (Alford, 2006; Ji, 2012). Before the fermentation is started the medium must be formulated and sterilized, the fermenter sterilized, and a starter culture, inoculum made available in sufficient amounts and in the right physiological state to ensure cell viability (Alford, 2006). At the Downstream processes the product is purified and further processed and the effluents produced by the process have to be treated or reused depending on the management system in place (Zhi-Long, 2008). Figure 2.1 illustrates the component parts of a generalized fermentation process.

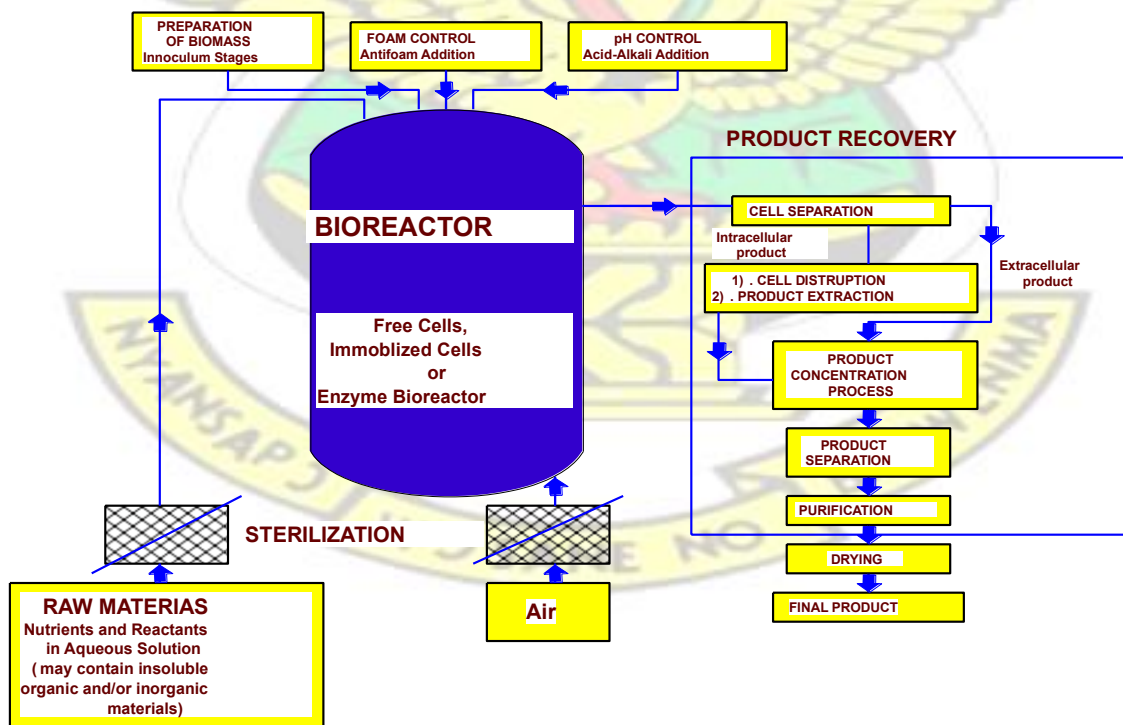


Figure 2.1: Process flow diagram for bioprocess manufacturing

2.2 Selection, Scale-Up, Operation and Control of Fermenters

2.2.1 Fermenter Design and Operation Modes

Literature has shown significant effects of fermenter design on the efficiency of a fermentation process and the proper selection and design of the bioreactor have been shown to determine the optimal commercial bioprocess and the corresponding capital investment (Williams, 2002; Qiangshan *et al.*, 2006). The design and mode of operation of a fermenter mainly depends on the type of cell in the culture, the optimal operating condition required for target product formation and scale of production (Williams, 2002). Based on, this we can have four basic fermenter configurations: (a) a batch process is where all the culture medium is directly available to the cell and no medium is added or withdrawn during the culture; (b) a fed-batch process is characterized by an addition of culture medium during the culture thanks to a predefined or a controlled flow rate (Modak, 1986); (c) a continuous culture mode is where fresh culture medium is added while the culture is continuously withdrawn; (d) Perfusion mode is where culture medium is added and withdrawn whereas the cells are maintained in the bioreactor (Williams, 2002). Most of the ethanol produced today is done by the batch operation since the investment costs in batch fermentation is low, does not require much control and can easily be adapted to many research (Mishra *et al.*, 2012).

2.2.2 Considerations in Fermenter Design

In bioprocess manufacturing, the fermenter provides the following facilities such as contamination-free environment, specific temperature maintenance, maintenance of agitation and aeration, pH control, monitoring Dissolved Oxygen (DO), ports for nutrient and reagent feeding, ports for inoculation (Williams, 2002; Alford, 2006). To maintain these requirements an optimal fermenter design with appropriate controls is

required to suppress the influence of external disturbances, ensure stability and optimize the performance of the process.

2.2.2.1 Economic Aspects in Fermenter Design

In bioprocess manufacturing as with conventional chemical processing, the main objective is to convert raw materials into the desired product in the most economical way. In meeting this objective, the fermenter, which is the center to bioprocessing must be designed to minimize process cost while maintaining key production requirements which include; safety, product specification, environmental requirements and other operational constraints (Vidyalakshmi *et al.*, 2009). This requires appropriate screening and selection of appropriate microbes to achieve objectives such as high yield and productivity, microbe Generally Regarded as Safe, and if applicable extracellular product producing microbe in order to minimize the cost of downstream processing since level of purification applied varies considerably depending on whether the product is intracellular or extracellular (Zhi-Long, 2008).

2.2.2.2 Biological Aspects in Fermenter Design

Due to the complexity in biological systems, the designing of a bioreactor also has to take into considerations the unique aspects of biological processes. In contrast to isolated enzymes or conventional chemical catalysts, microorganisms adapt the structure and activity of their products to the process conditions (Doran, 1995). Literature has shown that both the substrates and the products may inhibit bioreactions. For this reason the concentrations of substrates and products in the reaction mixture are frequently maintained at optimal levels required for cell growth. Certain substances acting as either inhibitors, effectors or precursors, influence the rate and the mechanism

of the reactions, some of which cause mutations of the microorganisms under sub-optimal biological conditions (Fischer *et al.*, 2008). Microorganisms are frequently sensitive to strong shear stress and to thermal and chemical influences. The downstream recovery processes should be designed considering the effects such as growth on the walls, flocculation, or autolysis of microorganisms which can occur during the reaction.

2.2.3 Types of Fermenters Used in Alcoholic Fermentation

Few of the bioreactor types that can be used for ethanol fermentation include: membrane bioreactors, stirred-tank, packed-bed, fluidized-bed and vacuum bioreactors. Many of the industrial bioprocesses are operated in batch mode and the stirred tank has been highly applicable due to its amenability of batch operation (William, 2002; Alford, 2006). However, though significant developments have taken place in the recent years in reactor design, the bioprocess industry, still prefers stirred tanks because in case of contamination or any other substandard product formation the loss is minimal (Williams, 2002). In recent years, Fluidized bed bioreactors (FBB) have received increased attention due to the advantages it provides including the segregation of the culture media into solid, liquid and gaseous phases in comparison to conventional mechanically stirred reactors, FBBs provide a much lower attrition of solid particles with relatively higher volumetric productivity (Qiangshan *et al.*, 2006). In comparison to packed bed reactors, FBBs can be operated with smaller size particles without the drawbacks of clogging, high liquid pressure drop, channeling and bed compaction hence facilitating higher mass transfer rates and better mixing (Qiangshan *et al.*, 2006). Packed bed or fixed bed bioreactors are commonly used with attached biofilms especially in wastewater engineering.

2.2.4 Process Scale-up and Scale-down in Alcohol Fermentation

Engineers trained in bioprocessing are normally involved in pilot-scale operations. Even though changing the size of the equipment and processes seems relatively trivial, loss or variation of performance often occurs. For the optimum design of a product-scale fermentation system (prototype), the data on a small scale (model) must be translated to the large-scale with similarity between the model and the prototype. The scale-up of submerged fermentation process seems to be much easier than those for aerobic processes such as penicillin fermentation, which have attracted the attention of many scholars, established scale-up theories and technologies, and founded modern biochemical engineering (Wang *et al.*, 2012). However, when we examine today's ethanol fermentation industry, its engineering design and plant operation are far behind other fermentations industries such as organic acids, amino acids, enzyme production antibiotics, and needless to say, modern recombinant pharmaceuticals (Fengwu, 2007). This coupled with research being geared towards developing new feedstock for ethanol production suggest need for more research into both reactor geometry and plant design for optimized ethanol fermentation.

2.2.5 Key Factors of Control in Submerged Fermentation

Due to the high requirements in terms of precision and sophistication in microbial cell cultivation, a process controller forms an integral part of a high-quality bioreactor, in maintaining operating conditions within required ranges. Regarding the use of controllers in bioreactions engineering, three possible configurations of sensors can be envisaged: In-line in which the directly measured value controls the process, e.g. antifoam probe, on-line sensors in which the measured value must be entered into the control system e.g. ion specific sensors, mass spectrophotometer and off-line sensors

which do not form integral part of fermenter and the measured value is stored into a database for future processing (Alford, 2006).

In ethanol fermentation, the main process parameters of interest to the process control engineer are the mineral content of water, temperature of fermentation, pitch rate of yeast, amount of aeration, length of fermentation, culture pH and carbon dioxide. The optimization of temperature is important in the control of fermentation duration and flavor-active compounds like esters and higher alcohols (Saerens *et al.*, 2008). High levels of gases such as CO₂ and O₂ have been shown to result in higher pressure with similar effects to that of an increased temperature and as yeast prefers aerobic conditions. The addition of additional oxygen would cause changes in the fermentation process by affecting the amount of unsaturated fatty acids present in the fermentation broth (Verbelen *et al.*, 2009). Results have shown the importance of the pitching rate on yeast physiology and activity and consistency during fermentation with increasing rate thus resulting in decreased fermentation time required and increased concentration of higher alcohols (Verbelen *et al.*, 2009).

2.3 Biochemical and Microbial Aspects of Submerged Fermentation

2.3.1 Microorganisms and Fermentation Conditions in Brewing

Fermentation principle consists of exploiting the metabolic reactions that take place in the cell of a microorganism for the production of valuable products (Olivier, 2001). During ethanol fermentation in brewing, the three most common yeast strains usually used include: (a) Ale yeasts, top-fermenting, which can ferment at higher temperatures and tend to produce more esters, (b) Lager yeasts which are bottom fermenting, withstand lower temperatures and produce a more crisp taste, and (c) the Wild yeasts which produce a lot of unusual compounds and contribute to a “horse sweat” flavour

that is more acidic and an acquired taste. In order to activate the metabolic pathways of interest within the cell, specific environmental conditions (temperature, pH, nutrient concentration) are applied to enable the yeast cell grow and produce the required ethanol. However, due to the dynamic nature of the culture medium, yeast cells often suffer from various stresses resulting from both the environmental conditions, and from both product and or substrate inhibition. Figure 2.2 illustrates some stresses that yeast cells could experience in ethanol fermentations.

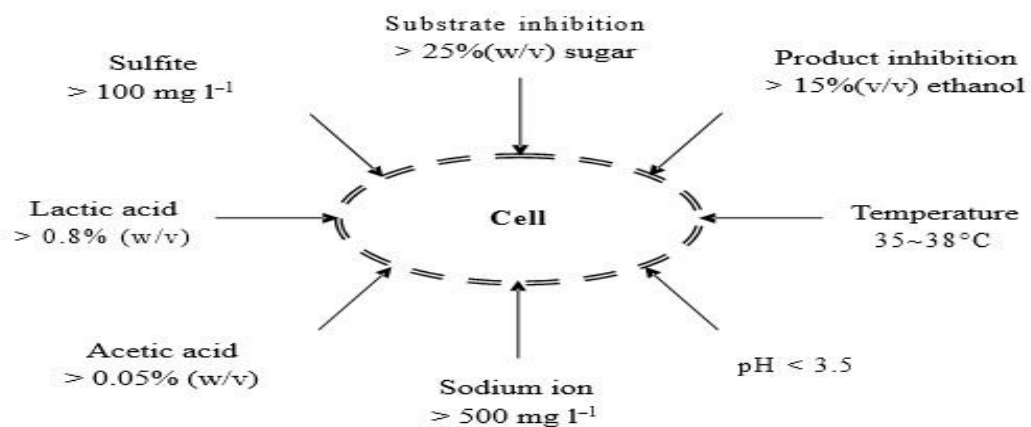


Figure 2.2: Environmental stresses exerted on *S. cerevisiae* during ethanol fermentation (Ingledew, 1999)

2.3.2 Biochemical Pathways in Yeast Fermentation

There are three pathways yeast (usually *S. cerevisiae*) can obtain energy through the oxidation of glucose. All three pathways start with the initial stage of glycolysis, the conversion of glucose into fructose-1, 6-bisphosphate. These pathways are: (a) alcoholic fermentation in which the pyruvate resulting from glycolysis is decarboxylated to acetaldehyde (ethanal) which is reduced to ethanol. This pathway yields only two more molecules of Adenosine Triphosphate (ATP) per molecule of glucose over the two resulting from glycolysis. This is the major pathway in ethanol fermentation, (b) Glyceropyruvic fermentation is important at the beginning of the alcoholic fermentation of grape when the concentration of alcohol dehydrogenase

(required to convert ethanal to ethanol) is low and (c) Aerobic respiration which occurs in the presence of oxygen. In the production of alcoholic beverages, the amount of oxygen is carefully controlled during the wine-making process and the latter pathway is forbidden. (Nelson and Cox, 2001). Figure 2.3 shows a simplified glycolytic scheme (Embden–Meyerhof–Parnas) in *S. cerevisiae*. The pathway is shown in Fig. 2.3.

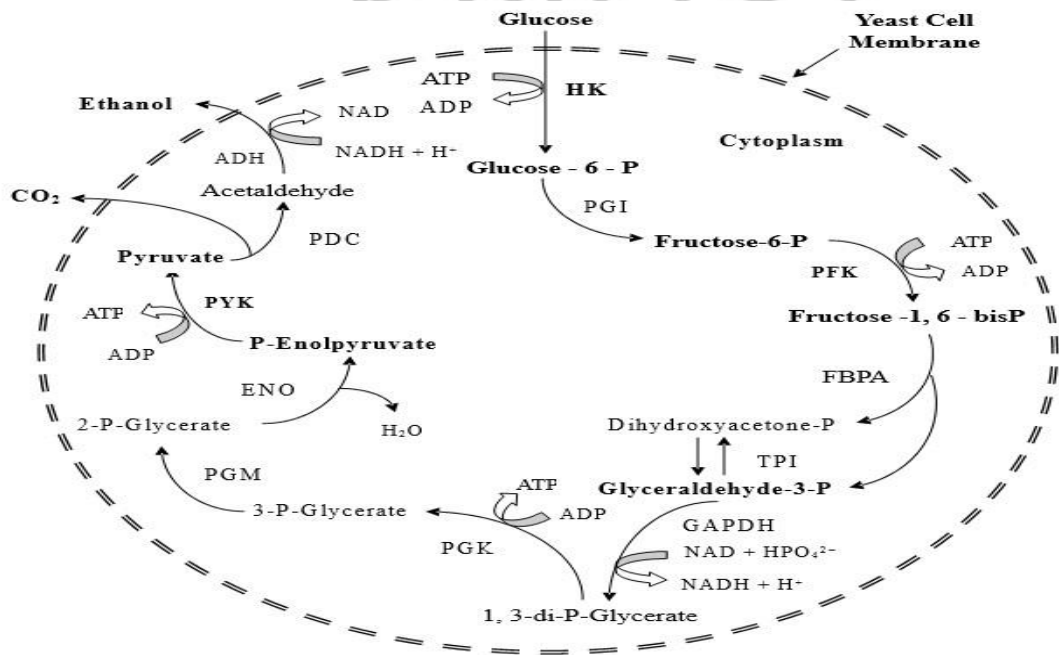


Figure 2.3: Simplified glycolytic scheme (Embden–Meyerhof–Parnas) in *S. cerevisiae* Abbreviations: HK: hexokinase, PGI: phosphoglucosomerase, PFK: phosphofructokinase, FBPA: fructose bisphosphate aldolase, TPI: triose phosphate isomerase, GAPDH: glyceraldehydes-3-phosphate dehydrogenase, PGK: phosphoglycerate kinase, PGM: phosphoglyceromutase, ENO: enolase, PYK: pyruvate kinase, PDC: pyruvate decarboxylase, ADH: alcohol dehydrogenase (Fengwu, 2007).

2.4 Industrial Applications of Alcoholic Fermentation

2.4.1 Production of Alcoholic Beverages and Bakeries

The production of alcoholic beverages by submerged fermentation vary widely depending primarily on these starchy material, fermentation conditions and on the type of micro-organism used for fermentation (Saerens *et al.*, 2008; Verbelen *et al.*, 2009).

Over the years various materials have been used ranging from grapes to berries, corn, rice, wheat, honey, potatoes, barley, hops, cactus juice, cassava roots, and other plant materials resulting various forms of beer, wine and distilled liquors which may be given specific names depending on the source of the feedstarch. Besides the production of ethyl alcohol used in alcoholic beverages, one other major application of fermentation in the food industry has been to harness the potential of yeast to produce carbon dioxide in improving bulkiness and texture of the dough during baking.

2.4.3 Production of Biofuels

Submerged fermentation of sugars from biowastes and agro residues is the most conventional way to produce bioethanol. Many laboratories and researchers in Ghana are involved in the design and construction of bioreactor systems for bioethanol production. Studies on biofuels potential in Ghana have been widely reported from three main types of biomass raw materials which are starchy materials like rice husk, cassava; sugar materials like sorghum juice (Osei et al., 2013; Kemausuor et al., 2014), and finally lignocellulosic materials such as bagasse, straw and wood biomass.

The main motivation for this subject has been to develop an alternative renewable transportation liquid from lignocellulosic resources which forms part of the goal of Ghana obtaining 10% of its energy from renewable sources by 2020 (Ghana Renewable Energy Act, 2011). However, energy efficiency, economic viability and environmental impact of these processes have not been fully investigated. Empirical methods have been traditionally used to scale-up bioreactor facilities in developing countries, but these have required construction of expensive prototype systems and time-consuming studies (Yu *et al.*, 2013). Alternatively, design and optimization of submerged

fermenters for bioethanol production can be enhanced via validated mathematical models.

2.5 Kinetic and Dynamic Modelling of Fermentation Processes

2.5.1 The Benefits of Modelling in Industrial Fermentation

The increasing study of realistic and practically useful mathematical models in bioprocess manufacturing, whether for the production of enzymes, alcoholic beverages, biofuels or other products of human and industrial importance, is a reflection of their use in helping to understand the dynamic processes involved and in making practical predictions. A mathematical model describing the dynamics of fermentation is a reliable tool in situations where experiments are very expensive and time consuming (Alford, 2006; Yu *et al.*, 2013). In addition to the context of cost and time reduction, a fermentation process model developed in the early research and development stage can go beyond the laboratory to benefit the routine manufacturing, guarantee the quality, supply information about the values of experimentally inaccessible parameters and help reveal possible underlying mechanisms involved in the process. This is illustrated by modelling recently attracting attention from industry (Velayudhan and Menon, 2007), with the Quality by Design (QbD) and Process Analytical Technology (PAT) being driving force behind this transition (Ji, 2012). These concepts and technologies aim to utilize mathematical modelling methods to enhance the understanding of complicated biochemical process, with the long term benefits for companies to develop and design processes more quickly and facilitate batch release (Mandenius and Brundin, 2008).

Several fermentation companies have applied modelling to processes and gained benefits arising from their utilization (Chhatre *et al.*, 2011; Ji, 2012). For instance, Novozyme, found modelling very helpful to identify the optimal feeding profile in a

fed-batch filamentous fungal fermentation for enzyme production system (Titica *et al.*, 2004). Ramirez and Maciejowski (2007) used mathematical modelling to develop a new tool to solve a wide range of optimal beer fermentation problems.

2.5.2 General Characteristics of Dynamic Models

Different kinds of models for biochemical processes are distinguishable according to their possible biological interpretation and before modeling the kinetics and dynamics of biosystems. It is important to understand some of the characteristics dynamic models present. A dynamic model can be linear, satisfying the superposition principle or nonlinear, represented by nonlinear differential equations (Constantinides and Mostoufi, 1999). The parameters of a model are lumped when the model is homogeneous with time being the unique independent variable but when some state varies within the system, the model becomes heterogeneous with distributed parameters. Many models are continuous; their independent variables are considered to be defined for any real values of time (Beers, 2007). However, measured data are usually obtained through discrete sampling which implies measurements at discrete time intervals. Unlike deterministic models which are based on the underlying mechanism of action of the system, stochastic models on the other hand present randomness which is usually introduced as the measurement noise (Lübbert and Jørgensen, 2001; Box *et al.*, 2002). A dynamic model can be structured or unstructured depending on whether it describes intracellular characteristics including the metabolic processes of the cell or considers the cell like an entity without internal structure (Shuler and Kargi, 1992; Zeng and Bi, 2006).

2.5.3 Modeling Methods in Bioprocess Engineering

Developing a model to describe a bioprocess is not an easy task, usually involve time consuming mathematical and computational analysis due to the nonlinearity of biosystems. However, an ideal process model for a bioprocess should be able to represent the characteristics of the process in a quantitative way and predict the system's behavior accurately and precisely through the application of computational analysis and optimization algorithms (Datta and Sabiani, 2007). Even though such an ideal process model may not always exist the idea is to strive as much as possible to arrive at a model which is closest to ideality and could represent the system as accurately as possible.

2.5.3.1 Traditional Modeling Procedure

The first part in modeling the dynamics of a bioprocess is to determine the type of model to describe the kinetics of the process reactions and proposing a model structure according to the developer's knowledge of the system and the objectives to achieve it. This is usually done based on theories, and detailed understanding of the mechanism of the process; and an example of such a model is the Michaelis-Menten model describing the kinetics of enzyme catalyzed reaction (Michaelis and Menten, 1913). When the process mechanism is unknown or too complicated to form a mathematical relationship, a common practice in engineering it to build an empirical process model using relatively simple mathematical equation which can then fit the data. For instance, the Monod's growth equation. The third approach to describe reaction kinetics is to use a hybrid model, combining the mechanistic knowledge with correlations of an empirical nature for aspects that are not yet fully understood (Galvanauskas *et al.*, 2004). When an appropriate formulation or choice of kinetic model has been made, the continuity equations of mass and/or energy involving substrate inputs, accumulation and dilution

terms as well as kinetics described by activation, inhibition and saturation coefficients are then applied to the system to develop systems of differential equations describing the dynamics of the system. No matter which type of model is used, experimental data must be used to fit and regress model parameters with subsequent evaluation and validation of results by statistical tests. Although the modeling process might seem quite simple and straightforward, differences between initial proposed structure and real experimental data may require model modifications and fine-tuning which further complicates the modelling activities and requires the model developer to have good mathematical background. Another drawback of this conventional modelling procedure is that the model does not interact readily with experiments. The experimental data may not be sufficient in number or quality for modelling, requiring the concern of experimental design in order to obtain effective information and achieve maximum process understanding with minimum experimental number.

2.5.3.2 Innovative artificial neural network modeling

In recent years, there has been significant interest in the use of artificial neural networks with hybrid process models for bioprocess modeling, and this approach has shown to be less time consuming, simple for engineers and solves the problems of proposing an initial model followed by subsequent modification as observed in traditional modeling. This approach has been well-studied and successfully applied in the modeling and optimization of fermentation processes including ethanol fermentation (Komives and Parker 2003; Alford, 2006). The structure of the neural network based process model may be considered generic, in the sense that no *a priori* understanding or information about the system is required (Massimo et al., 1991; Montague and Morris, 1994). A neural network model consists of highly interconnected layers of simple ‘neuron-like’ nodes, which act as non-linear processing elements within

the network and one very interesting property of using neural networks is that given the appropriate network topology, they are capable of learning and characterizing non-linear functional relationships through experimental data. Literature shows the use of artificial neural network to predict the pH, temperature, substrate, biomass, carbon dioxide (CO₂) and alcohol (ethanol) evolution during batch fermentation of sorghum (Kouame et al., 2015). Assidjo *et al.* (2009) combined the neural network to differential equations in the simulation of an ethanol fermentation process using malt, with a predictive error of less than 0.030. The use of neural network to estimate the effect of temperature on an industrial ethanol fermentation process was presented by Mantovanelli *et al.* (2007).

2.5.4 Kinetic Models for Cell Growth Kinetics

As seen in section 2.5.3, modeling the dynamics of bioprocesses require a kinetic model describing the variation of the substrate and/or product concentration with the cell growth and which can also express the influences of other process variables such as pH, pO₂, pCO₂ and temperature. Generally, in ethanol fermentation the specific growth rate μ is the key variable (Moser, 2004) as it is time dependent and also dependent on wide range of physical, biological and chemical parameters including the concentration of cells, substrate and product, and temperature, pH and different inhibitors. These assumptions were studied in detail by Bastin and Dochain (1990) who also proposed a generalized approach to bioprocess modeling and conforming to several models that exist in literature describing the dependence of the specific growth rate on different process parameters represented mathematically as equation (1):

$$\mu = f(S, X, pH, C, I, \dots, t) \quad (1)$$

2.5.4.1 Growth Limitation through Substrate Concentration

Bellgardt (1991, 2000) studied various kinetic models showing the dependence of specific growth rate on substrate limitation as presented in Table 2.1 below

Table 2.1: kinetic models with growth limitation through substrate concentration

Model Equations	Constants	Authors	Comments
$\mu(S) = \frac{\mu_{max} S}{K_s + S}$	μ_{max} is the maximum specific growth rate (1/h) and K_s is the saturation constant (g/L)	Monod equation (1942, 1949)	Empirically derived from Michaelis-Menten equation
$\mu(S) = \frac{\mu_{max} S^n}{K_s + S^n}$		Moser equation (1988)	Analogy with a Hill kinetic ($n > 0$)
$\mu(S) = \frac{\mu_{max} S}{K_s + K_D + S}$	K_D is the diffusion constant	Powell equation (1958)	Influence of cell permeability, substrate diffusion and cell dimensions through K_D parameter

2.5.4.2 Growth Limitation through Substrate and Cell Concentration

The kinetic models with growth limitation through substrate concentration $\mu = \mu(X, S)$ form (Bellgardt, 1991; Bellgardt, 2000) are presented in Table 2.2 below

Table 2.2: Kinetic models with growth limitation through substrate and cell concentration

Model Equations	Constants	Authors	Comments
$\mu(X) = \mu_{max}(1 - K_x X)$	K_x is the kinetic constant	Verhulst (1845)	It is known as growth logistic model
$\mu(S) = \frac{\mu_{max} S}{K_x X + S}$	K_x is the kinetic constant	Contois (Contois – Fujimoto) equation (1959):	If $S = \text{constant}$, the only dependence remains $\mu = f(X)$.
$\mu(X, S) = \mu_{max} \frac{S_0 - \frac{X}{Y}}{K_s + S_0 - \frac{X}{Y}}$	S_0 is the initial substrate concentration Y is the substrate/cell yield	Meyrath (1973)	It is based on Monod kinetics.

2.5.4.3 Growth kinetics with substrate inhibition

Just like the Monod kinetic model derived empirically by comparing experimental with the nature of Michaelis-Menten equation most of the kinetic models describing substrate and/or product inhibition were derived from the inhibition theory of

enzymatic reactions and are consequently not generally valid requiring application with experimental data (Bellgardt, 1991, 2000)

Table 2.3: Kinetic models with substrate inhibitions

Model Equations	Constants	Authors	Comments
$\mu = \mu_{max} \frac{S}{K_s + S} e^{-\frac{S}{K_{i,S}}}$		Aiba model (1965)	
$\mu = \mu_{max} \frac{1}{1 + \frac{K_s + K_i S}{S}}$	K_i is the inhibition constant	Andrews model (1968)	Substrate inhibition in a chemostat

2.5.4.4 Growth Kinetics with Product Inhibition

Hinshelwood (1946) studied product inhibition influences upon the specific growth rate and linear decrease, exponential decrease, growth sudden stop, and linear/exponential decrease in comparison with a threshold value of product were detected. This requires more research into the mechanism of substrate and or product inhibition applies in ethanol fermentation so as to guarantee the accuracy of the model.

Table 2.4: Models showing growth kinetics with product inhibition

Model Equations	Constants	Authors
$\mu(P) = \mu_{max} K_1 (P - K_2)$	$k_1, k_2 = \text{constants } (>0)$	Holzberg model (1967)
$\mu(P) = \mu_{max} e^{-K_1 P}$	$k_1 = \text{constant}$	Aiba (1982)
$\mu(P) = \mu_{max} \frac{P}{P_{max} (1 + \dots)}$	$P_{max} = \text{maximum product concentration}$	Ghose and Tyagi model (1979)

2.5.4.5 Unstructured Kinetic Models for Product Formation

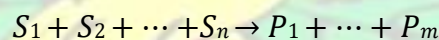
In this section, a combination of the kinetics of product formation and the cell growth is considered and based on the Gaden classification, four categories of kinetic models can be defined (Schugerl, 1991). Type 0, involves only a little substrate with cells functioning only as enzyme carriers, a typical example is the transformation of steroids

and synthesis of vitamin E by *Saccharomyces cerevisiae*. Type 1: where product formation is directly linked to cell growth, case of ethanol fermentation and situations in biological wastewater treatment. Type 2: with no direct connection between growth and product formation, case of penicillin and streptomycin synthesis. Type 3: Involves pathways that have a partial association with growth and thus indirect link to energy, e.g. citric acid and amino acid production.

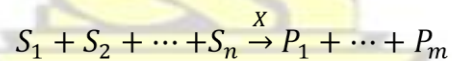
2.5.5 Reaction Schemes in Biochemical Process Modeling

The reaction scheme of a biochemical process is a macroscopic description of the set of biological and chemical reactions which represent the main mass transfer within the fermenter. A formalism close to that used in chemistry is adopted. In such a scheme a set of substrates S_i is converted to a set of products P_i following three possibilities models (Bastin and Dochain, 1990):

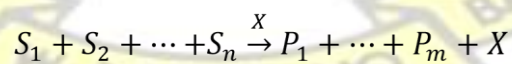
- a) The reaction is a pure chemical reaction and no biomass is involved. The reaction is therefore a pure chemical reaction:



- b) The reaction is catalyzed by a biomass X. The biomass acts only as a catalyzer and the reaction is not associated with the growth of the microorganism:



- c) The reaction is associated with growth of microorganism. Therefore biomass is also a product:



2.6 Parameter Estimation in Bioprocess Modeling

One very efficient method in studying and predicting the behavior of industrial bioprocesses is the use of mathematical models to quantitatively describe the dynamics

of cell growth and product formation (Hamilton, 2011). The central idea of bioprocess modeling, to help reveal possible underlying mechanisms involved in a biological processes by the analysis of mathematical models is often hampered by the fact that parameters like rate constant are not known (Peifer and Timmer, 2007).

Numerical simulations of the system often involve estimating parameter values and evaluating the sensitivity of the system to small changes in parameters (Wang, 2012).

The challenging problems related to parameter estimation in Ordinary Differential Equations are numerous. The existence of noise in measurements and nonlinearity of bioprocess dynamics makes it more challenging in estimating model parameters which complicates the adoption of most optimization techniques. Several approaches for estimating parameters in ordinary differential equations have either a small convergence region or suffer from an immense computational cost and if the parameters of a model are unknown, the results from simulation studies can be misleading (Peifer and Timmer, 2007). There is therefore need for appropriate choice and validation of parameter estimation method used in bioprocess modeling.

2.6.1 Parameter Estimation Methods

Due to the nonlinearity of ODEs used in describing the dynamics of bioprocess, all methods regarding parameter estimation show an interplay between simulating the system's trajectory and optimization (Peifer and Timmer, 2007; Wang, 2012). The simulation of trajectory is usually done by convenient numerical methods for ODE; whereas the optimization differs drastically and can be broadly classified into global, clustering methods (Rinnooy-Kan and Timmer, 1987), evolutionary computation (Holland , 1992) and simulated annealing and Cross-Entropy method and local optimization methods, sequential quadratic programming (SQP), Newton methods,

quasi-Newton methods and so on. Global optimization (GO) methods can be roughly classified as deterministic (Horst and Tuy, 1990; Grossmann, 1996) or stochastic (Ali et al., 1997; Torn and Viitanen, 1999). One weakness of stochastic GO methods is the lack of strong theoretical guarantees of convergence to the global optima, since stochastic techniques for global optimization ultimately rely on probabilistic arguments. Deterministic GO methods are, on the other hand, generally able to achieve a level of assurance that the global optimum will be located. In the case of parameter identification in ODEs, the problem of convergence to local minima is predominant if the so-called initial value approach is considered.

2.7 Theory of Optimal Control in Submerged Fermentation

Optimal control is a subject where it is desired to determine the inputs to a dynamical system that optimize (i.e., minimize or maximize) a specified performance index while satisfying any constraints on the motion of the system (Bryson, 1996). Optimal control is an extension of the calculus of variations and most fruitful applications of the calculus of variations have been to theoretical physics, in connection with Hamilton's principle. Early applications of optimal control in resources economics appeared in the late 1920s and early 1930s by Ross, Evans, Hotelling and Ramsey, with further applications published occasionally thereafter (Sussmann and Willems, 1997). The application of optimal control in the development of suitable procedures for the optimization of fermentation processes is very important, since obtaining the global optimum may be very difficult (Alford, 2006). In regards to this, optimal temperature profiles have been determined to maximize beer flavor (Ramirez and Maciejowski, 2007), maximize ethanol formation from sugarcane molasses (Marcus and Normey-Rico, 2011), minimize acetyl acetate production, (Carrillo-Ureta et al., 1999), and maintain cell viability and reduce glycerol production (Atala et al. 2001).

2.7.1 Performance Criteria of an Optimal Control Problem

The general objective of an optimal control problem is to determine the control signals that will cause a controlled system to satisfy the physical constraints and, at the same time, minimize (or maximize) some performance criterion”, which can take various forms including Lagrange form, Mayer form and Bolza form. The controlled system is characterized by: State variables describing its internal behavior, called the phase space e.g., coordinates, velocities, concentrations, flowrates, etc. and Control variables describing the controller positions, called the control space e.g., force, voltage, temperature, etc. (Luus, 1990).

A function used for quantitative evaluation of a system’s performance can depend on both the control and state variables and on the initial and/or terminal times too (if not fixed). The three general forms of the performance criterion are presented in equations (2.1), (2.2) and (2.3):

$$\text{Lagrange form: } J(u) = \int_{t_0}^{t_f} \mathcal{L}[x(t), u(t), t; p] dt \quad (2.11)$$

$$\text{Mayer form: } J(u) = \Phi[x(t_0), t_0, x(t_f), t_f; p] \quad (2.12)$$

$$\text{Bolza form: } J(u) = \Phi[x(t_0), t_0, x(t_f), t_f; p] + \int_{t_0}^{t_f} \mathcal{L}[x(t), u(t), t; p] dt \quad (2.13)$$

The Lagrange, Mayer and Bolza functional forms are equivalent (Chachuat, 2007; Zabczyk, 2008).

2.7.2 Solution Methods for Optimal Control

Generally the approaches used in solving optimal control problems can be divided into two broad categories; the indirect methods and direct methods. The major methods that fall into each of these two broad categories are described in the following sections.

2.7.2.1 Indirect Methods of Solving Optimal Control Problems

In an indirect method, calculus of variations is applied to determine the first-order optimality conditions and unlike ordinary calculus (where the objective is to determine points that optimize a function), the calculus of variations is the subject of determining functions that optimize a function of a function, referred to as functional optimization (Athans and Falb, 2006; Leitman, 1981).

2.7.2.2 Direct Methods for Solving Optimal Control Problems

Direct methods are fundamentally different from indirect methods. In a direct method, the state and/or control of the original optimal control problem are approximated in some appropriate manner. In the case where only the control is approximated, the method is called a control parameterization method (Goh and Teo, 1988). When both the state and control are approximated the method is called a state and control parameterization method. In either a control parameterization method or a state and control parameterization method, the optimal control problem is transcribed to a nonlinear optimization problem or nonlinear programming problem (Betts, 1998; Gill et al., 1981). The three most common direct methods are the shooting method, the multiple-shooting method, and collocation methods.

2.7.3 Numerical Methods in Optimal Control

Due to the nonlinearity often observed in the HBVP extremal trajectories (i.e., solutions of the HBVP) are determined numerically. At the heart of a well-founded method for solving optimal control problems are the following three fundamental components: The three most common indirect methods are the shooting method, the multiple-shooting method, and collocation methods. Methods for solving differential equations and integrating functions are required for all numerical methods in optimal control. In an

indirect method, the numerical solution of differential equations is combined with the numerical solution of systems of nonlinear equations while in a direct method the numerical solution of differential equations is combined with nonlinear optimization (Logsdon and Biegler, 1989; Biegler *et al.*, 2002).

2.8 Perspective and Motivation

From the detailed background in this area of study, it is observed that the current information regarding mathematical modeling and fermentation processes is not adequate to conveniently establish the mathematical structure and mechanism of substrate and/or product inhibition in the alcoholic fermentation of maize, sorghum and cassava extracts. There is therefore a need for more research and development in the area of mathematical modeling to determine the nature of process stresses in the three substrates followed by the application of optimal control to minimize the effect of such inhibitions.

CHAPTER THREE MATHEMATICAL MODELING, AND PARAMETER ESTIMATION

3.1 Introduction and Chapter Overview

The obstacles which include the complexity of the biological systems, the limited understanding of the biological processes, and the resulting lack of adequate process models hinder the adaptation of traditional process engineering approaches to bioprocessing. The evolution of micro-organisms is very complex and does not obey some clear physical laws which make modelling of biological processes complex because it is not based on validated laws like in other fields (mechanics, electronics, etc.). Nevertheless, like all physical systems, biosystems respect some laws like mass

conservation and energy conservation. In this section, all these aspects were considered in the model development in order to ensure that the mass balance approach would guarantee robustness of the model to describe the fermentation process. The model parameters were estimated using experimental data and a Matlab code which was written for parameter estimation in each of the scenarios considered. The capability of the mathematical model to describe the ethanol fermentation process was tested statistically using the F– tests using STATA software at a confidence interval of 99%.

3.2 Experimental Methods and Data Collection

This study involved a batch process where all the culture medium was directly available to the cell and no medium was added or withdrawn from the culture. The fermentation was carried out in industrial scale dual purpose fermenters and a series of peripheral devices were used to control and monitor the fermentation process.

Three different fermentation worts were used- cassava, maize and sorghum and the environmental and state variables were measured at regular time intervals. Sorghum was top fermented with *S. cerevisiae* for a duration of 64 h, using an initial cell and substrate concentration of 0.1 million cells/ 0.1ml and 16.8g/100g respectively, with data taken every 4 h. Cassava and maize were bottom fermented separately, using *S. carlsbergensis* for a duration of 120 h and data collected every 12 h. The fermenters were inoculated with cell and substrate concentration of 0.16 million cells/0.1ml and 15.28g/100g respectively in the case of maize and 0.16 million cells/0.1ml and 12.79g/100g respectively in the case of cassava. The environmental variables that were controlled are pH and temperature. pH was measured with a pH probe and temperature monitored by a thermocouple. Besides these environmental

considerations, the substrate (glucose), cell and product concentrations were the main variables of interest.

3.3 Model Development and Validation Methodology

In developing the systems of differential equations for the batch fermenters, a Monod type model that accounts for product and/or substrate inhibition was used to approximate the kinetics of cell growth, substrate utilization and product formation in the fermentation process. The continuity equation of mass was applied to the fermenters to develop a system of differential equations that will be used to monitor the dynamics of substrate utilization, biomass formation and product formation during ethanol fermentation. All the system of linear ordinary differential equations obtained was simulated numerically using the 4-5th order Runge-Kutta method and all parameters in the model was estimated using experimental model fitting techniques. The formulation of mathematical fermentation process models, from the standpoint of system analysis, was usually realized in three stages:

- a) Qualitative analysis of the structure of a system, usually based on the knowledge of metabolic pathways and biogenesis of the desired product,
- b) Formulation of the model in a general mathematical form. This stage is sometimes called the structure synthesis of the process functional operator;
- c) Identification and determination of numerical values of model constants and/or parameters which are based on experimental or other operating data from a real process.

Figure 3.1 presents the different stages that were used for the model development

KNUST



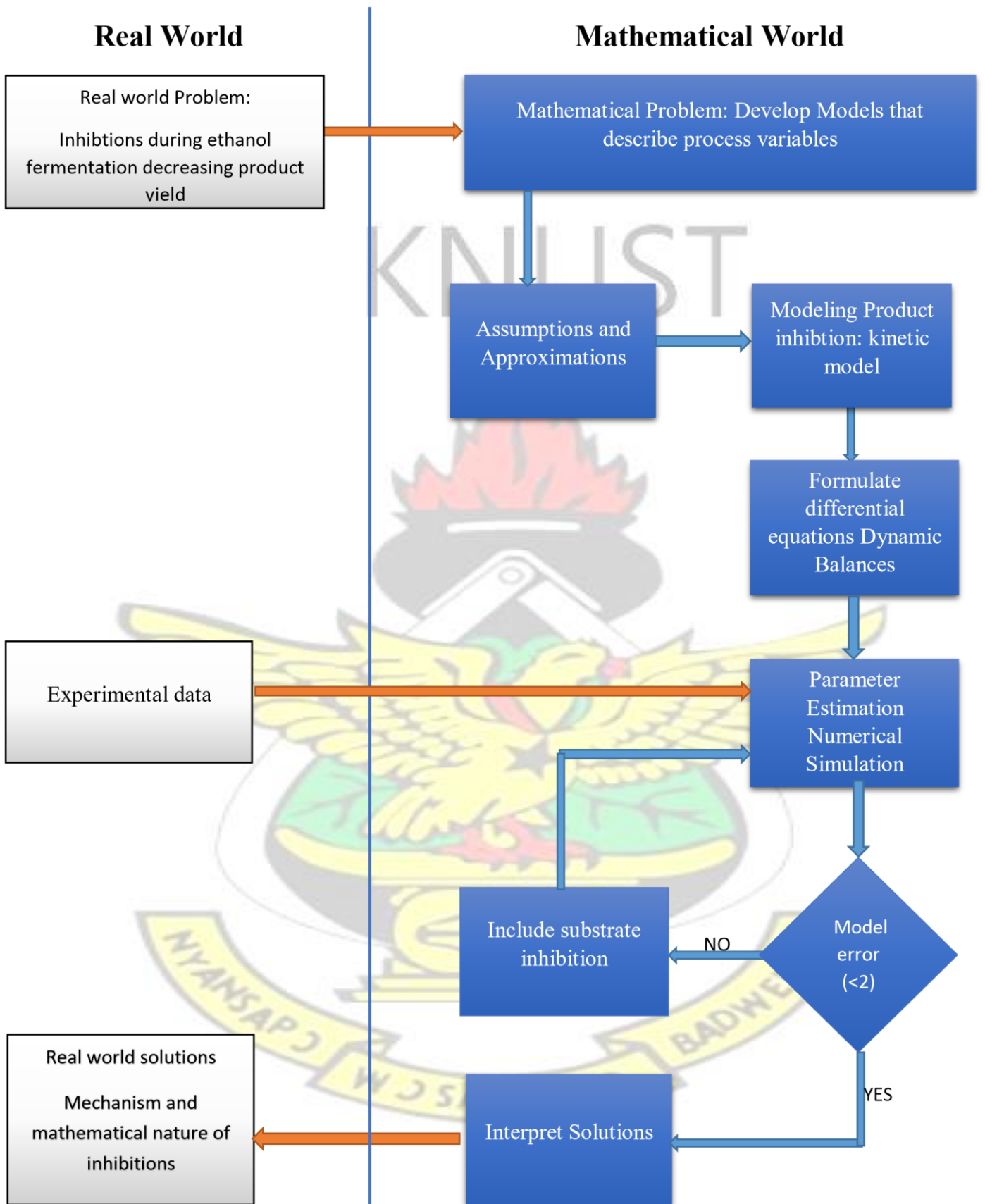


Figure 3.1: procedure used for model development and validation

3.4 Kinetic Modeling

3.4.1 Modeling of Growth Kinetics and Product Inhibition

The Monod's growth model is found to be the most simple and fundamental model to explain microbial growth and was chosen to describe the growth kinetics of ethanol fermentation in this study.

Similar type of equation which describes the specific rate of product formation was used to describe the kinetics of product formation as shown in equation (3.1). Starting from the Monod Equation for cell growth and product formation, three inhibition patterns were considered in modeling product inhibition; linear, sudden growth stop and exponential as shown in Table 3.1.

$$\left. \begin{aligned} \mu(S) &= \frac{\mu_{max}S}{K_{sx} + S} \\ q_p(S) &= \frac{q_{pmax}S}{K_{sp} + S} \end{aligned} \right\} \quad (3.1)$$

Table 3.1: Mathematical expressions used in modeling product Inhibition

Product Inhibition Factor	Mathematical Expression
Linear	$(1 - K_2P)$
Sudden Growth Stop	$\left(1 - \frac{P}{P_{max}}\right)$
Exponential	e^{-K_1P}

To introduce the effect of product inhibition on the Monod equation, the respective inhibition factor results in the following kinetic models: (a) Linear product Inhibition (equation 3.1.1 known as the Hinshelwood-Dagley model), (b) Sudden growth stop product inhibition (equation 3.1.2 which was first proposed by Ghose and Tyagi,

(1979)), and (c) exponential product inhibition (equation 3.1.3 known as the Aiba and Shoda model (1989)).

$$\left. \begin{aligned} \mu(S, P) &= (1 - K_{ix}P) \frac{\mu_{max}S}{K_{sx} + S} \\ q(S, P) &= (1 - K_{ip}P) \frac{q_{max}S}{K_{sx} + S} \end{aligned} \right\} \quad (3.1.1)$$

$$\left. \begin{aligned} \mu(S, P) &= \left(1 - \frac{P}{P_{max}}\right) \frac{\mu_{max}S}{K_{sx} + S} \\ q(S, P) &= \left(1 - \frac{P}{P_{pmax}}\right) \frac{q_{max}S}{K_{sx} + S} \end{aligned} \right\} \quad (3.1.2)$$

$$\left. \begin{aligned} \mu(S, P) &= \exp(-K_{ix}P) \frac{\mu_{max}S}{K_{sx} + S} \\ q(S, P) &= \exp(-K_{ip}P) \frac{q_{max}S}{K_{sx} + S} \end{aligned} \right\} \quad (3.1.3)$$

3.4.2 Modeling Substrate Inhibition

The substrate Inhibiton was modelled taking into consideration the presence of product inhibition, and the patterns that were considered are shown in Table 3.2 below. To introduce the effect of substrate inhibition on kinetics of cell growth and product formation resulted in four different inhibition patterns: (a) Linear Substrate-Linear Product (equation 3.1.4), (b) Linear Substrate-Exponential Product (equation 3.1.5), (c) Exponential substrate-linear product (equation 3.1.6) and (d) Exponential

Substrate-Exponential Product (equation 3.1.7) as shown in the following section.

Table 3.2: Mathematical expressions for the substrate and product inhibition factors

Inhibition Factor	Mathematical Expression
Linear substrate	$(1 - K_2S)$
Exponential Substrate	$e^{-\kappa_1S}$

$$\left. \begin{aligned} \mu(S, P) &= (1 - K_{ix}P)(1 - K_{isx}S) \frac{\mu_{max}S}{K_{sx} + S} \\ q(S, P) &= (1 - K_{ip}P)(1 - K_{isx}S) \frac{q_{max}S}{K_{sx} + S} \end{aligned} \right\} (3.1.4)$$

$$\left. \begin{aligned} \mu(S, P) &= (1 - K_{isx}S) \exp(-K_{ix}P) \frac{\mu_{max}S}{K_{sx} + S} \\ q(S, P) &= (1 - K_{isp}S) \exp(-K_{ip}P) \frac{q_{max}S}{K_{sx} + S} \end{aligned} \right\} (3.1.5)$$

$$\left. \begin{aligned} \mu(S, P) &= (1 - K_{ix}P) \exp(-K_{isx}S) \frac{\mu_{max}S}{K_m + S} \\ q(S, P) &= (1 - pP) \exp(-K_{isp}S) \frac{q_{max}S}{K_m + S} \end{aligned} \right\} (3.1.6)$$

$$\left. \begin{aligned} \mu(S, P) &= \exp(-K_{ix}P) \frac{\mu_{max}S}{K_{sx} + S} \exp(-K_{isx}S) \\ q(S, P) &= \exp(-K_{ip}P) \frac{q_{max}S}{K_{sp} + S} \exp(-K_{isp}S) \end{aligned} \right\} (3.1.7)$$

3.5 Dynamic Balances and Governing Differential Equations

The dynamic equations for each of the process variables were developed by applying the continuity law of mass to the batch fermenter and presented as follows;

$$\begin{aligned} \text{Rate of mass} & & \text{Rate of mass} & & \text{Rate of Mass} & & \text{Rate of} & & \text{Rate of} \\ \left(\frac{\Delta S}{\Delta t} \right) & = & \left(\frac{\Delta S}{\Delta t} \right) & - & \left(\frac{\Delta S}{\Delta t} \right) & + & \left(\frac{\Delta S}{\Delta t} \right) & - & \left(\frac{\Delta S}{\Delta t} \right) \\ \text{Accumulation} & & \text{Input} & & \text{Output} & & \text{Generation} & & \text{Consumption} \end{aligned} \quad (3.1.8)$$

Since the study involved a batch configuration the continuity equation can be simplified to:

$$\begin{aligned} \text{Rate of Component} & & \text{Rate of component} & & \text{Rate of component} \\ \left(\frac{\Delta S}{\Delta t} \right) & = & \left(\frac{\Delta S}{\Delta t} \right) & - & \left(\frac{\Delta S}{\Delta t} \right) \\ \text{Accumulation} & & \text{Generation} & & \text{Consumption} \end{aligned} \quad (3.1.8a)$$

It was considered in modeling the substrate dynamics that when substrate is consumed the rate of substrate consumption depends on

$$\Delta S = \left(\frac{\Delta S}{\Delta t} \right)_{\text{into biomass}} + \left(\frac{\Delta S}{\Delta t} \right)_{\text{extracellular pdt}} + \left(\frac{\Delta S}{\Delta t} \right)_{\text{Growth energy}} + \left(\frac{\Delta S}{\Delta t} \right)_{\text{Mentainance energy}} \quad (3.1.8b)$$

This implies the rate of substrate utilization $K\phi$ is given by

$$K\phi = \frac{1}{Y_x} \mu(S, P)X + \frac{q_p}{Y_p} X + G_s X + M_s \quad (3.1.9)$$

where,

$$\frac{1}{Y_x} \mu(S, P)X = \text{substrate assimilation into biomass} \quad (3.1.9a)$$

$$\frac{q_p}{Y_p} X = \text{subtrate assimilation into extracellular product} \quad (3.1.9b)$$

$$G_s X = \text{substrate utilization for growth} \quad (3.1.9c)$$

$$M_s X = \text{substrate utilization for maintainace energy} \quad (3.1.9d)$$

By applying the principle of conservation of mass and using the specific rates of biomass, substrate and product formation, batch kinetics and mathematical correlations, the approximate representation (description) of the fermentation process was done using systems of first order ordinary differential equations presented by equation (3.2). It consists of the system of mass balances for each of the state variables that were considered in the experiment, where S represents substrate concentration, P product concentration and X biomass.

$$\left. \begin{aligned} \frac{dX}{dt} &= \mu X \\ \frac{dP}{dt} &= qX \\ \frac{dS}{dt} &= -\bar{Y}_x \frac{dX}{dt} - \bar{Y}_p \frac{dP}{dt} - G_s X - M_s X \end{aligned} \right\} (3.2) dt$$

3.5.1 Systems Dynamics with Product Inhibition

Using the batch kinetic models developed above and substituting μ and q in equation (3.2) with each of their product inhibition expressions, the approximate representation of the fermentation process was described by equation (3.2.1) (Linear product inhibition), equation (3.2.2) (sudden growth stop product inhibition and equation (3.2.3) for exponential product inhibition, presented in the following section.

$$\left. \begin{aligned} \frac{dX}{dt} &= \left(1 - \frac{\mu_{max} S}{K_{ix} P + S}\right) X \\ \frac{dP}{dt} &= q X \\ \frac{dS}{dt} &= -\frac{1}{Y_x} \frac{dX}{dt} - \frac{1}{Y_p} \frac{dP}{dt} - G_s X - M_s X \end{aligned} \right\} (3.2.1)$$

$$\left. \begin{aligned} \frac{dX}{dt} &= \left(1 - \frac{P}{P_{max}}\right) \frac{\mu_{max}S}{K_{sx} + S} X \\ \frac{dP}{dt} &= \left(1 - \frac{P}{P_{pmax}} - \frac{q_{max}S}{K_{sp} + S}\right) X \end{aligned} \right\} (3.2.2) \frac{dt}$$

$$\frac{dS}{dt} = -\frac{1}{Y_x} \frac{dX}{dt} - \frac{1}{Y_p} \frac{dP}{dt} - G_s X - M_s X$$

$$\left. \begin{aligned} \frac{dX}{dt} &= \exp(-K_{ix}P) \frac{\mu_{max}S}{K_{sx} + S} X \\ \frac{dP}{dt} &= \exp(-K_{ip}P) \frac{q_{max}S}{K_{sp} + S} X \end{aligned} \right\} (3.2.3)$$

$$\frac{dS}{dt} = -\frac{1}{Y_x} \frac{dX}{dt} - \frac{1}{Y_p} \frac{dP}{dt} - G_s X - M_s X$$

3.5.2 Systems Dynamics with Substrate and Product Inhibition

Using the batch kinetic models developed above and substituting μ and q in equation (3.2) with each of their kinetic expressions that take into consideration substrate and product inhibition, the approximate representation of the fermentation process was described by (a) equation (3.2.4) (Linear Substrate-Linear Product inhibition), (b) equation 3.2.5 (Linear Substrate Exponential Product inhibition) (c) equation 3.2.6 (Exponential substrate linear product inhibition and (d) equation 3.2.7 (Exponential Substrate Exponential Product inhibition as presented in the following section.

$$\left. \begin{aligned} \frac{dX}{dt} &= (1 - K_{ix}P)(1 - K_{isx}S) \frac{\mu_{max}S}{K_{sx}+S} X \\ \frac{dP}{dt} &= (1 - K_{ip}P)(1 - K_{isp}S) \frac{q_{max}S}{K_{sp} + S} X \\ \frac{dS}{dt} &= -\frac{1}{Y_x} \frac{dX}{dt} - \frac{1}{Y_p} \frac{dP}{dt} - G_s X - M_s X \end{aligned} \right\} (3.2.4)$$

$$\left. \begin{aligned} \frac{dX}{dt} &= (1 - K_{isx}S) \exp(-K_{ix}P) \frac{\mu_{max}S}{K_{sx}+S} X \\ \frac{dP}{dt} &= (1 - K_{ip}P) \exp(-K_{isp}S) \frac{q_{max}S}{K_{sp} + S} X \end{aligned} \right\} (3.2.5)$$

$$\left. \begin{aligned} \frac{dX}{dt} &= (1 - K_{isx}S) \exp(-K_{ix}P) \frac{\mu_{max}S}{K_{sx}+S} X \\ \frac{dP}{dt} &= (1 - K_{ip}P) \exp(-K_{isp}S) \frac{q_{max}S}{K_{sp} + S} X \end{aligned} \right\} (3.2.6)$$

$$\frac{dP}{dt} = (1 - K_{ip}P) \exp(-K_{isp}S)$$

$$\frac{dX}{dt} = (1 - K_{ix}P) \exp(-K_{isx}S) \mu$$

$$\frac{dP}{dt} = (1 - K_{ip}P) \exp(-K_{isp}S)$$

$$\frac{dS}{dt} = -\frac{1}{Y_x} \frac{dX}{dt} - \frac{1}{Y_p} \frac{dP}{dt} - G_s X - M_s X$$

$$\frac{dX}{dt} = \exp(-K_{ix}P) \frac{\mu_{max}S}{K_{sx}+S} \exp(-K_{isx}S)X$$

$$\frac{dX}{dt} = \frac{q_{max}S}{S \exp(-K_{isp}S)X} \quad (3.2.7)$$

$$\frac{dS}{dt} = -\frac{1}{Y_x} \frac{dX}{dt} - \frac{1}{Y_p} \frac{dP}{dt} - G_s X - M_s X$$

3.6 Parameter Estimation and Model Statistical Validity

The identification of model parameters for the different systems of equations was determined with Matlab and the *ode45* solver used to simulate the differential equations. This was done by minimizing the overall sum of squared error (equation (11)) between the model simulation and experimental data points of the process variables (biomass, substrate and product).

$$\varepsilon = \min \sum (X(k_1, k_2, \dots, k_n) - X^e)^2 + (S(k_1, k_2, \dots, k_n) - S^e)^2 + (P(k_1, k_2, \dots, k_n) - P^e)^2 \quad (11)$$

For that purpose, the Matlab routine “fmincon” was applied. Here, $k_i, i = 1 \div n$ was vector of model parameters to be determined as output of minimization procedure. A Matlab code was written which imports the experimental data from Microsoft Excel, simulates the differential equations, calculates and minimizes the total error, displays the parameter values and plots the model and experimental values. Once the model parameters were estimated, the capability of the mathematical model to describe the ethanol fermentation process was tested statistically using the F-tests and this was done

using STATA software at a confidence interval of 99% to determine the confidence level for the developed mathematical model.

KNUST



CHAPTER FOUR RESULTS AND DISCUSSIONS: MODEL SIMULATION AND PARAMETER ESTIMATION

4.1 Overview of Chapter

This chapter presents the results from the kinetic modeling, parameter estimation and dynamic simulation for the three substrates considered for the fermentation (sorghum, maize and cassava). The results for model statistical validity using F-test variance comparison test for the model and experimental data are also presented. Simulations showing the variation of substrate and product concentration in the fermenter as the cells grow are also presented for the three different substrates used. Finally, 3D profiles revealing more in-depth mechanism of the fermentation process are presented. The chapter is divided into four main sections: the first presents the results for sorghum extracts, second for maize extracts, the third for cassava extracts and a conclusion on the results.

4.2 Alcohol Fermentation with Sorghum Extracts

Figures 4.21 to 4.24 presents the fitting of the models with respect to the experimental data. The results led to the following conclusions: First alcoholic fermentation of sorghum extracts using *Saccharomyces cerevisiae* shows the existence of product inhibition, and the patterns of inhibition could be described as linear or exponential (models which showed lowest error). This is justified by the observation that the errors for the models showing product inhibition were all lower than that of the Monod in which case was used as the control. The results confirmed previous observations by Chen and McDonald (1990a, b) Beuse et al. (1998, 1999) and Fengwu (2007) that ethanol, whether produced by yeast cells during fermentation or externally added into

a fermentation system, can trigger inhibitions once its concentration approaches inhibitory levels. Also important in fermentation kinetics is the product yield, growth and maintenance coefficients. The linear model showed a relatively high product yield coefficient with a relatively low growth and maintenance coefficient compared to the exponential model. This suggest that even though both models showed similar accuracy in describing the fermentation dynamics, designing a control policy with the Linear model will result in more substrate being accumulated into extracellular product and lesser amount for cell growth and maintenance hence higher productivity and yield. Tables 4.22 and 4.23 present the model statistical validity using two sample F-test for variance and the results show that at 99% confidence interval, the states' prediction of the linear and exponential models showed no significant difference with the experimental data.

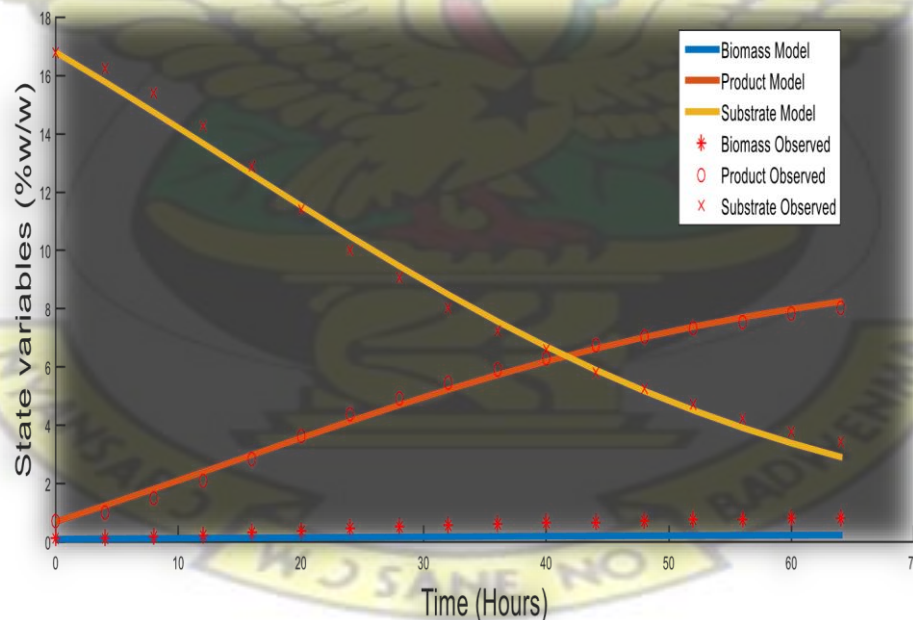


Figure 4.21: Experimental results and model fitting of no inhibition (Monodmodel)

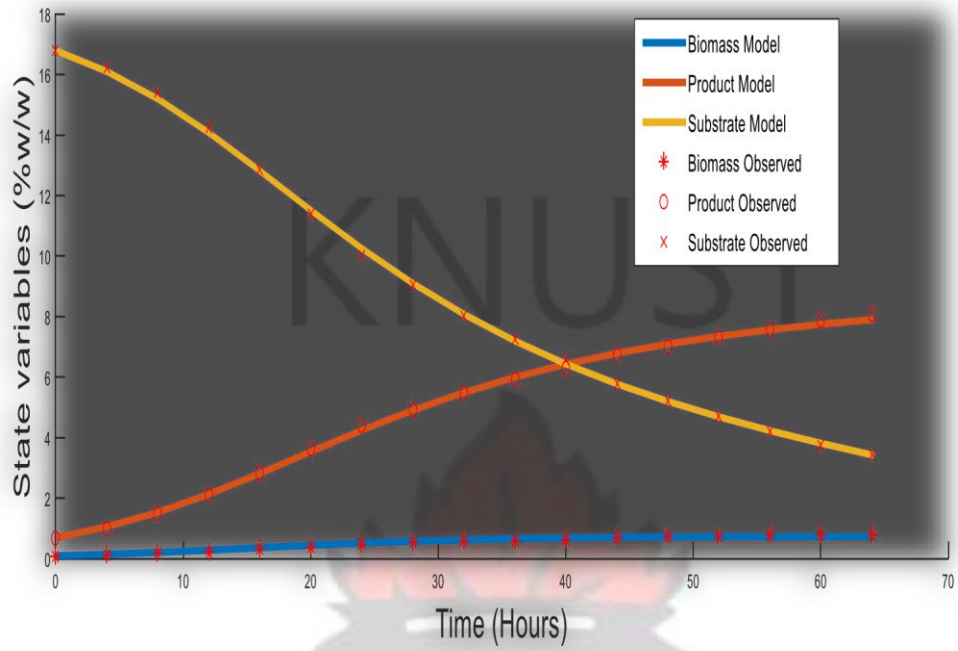


Figure 4.22: Experimental results and model fitting, case of linear inhibition model

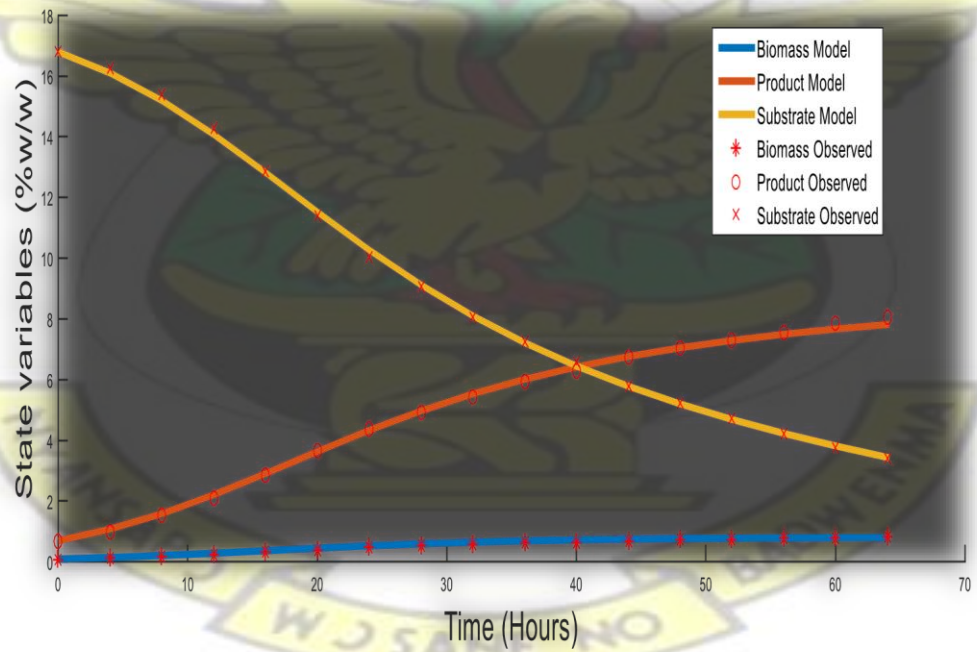


Figure 4.23: Experimental results and model fitting of Sudden Growth Stop inhibition

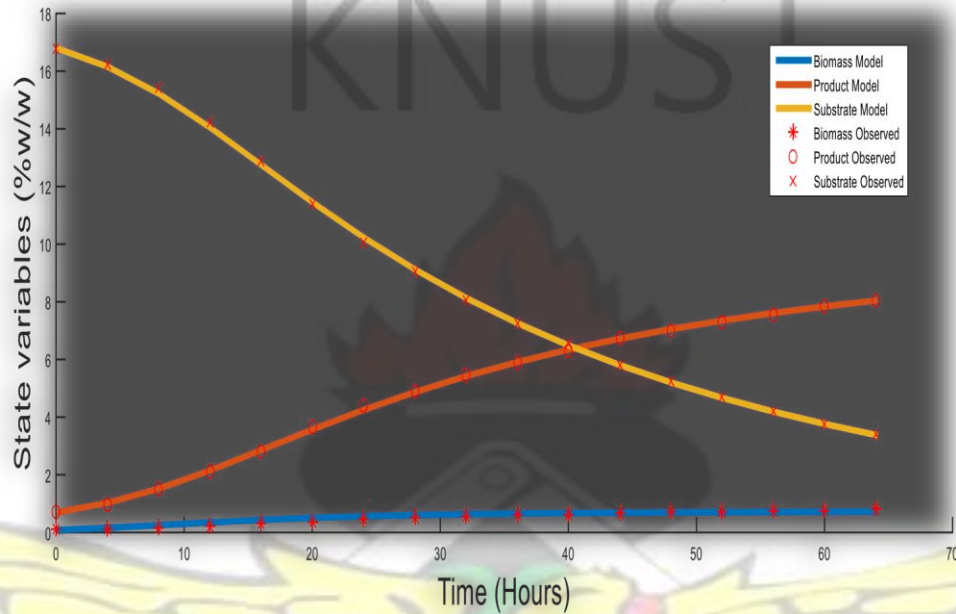


Figure 4.24: Experimental results and model fitting of Exponential inhibition model
 Table 4.21 presents the parameters for the four different models used to describe the dynamics of fermentation and

Table 4.21: Model Parameters for beer fermentation using Sorghum Extracts

		Inhibition			
		No Inhibition	Linear	SGS	Exponential
Model Parameters	μ_{max}	0.3887	0.9557	0.6582	2.2628
	q_{pmax}	17.4649	2.2101	4.7227	9.0145
	P_{xmax}	□	□	7.9885	□
	P_{pmax}	□	□	9.8916	□
	K_{ix}	□	0.1294	□	0.4210
	K_{ip}	□	0.1004	□	0.1030
	K_{sx}	249.9922	125.433	81.8551	179.2911
	K_{sp}	199.9980	29.213	74.8407	199.8710
	Y_x	0.1001	0.1086	0.1368	1.0000
	Y_p	0.6085	1.8895	1.2710	0.5936

G_s	0.0010	0.0502	0.0345	0.0010
M_s	0.0100	0.0564	0.0423	0.0100
Model Error	5.4262	0.3407	0.4054	0.3270

47

KNUST



Table 4.22: Model Statistical Validity with kinetics of linear inhibition, two sample F-test for variance (Biomass)

	Biomass		Product		Substrate	
	Experimental (Xobs)	Model (Xpred)	Experimental (Pobs)	Model (Ppred)	Experimental (Sobs)	Model (Spred)
Mean	0.508	0.533	4.903	4.893	9.126	9.107
Standard Error	0.059	0.055	0.610	0.605	1.114	1.105
Standard Deviation	0.244	0.228	2.514	2.495	4.595	4.558
Observations	17	17	17	17	17	17
Confidence Interval	0.990		0.990		0.990	
F	0.8664		0.9842		0.9840	
Pr(F < f) Two-tailed	0.7778		0.9750		0.9747	

Table 4.23: Model Statistical Validity with kinetics of Exponential inhibition, two sample F-test for variance

	Biomass		Product		Substrate	
	Experimental (Xobs)	Model (Xpred)	Experimental (Pobs)	Model (Ppred)	Experimental (Sobs)	Model (Spred)
Mean	0.508	0.549	4.903	4.903	9.126	9.105
Standard Error	0.059	0.050	0.610	0.610	1.114	1.1061
Standard Deviation	0.244	0.207	2.514	2.514	4.595	4.561
Observations	17	17	17	17	17	17
Confidence Interval	0.990		0.990		0.990	
F	0.7209		0.9994		0.9850	

Also important in a fermentation process is how the substrate and product vary in the fermenter as the cells grow. The linear and exponential inhibition models were both

used to simulate this variation. Both showed a decrease in substrate concentration and an increase in product concentration with cell growth. However, with the linear model the process reached a steady state within the time used for the simulation (seen in figure 4.25 by the curve at the edges of the plots) which was not observed in the exponential model. This confirmed the earlier assertions with the yield coefficients that using the linear model in a control policy will result in high productivity. 3D profiles using the proximal interpolant method implemented using the Matlab curve fitting tool also revealed interesting findings regarding the fermentation process. This was to observe the formation of product as cells grow and consume substrate.

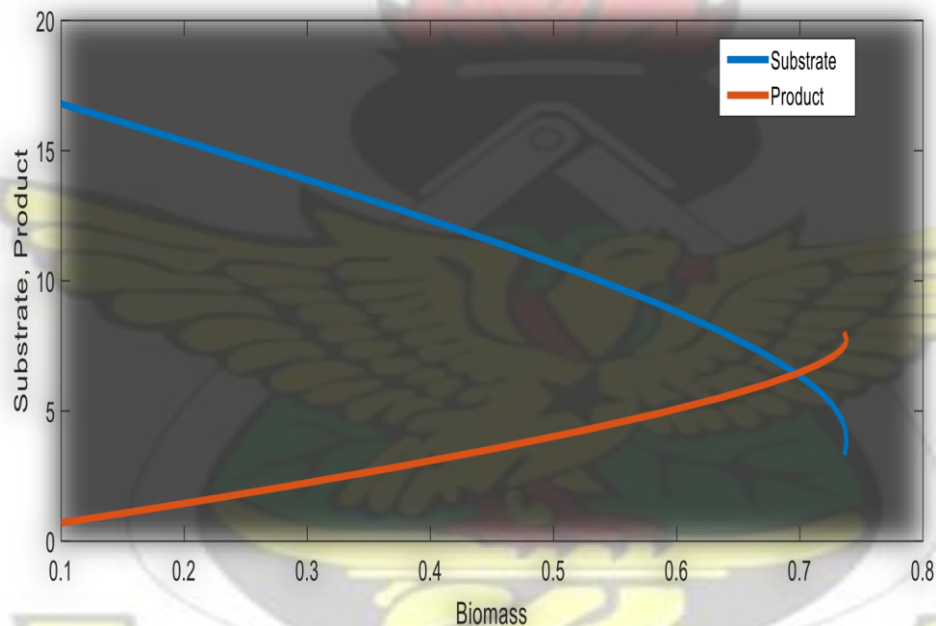


Figure 4.25: Simulation of substrate and Product variation as a function of biomass during fermentation using Linear Inhibition kinetics.

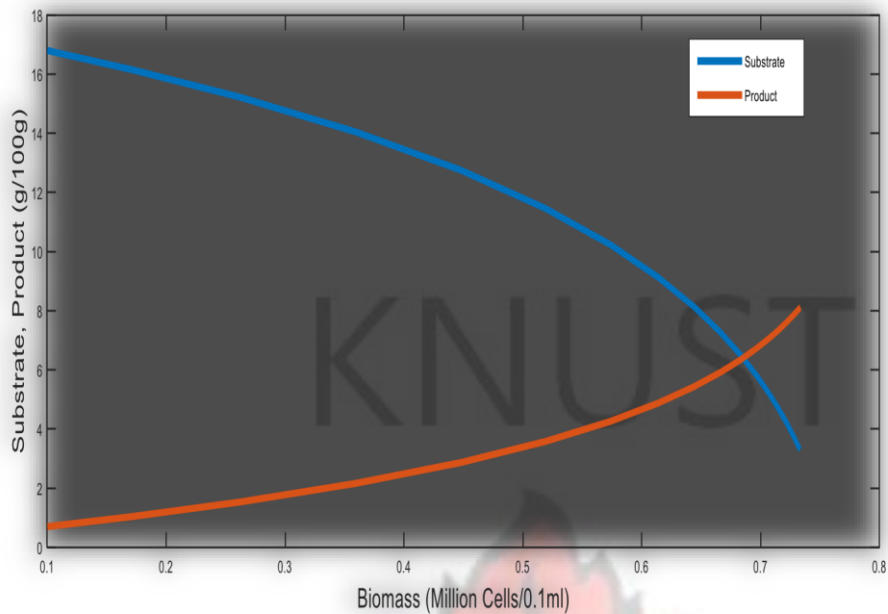


Figure 4.26: Simulation of substrate and product as a function of biomass during fermentation using Exponential Inhibition kinetics.

Figure 4.27 presents product variation with cell growth and substrate consumption using the linear model and figure 4.28 using the exponential model. It can be found that with the linear model, as ethanol accumulated in the fermenter up to a certain concentration, non-linearities, described as instabilities were observed in the product profile. This can be attributed to the higher product yield coefficient of the linear model compared to the exponential model which resulted in ethanol accumulating faster in the fermenter and rapidly reaching inhibitory levels, resulting in transient instabilities in the fermenter showed by the non-linearity (Ingledew, 1999; Fengwu, 2007). This high ethanol concentration is inhibitory to the yeast cell by disrupting the integrity of the cell membrane (Russell, 2003; Sutton, 2011)

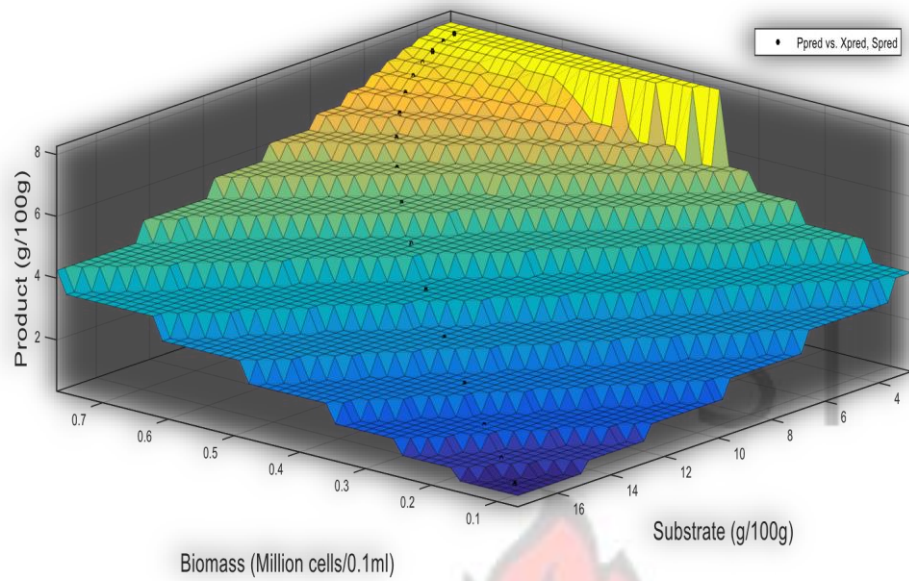


Figure 4.27 3D proximal interpolant simulation of product variation as a function of substrate and biomass using linear Inhibition Kinetic Model

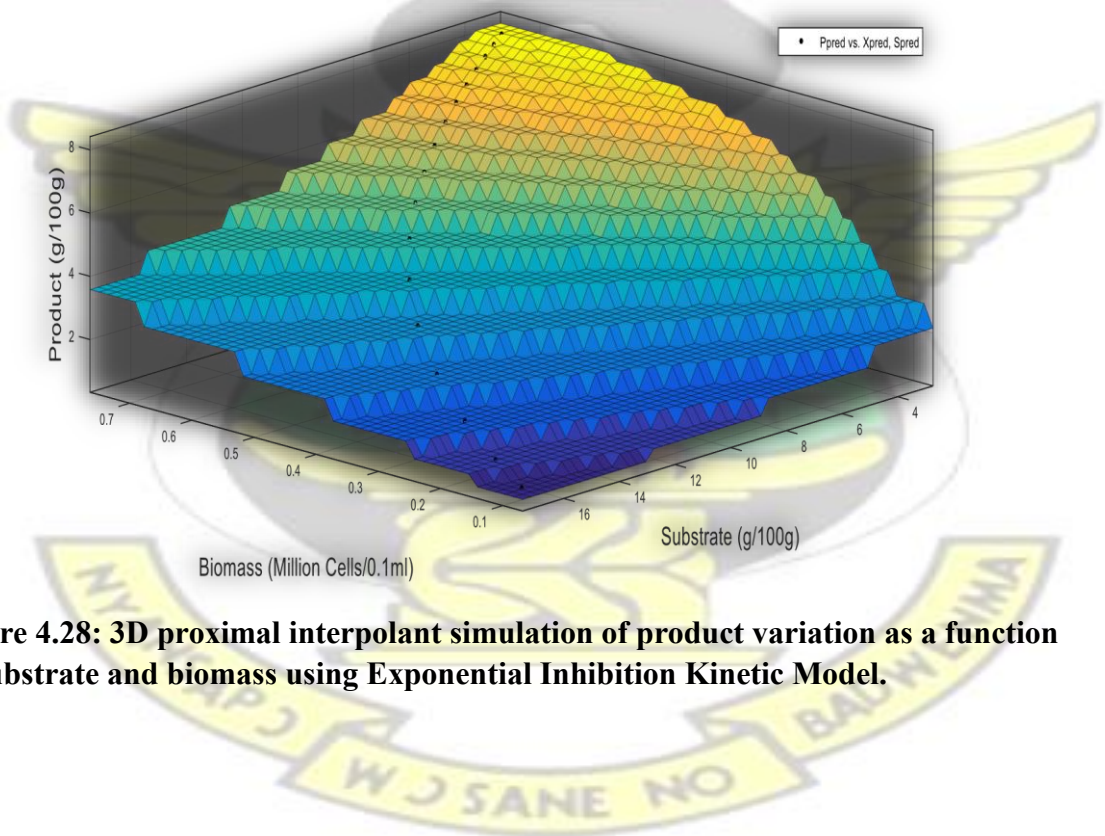


Figure 4.28: 3D proximal interpolant simulation of product variation as a function of substrate and biomass using Exponential Inhibition Kinetic Model.

4.3 Alcohol Fermentation with Maize Extracts

Alcohol fermentation with maize extracts also showed the existence ethanol inhibition but in this case the patterns of inhibition could be described as linear decrease on the inhibitory ethanol concentration or sudden growth ceasure at inhibitory concentration.

Table 4.31 presents the parameters for the four different models used to describe the dynamics of fermentation and Figures 4.31 to 4.34 presents the fitting of the models with respect to the experimental data. Even though the linear and sudden growth stop models described the dynamics of ethanol inhibition, the sudden growth stop model showed a very high maximal rate of ethanol accumulation compared to the exponential model. This suggests that designing a control policy with this model will result in high process productivity. Tables 4.32 and 4.33 present the model statistical validity using two sample F-test for variance and the results show that at a 99% confidence interval, the states' prediction of the linear and exponential models showed no significant difference with the experimental data.

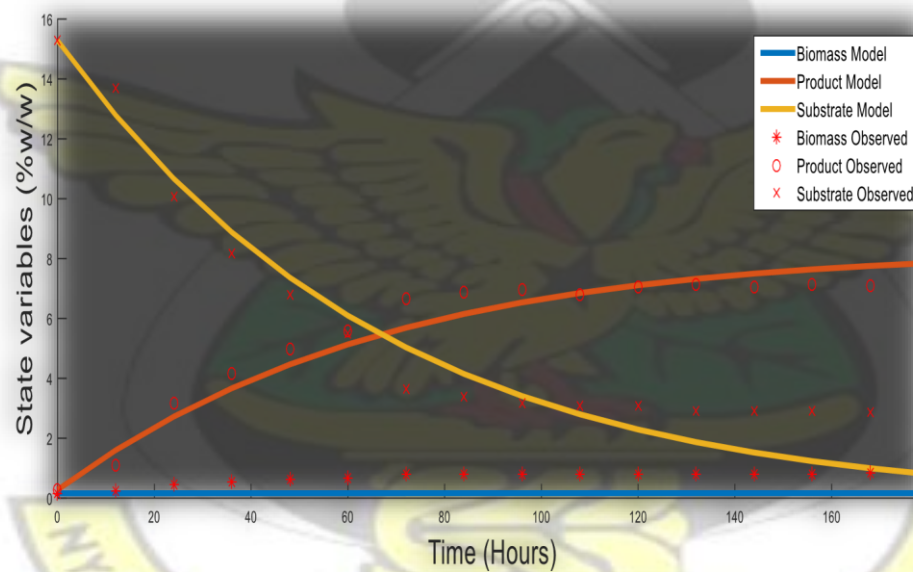


Figure 4.31: Experimental results and model fitting of no inhibition (Monodmodel).

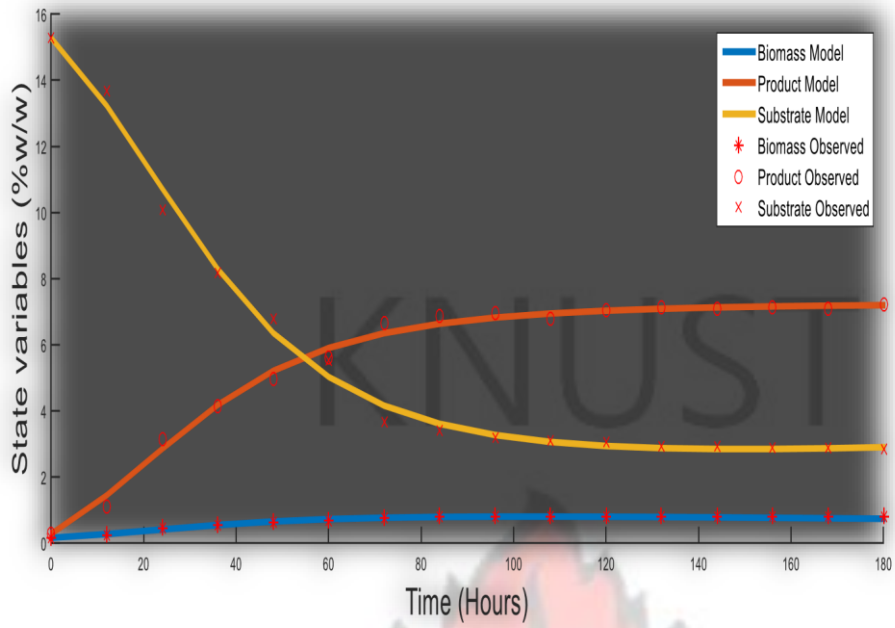


Figure4.32: Experimental results and model fitting of linear inhibition model.

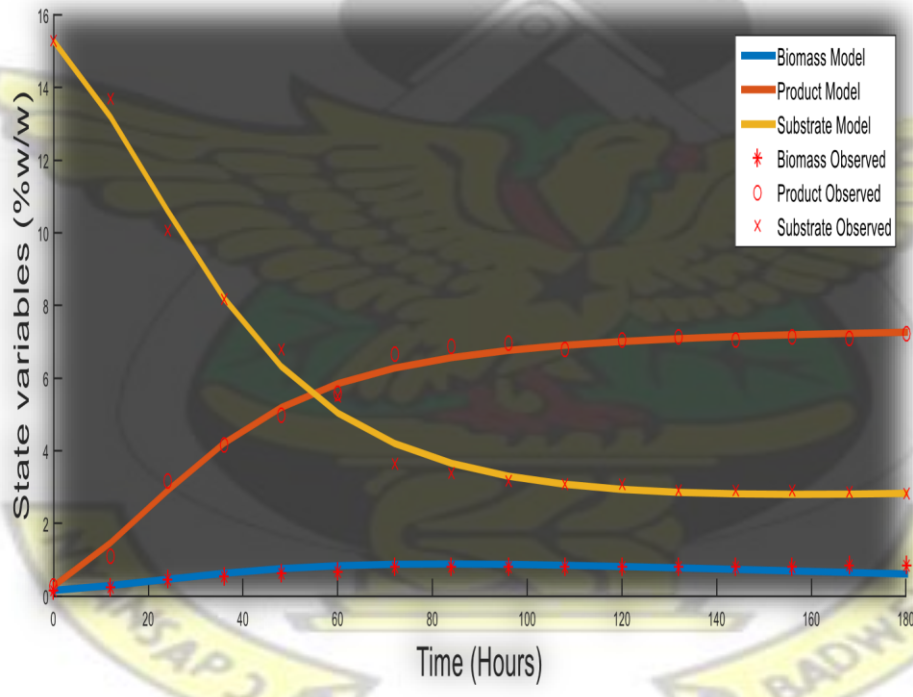


Figure 4.33: Experimental results and model fitting of Sudden Growth Stop inhibition model.

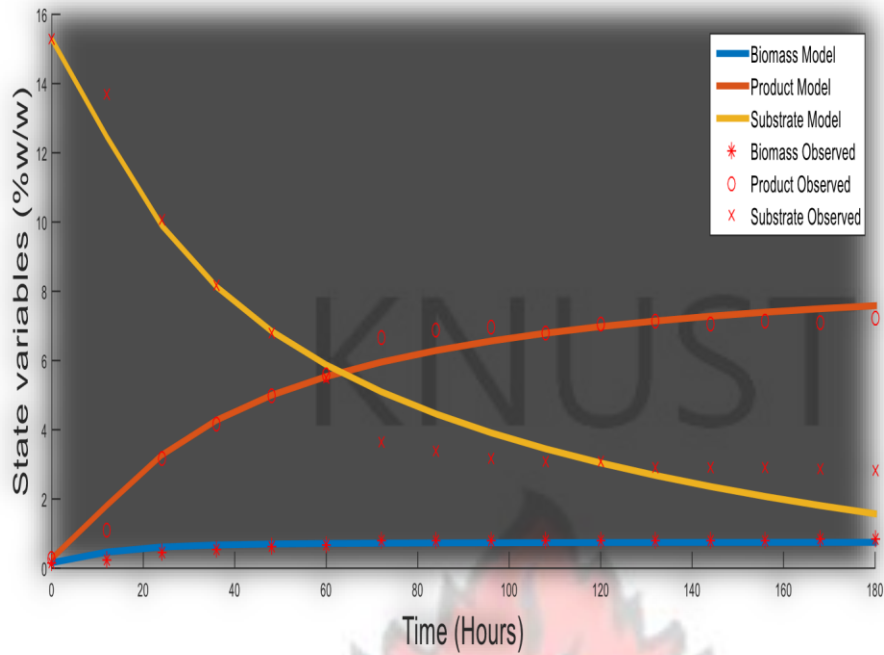


Figure 4.34: Experimental results and model fitting of Exponential Inhibition Model.

Table 4.31: Model Parameters for beer fermentation using Maize Extracts

		Inhibition			
		No Inhibition	Linear	SGS	Exponential
Model Parameters	μ_{max}	0.0100	0.0567	0.0630	2.9922
	q_{pmax}	10.4778	0.7784	0.9338	8.2438
	P_{xmax}	□	□	6.7249	□
	P_{pmax}	□	□	7.3560	□
	K_{ix}	□	0.1459	□	0.7179
	K_{ip}	□	0.1375	□	0.2631
	K_{sx}	250.000	1.2621	1.9085	231.9805
	K_{sp}	200.00	7.1081	11.7803	199.9890
	Y_x	0.1000	0.1084	0.1108	1.0000
	Y_p	0.5370	1.2548	1.3938	0.6210
	G_s	0.0010	0.0018	0.0051	0.0010
M_s	0.010	0.0108	0.0141	0.0100	
Model Error	27.9231	2.0381	2.0941	11.340	

Another important finding that was observed was with the variation of substrate and product concentration in the in the fermenter as the cells grow. The linear and sudden

growth stop models inhibition models were both used to simulate this variation and both showed a decrease in substrate concentration and an increase in product concentration with cell growth. What was intriguing is the curve-like behavior that was observed at the end of the profiles as shown in Figures 4.35 and 4.36. There are two theories to explain this behavior: ethanol inhibition and stationary/decline phases in batch growth kinetics. In the case of ethanol inhibition, accumulated ethanol to inhibitory levels leading to disruption of the cell membrane and the corresponding non-linearity in the substrate consumption and product formation profiles (Chen and McDonald, 1990a,b; Beuse et al., 1998, 1999; Fengwu, 2007; Sutton, 2011). The more intense curvature observed with the sudden growth model is due to its relatively high maximal rate of product formation, hence rapidly accumulated ethanol to inhibitory concentration. Regarding the stationary and decline phase theory in batch growth kinetics, the curve-like behavior observed in the linear model can be attributed to the fact the cells grow and get to the stationary and decline phases, and no longer consume substrate and produce ethanol as in the exponential phase, resulting in the observed non-linearity. These theories are further confirmed in Figures 4.37 and 4.38 which respectively simulated cell growth and product formation throughout the duration of the fermentation. It can be observed that cells in the fermenter start declining after a certain time of fermentation which confirms the attainment of ethanol inhibition and disruption of cell membrane leading to cell death. The nonlinear patterns observed at the start of the fermentation can be attributed to high sugar concentrations encountered immediately after hydrolysis which exert osmotic stress on yeast leading to non-linearity in their pattern of growth and product formation (Russell, 2003; Sutton, 2011).

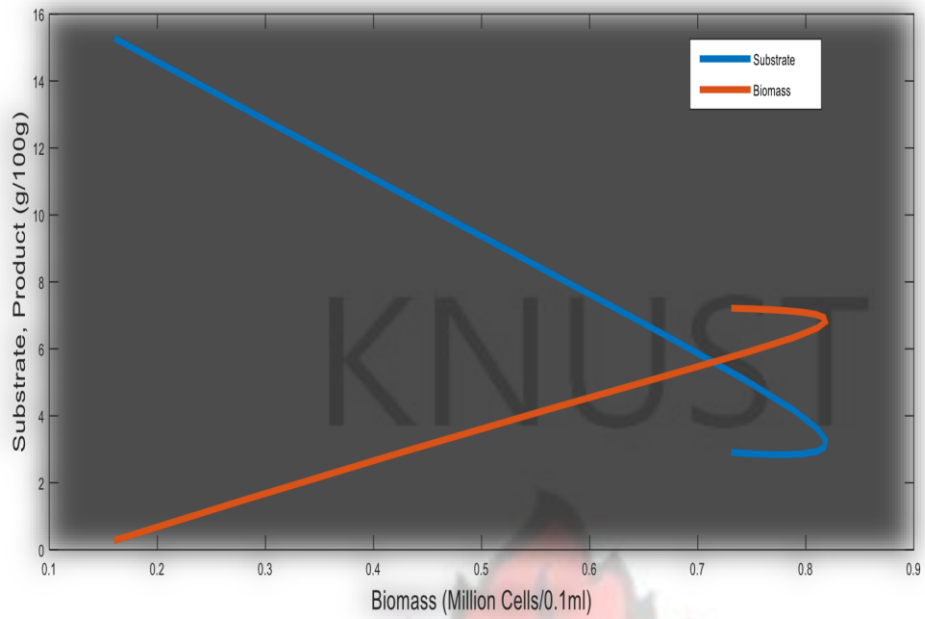


Figure 4.35: Simulation of substrate and Product variation as a function of biomass during fermentation of maize extracts using Linear Inhibition kinetic model.

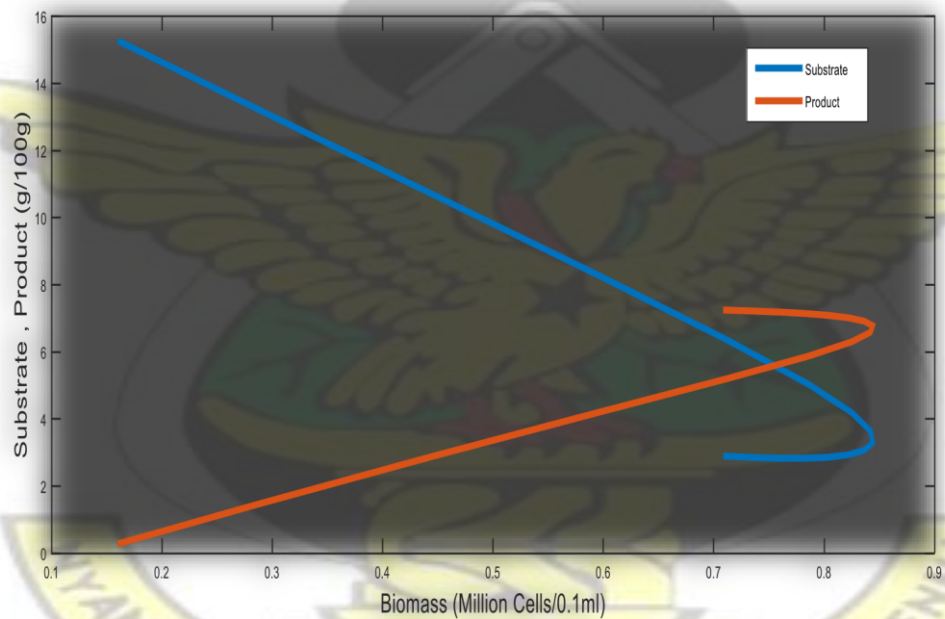


Figure 4.36: Simulation of substrate and Product as a function biomass during fermentation, using Sudden Growth Stop Inhibition kinetic.

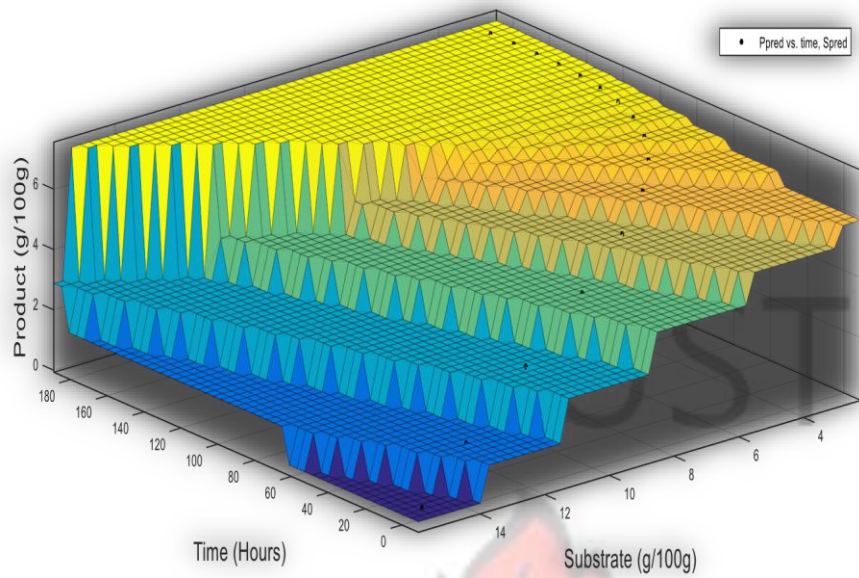


Figure 4.37 3D proximal interpolant simulation of product dynamics during fermentation using linear inhibition kinetic Model. -

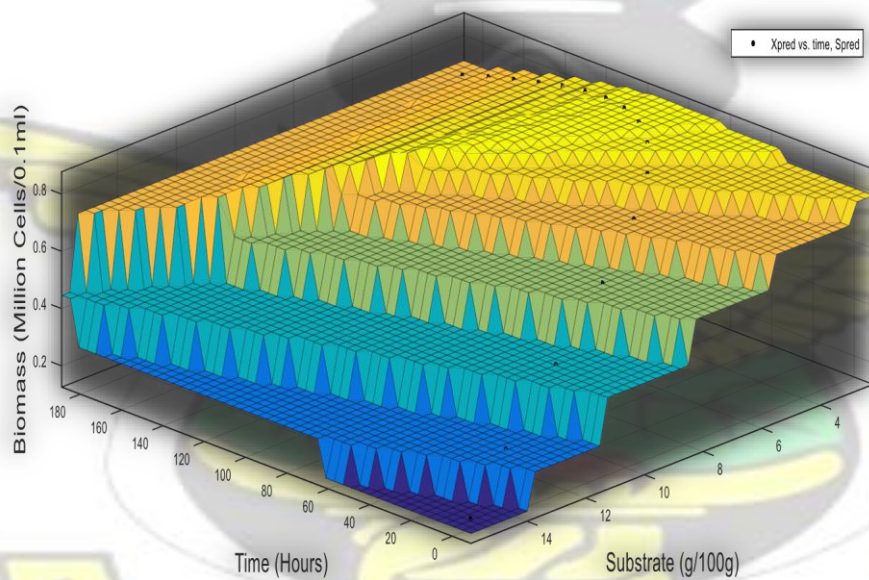


Figure 4.38: 3D proximal interpolant simulation of biomass variation during fermentation using Sudden Growth Stop inhibition kinetic Model.

4.4 Alcohol Fermentation with Cassava Extracts

4.4.1 Product Inhibition

The fermentation of cassava extracts also showed the existence of product inhibition, described as linear or exponential decrease in product concentration (models which showed lowest error). However, unlike maize (minimum model error of **2.0381**) and sorghum (minimum model error of **0.3270**), cassava fermentation had a minimum model error of **4.8107**. This was suggested to be due to the presence of substrate inhibition as explained by the presence of hydrogen cyanide in the cassava which is toxic to the growth of microorganisms. This resulted in low model fit since the modeling of substrate toxicity was not yet considered and hence the model did not represent the reality in the fermenter, substrate and product inhibition. Figures 4.41 to 4.44 presents the fitting of the models with respect to the experimental data.

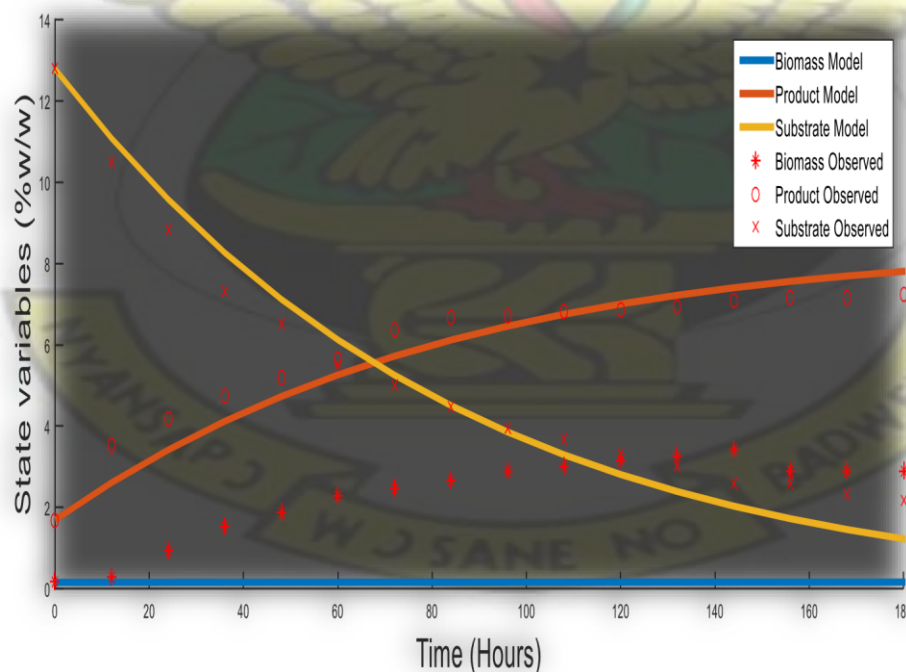


Figure 4.41: Experimental results and model fitting, case of no inhibition (Monod-Model).

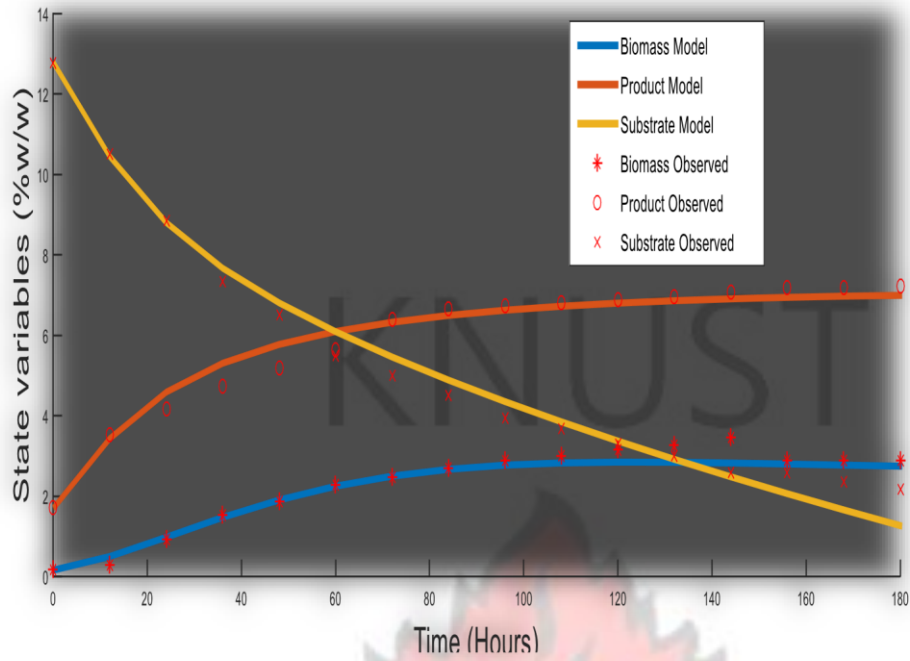


Figure 4.42: Experimental results and model fitting, case of linear inhibition model

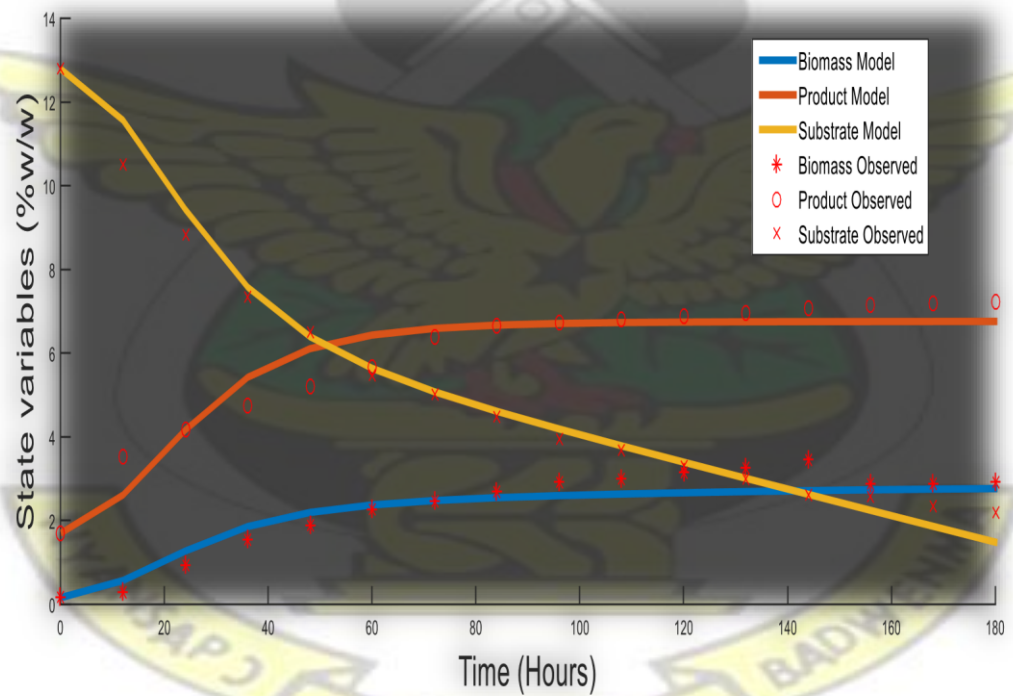


Figure 4.43: Experimental results and model fitting, case of Sudden Growth Stop inhibition model.

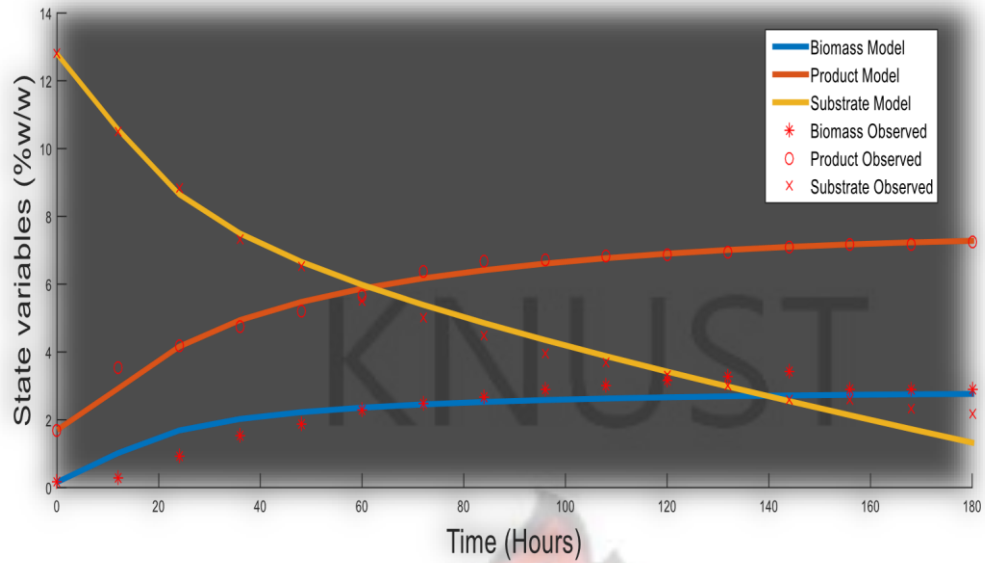


Figure 4.4 4: Experimental results and model fitting, case of Exponential inhibition model

Table 4.41 presents the parameters for the four different models used to describe the dynamics of fermentation in the case where only product inhibition was considered

Table 4.41: Model Parameters for beer fermentation using Cassava Extracts, case of product inhibition

		Inhibition			
		No Inhibition	Linear	SGS	Exponential
Model Parameters	μ_{max}	0.0100	0.3326	2.9996	4.9991
	q_{pmax}	8.4851	51.3560	5.8755	2.6067
	P_{xmax}	□	□	6.8884	□
	P_{pmax}	□	□	6.7637	□
	K_{ix}	□	0.1466	□	0.8290
	K_{ip}	□	0.1013	□	0.6347
	K_{sx}	249.9991	13.5297	231.0673	52.4603
	K_{sp}	199.9997	249.9655	199.9957	25.2593
	Y_x	0.1002	19.9983	1.0000	0.4297
	Y_p	0.5464	0.7589	1.1878	6.9998
	G_s	0.0010	0.0010	0.0010	0.0010
	M_s	0.0100	0.0100	0.0100	0.0100
Model Error		94.0344	4.8107	7.8655	5.5755

4.4.2 Substrate and Product Inhibition

Table 4.42 presents the parameters for the four different models used to describe the dynamics of fermentation and Figures 4.45 to 4.48 present the fitting of the models with respect to the experimental data. The results led to the following findings: first, there exist both substrate and product inhibition in the alcoholic fermentation of cassava extracts, with the LS-EP and ES-EP models, describing the inhibition dynamics with relatively high accuracy (having lower model errors); secondly, the results confirmed my previous observations that modeling only product inhibition did not describe with high accuracy the alcoholic fermentation of cassava extracts suggesting the presence of substrate inhibition. The dynamics described by conventional Monod equation (case of no inhibition) showed a very high error confirming the presence of inhibitions. Also important in fermentation kinetics is the specific rate of ethanol accumulation in the medium. The parameter estimation results indicated high maximal rate of product formation, $183.4561 h^{-1}$ with the ES-EP model compared to $7.1381 h^{-1}$ for LS-EP model. This suggests that even though both models showed similar accuracy in describing the fermentation dynamics, to design a control policy with the ES-EP model will result in a high process productivity in terms of ethanol accumulation. It highlights that the product inhibition had a higher effect on the fermentation process than substrate inhibition, as shown by the product inhibition coefficients being very high compared to those for substrate inhibition. This is explained by the fact that most of the cyanide in the cassava which could have resulted in substrate toxicity was removed during upstream process which resulted in smaller amounts left in the fermentation wort.

Table 4.42: Model Parameters for beer fermentation using Cassava Extracts, case of substrate and product inhibition

Inhibition

		Monod (No Inhibition)	Linear S Linear P	Linear S Exponential P	Exponential S Linear P	Exponential S Exponential P
Model Parameters	μ_{max}	0.0100	0.0100	3.0000	2.4342	2.9996
	q_{pmax}	8.4851	14.5352	7.1381	7.1395	183.4561
	K_{isx}	□	0.3131	0.0001	0.0001	0.0001
	K_{isp}	□	0.0010	0.0021	0.0010	0.2002
	K_{ix}	□	0.9539	0.5411	0.1264	0.5453
	K_{ip}	□	0.1475	0.8968	0.1450	1.2437
	K_{sx}	249.9991	1.0090	67.607	249.9969	66.2282
	K_{sp}	199.9997	198.8989	9.5495	199.9999	11.9572
	Y_x	0.1002	2.9782	3.0000	3.0000	2.9999
	Y_p	0.5464	0.6497	0.6131	0.6389	0.6131
	G_s	0.0010	0.0017	0.0001	0.0011	0.0001
	M_s	0.0100	0.0017	0.0001	0.0011	0.0001
Model Error		94.0344	7.3934	2.8012	7.5115	2.7975

The high product inhibition is in accordance to the work of Ingledew (1999) who showed substrate and product to be among the environmental stresses to *S. cerevisiae* during alcoholic fermentation Table 4.43 and 4.44 presents the model statistical validity using two sample F-test for variance and the results show that at a 99% confidence interval, the states' prediction of the LS-EP and the ES-EP models showed no significant difference with the experimental data.

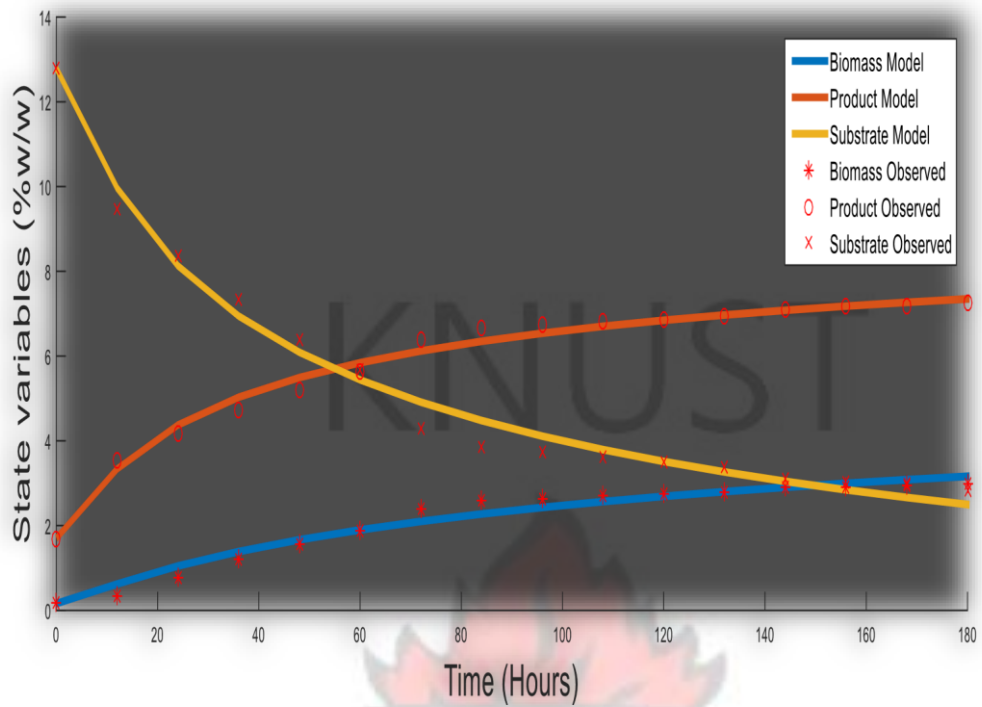


Figure 4.45: Experimental results and model fitting (LS-EP model).

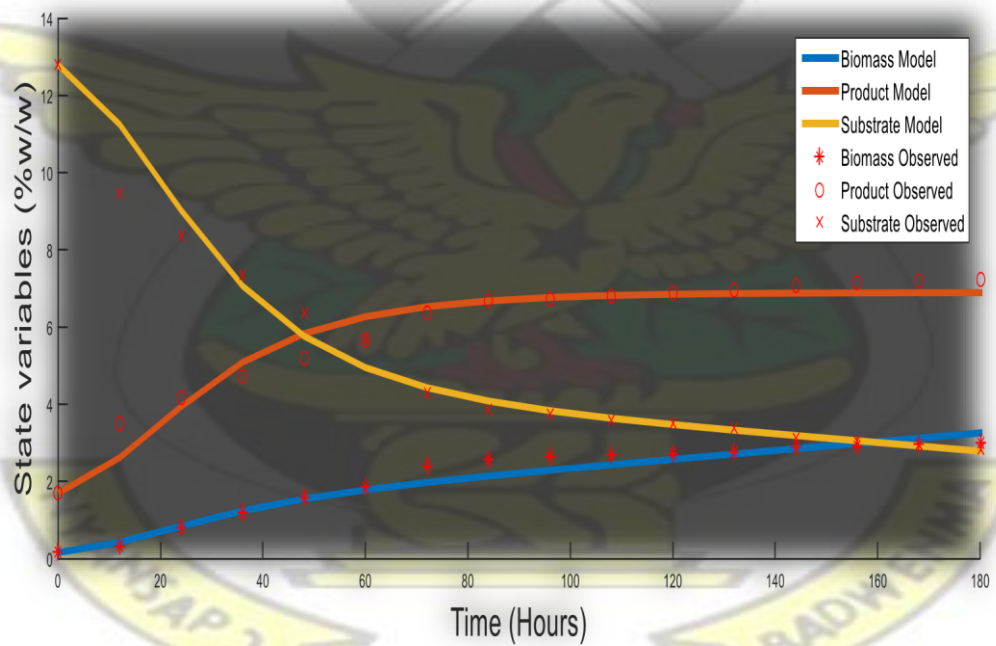


Figure 4.47: Experimental results and model fitting (ES-LP).

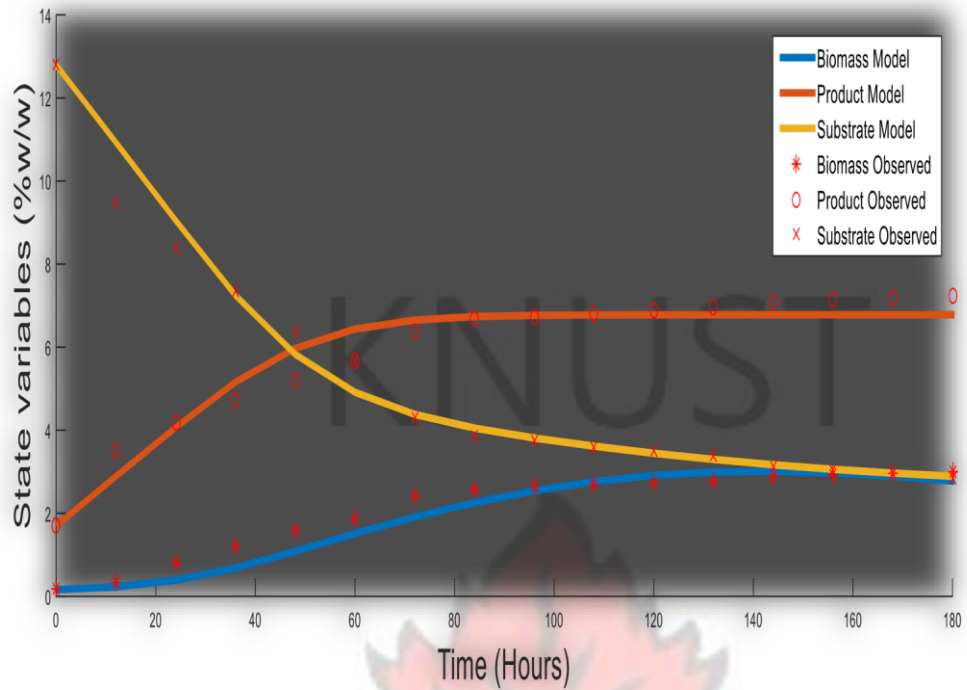


Figure 4.46: Experimental results and model fitting (LS-LP model).

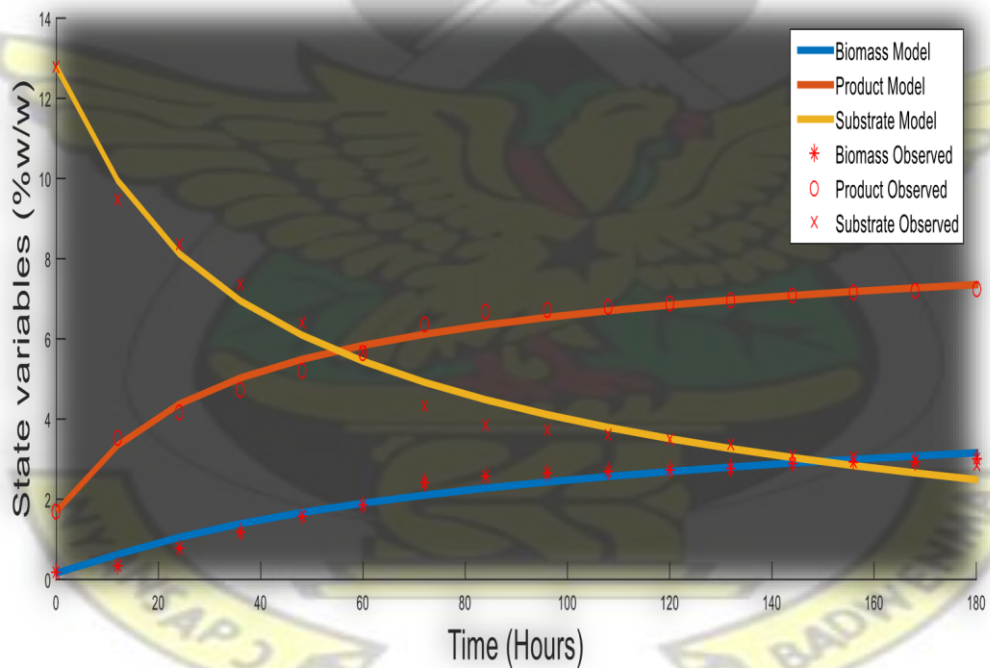


Figure 4.48: Experimental results and model fitting (ES-EP model).

3D profiles using the proximal interpolant method, implemented using the Matlab curve fitting tool showed interesting findings. Figure 4.49 shows the dynamics of product interpolated with substrate and time. It can be found that early in the fermentation

process there exist steps in the product profile which decreases in intensity as substrate concentration decreases in the reactor. This observed behavior can be attributed to high sugar concentrations encountered immediately after hydrolysis which exert osmotic stress on yeast cells resulting in transient instabilities in the bioreactor (Russell, 2003; Fengwu, 2007; Sutton, 2011). This behavior decreases in magnitude as the sugar concentration decreases up to a point where the systems achieves a stable steady state and the rate of product formation becomes constant. Figure 4.5 shows product, against biomass and substrate.

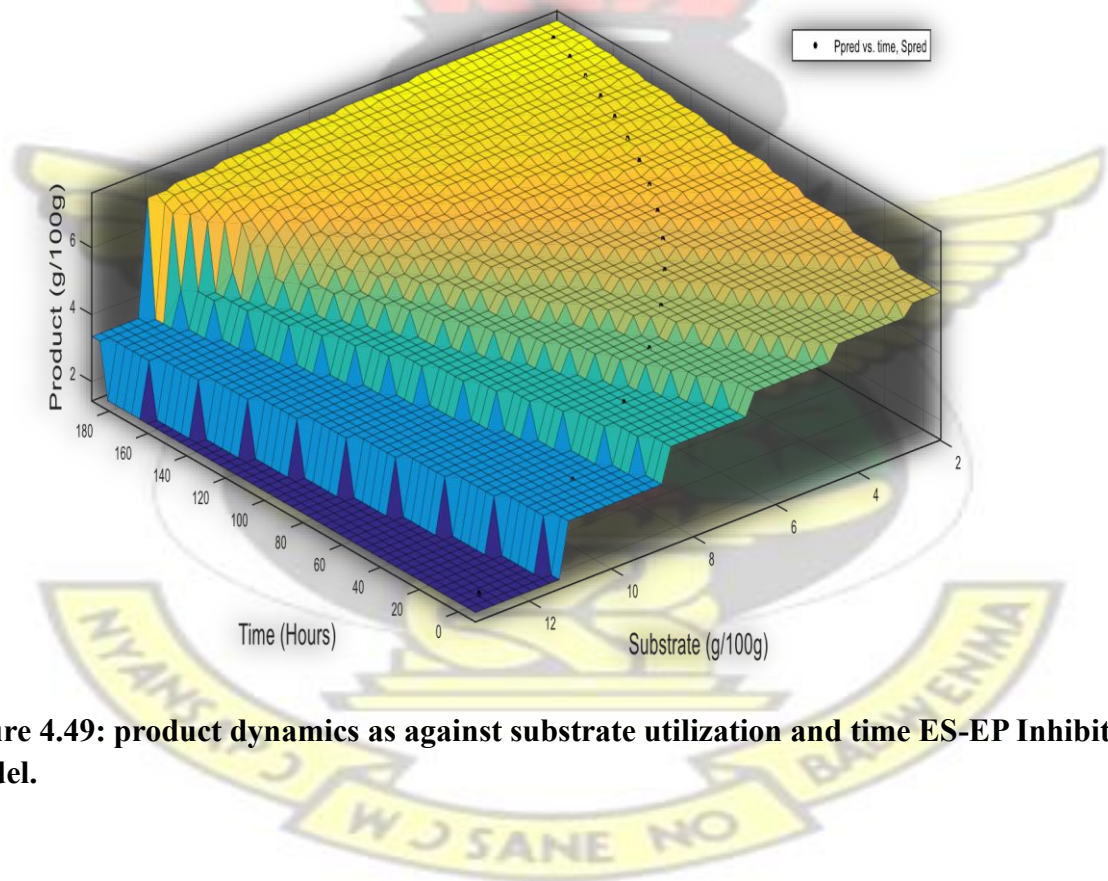


Figure 4.49: product dynamics as against substrate utilization and time ES-EP Inhibition Model.

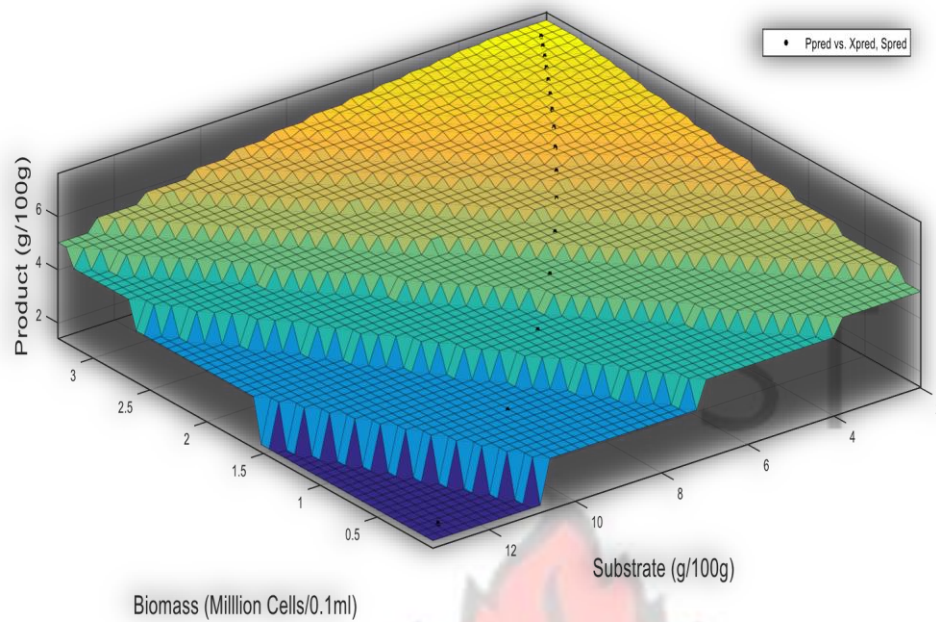


Figure 4.5: Dynamics of product formation as against substrate utilization and cell growth (ES-EP Inhibition Model)

4.5 Conclusion

A mathematical approach to study the kinetics of substrate and product Inhibition during alcoholic fermentation with three different substrates has been presented. Substrates considered were sorghum, maize and cassava and the results show that there exist both ethanol inhibition in the alcoholic fermentation of sorghum and maize extracts while cassava extracts show both ethanol and substrate inhibition. At a 99% confidence interval the pattern of these inhibitions can be described as a linear or an exponential decrease on ethanol concentration in the case of sorghum, linear and sudden growth stop in the case of maize, linear substrate exponential product, and exponential substrate exponential product in the case of cassava.

CHAPTER FIVE OPTIMAL CONTROL PROBLEM FORMULATION AND SOLUTION TECHNIQUE

5.1 Introduction and Overview

The transfer of laboratory scale experiments to production scale fermentation is becoming more time consuming, involving expensive prototype systems and complex experimental design to determine the optimal industrial scale operating conditions (Alford, 2006). This makes it very important to propose a systematic approach to effectively tackle these difficulties and achieve optimized design efficiently with minimal cost and time. Under this scope, several optimization strategies can be delineated, depending on the defined purposes. The process engineer point of view aims at optimizing the fermentation process by exploiting the maximum capabilities of an already selected microorganism and by manipulating environmental and operational variables, therefore using potentially similar tools, but with a different perspective when compared with optimization strategies that envisage the design of improved strains (Koutinas, 2012). This chapter includes the description of a batch alcohol fermentation process that has been optimized using a technique based on the application of mathematical modeling and optimal control. Calculus of variation is introduced as a valuable tool to derive and solve the necessary conditions for optimality and the obtained results show the optimal temperature and pH profiles for the fermentation of sorghum extracts. A Simulink model of the fermentation process shows that using the proposed control strategy increases ethanol yield by 14.18%, cell growth by 71.96% decreases the residual substrate by 84.77%

5.2 Objectives of the Optimal Control Strategy

The objective of the optimal control, which is to operate the fermenter in order to obtain maximum ethanol in the most economical way, is divided into two stages:

- a) **First Stage Control:** Determine the temperature and pH trajectories that maximizes cell growth and ethanol production.

- b) **Second Stage Control:** Design a Fermenter model using Simulink to confirm the optimal temperature and pH profiles

5.3 Control Assumptions and Approximations

- a) The maintenance and growth coefficient are temperature independent and hence will not be considered in the model
- b) Product formation and substrate utilization are directly linked to the cell specific growth rate
- c) Since the objective is to find a balance between two major controls, temperature and pH on the effect of the controls will be modelled only on the maximum specific growth rate.

5.4 Modeling Temperature and pH dependence

The temperature dependency of the cellular activity was modelled using the Arrheniuslike equation, equations (5.4a) and (5.4b).

$$\mu = f \left\{ \left[\mu_{max} \exp \left(-\frac{E_g}{RT} \right) \right] \right\} \quad (5.4a)$$

$$k_d = f \left\{ \left[k_d \exp \left(-\frac{E_g}{RT} \right) \right] \right\} \quad (5.4b)$$

Typical values for these parameters were taken from the literature (Shuler and Kargi, 2002).

A typical term, equation (5.41) that accounts for pH dependence was also introduced into the specific growth rate expression. Although this simple model cannot possibly explain pH dependence, literature shows that it gives an adequate fit for many microorganisms (Nielsen and Villadsen, 1994). The additional term is in the form:

$$\mu = f \left(\frac{\mu_{max}}{1 + \frac{k_1}{10^{-pH}} + \frac{10^{-pH}}{k_2}} \right) \quad (5.41)$$

The values of k_1 and k_2 that were used for the numerical simulations were chosen to be in their typical ranges from literature (Nielsen and Villadsen, 1994; Shuler & Kargi, 2002).

5.5 Modeling the Effect of Controls on State Equations

In order to minimize the effect of substrate and/or product inhibition during fermentation and correspondingly maximizes ethanol yield, the dynamic models that were developed in Chapter Three will now be used to control the process optimally. To introduce the effect of temperature and pH into equations, equation (5.51) (dynamics with linear product inhibition), equation (5.52) (dynamics with sudden growth stop product inhibition), equation (5.53) dynamics with exponential product inhibition, equation (5.54) (dynamics with linear substrate exponential product inhibition), equation (5.55) (dynamics with exponential substrate exponential product inhibition) were derived

$$\frac{dX}{dt} = \left(\frac{\mu_{max}(1-K_{ix}P)k_g \exp\left(-\frac{E_g}{RT}\right)}{1 + \frac{k_1}{10^{-pH}} + \frac{10^{-pH}}{k_2}} \right) \frac{S}{K_{sx} + S} X$$

$$\frac{dP}{dt} = \left(\frac{q_{max}(1-K_{ip}P)k_g \exp\left(-\frac{E_g}{RT}\right)}{1 + \frac{k_1}{10^{-pH}} + \frac{10^{-pH}}{k_2}} \right) \frac{S}{K_{sp} + S} X \quad (5.51)$$

$$\frac{dS}{dt} = \left(-1 + X \frac{S k_g \exp\left(-\frac{E_g}{RT}\right)}{K_{sx} + S} \right) \left(\mu_{max}(1-K_{ix}P) + q_{max}(1-K_{ip}P) \right) - X(G_s + M_s)$$

$$= \frac{k_1}{10^{-pH}} + \frac{10^{-pH}}{k_2} \quad Y_x(K_{sx} + S) \quad Y_p(K_{sp} + S)$$

$$\frac{dX}{dt} = \left(\frac{\mu_{max} \left(1 - \frac{P}{P_{xmax}} \right) k_g \exp\left(-\frac{E_g}{RT}\right)}{1 + \frac{k_1}{10^{-pH}} + \frac{10^{-pH}}{k_2}} \right) \frac{S}{K_{sx} + S} X$$

$$\frac{dP}{dt} = \frac{\frac{P}{10^{-pH}} \frac{E_g}{k_2} - \frac{S}{K_{sp} + S}}{\left(1 + \frac{k_1}{10^{-pH}} + \frac{1}{k_2}\right)} X \quad (5.52)$$

$$\frac{dS}{dt} = \frac{-X k_g \exp\left(-\frac{E_g}{RT}\right)}{10^{-pH}} + \frac{P}{k_2} \frac{\mu_{max} S}{(1 - P_{xmax}) Y_x (K_{sx} + S)} + \frac{P}{k_2} \frac{q_{max} S}{(1 - P_{pmax}) Y_p (K_{sp} + S)} - X(G_s + M_s)$$

$$\frac{dX}{dt} = \left(\frac{\mu_{max} \exp\left(-\frac{E_g}{RT}\right) k_g \exp\left(-\frac{E_g}{RT}\right)}{1 + \frac{k_1}{10^{-pH}} + \frac{1}{k_2}} \right) \frac{S}{K_{sx} + S} X$$

$$\frac{dP}{dt} = \left(\frac{q_{max} \exp\left(-\frac{E_g}{RT}\right) k_g \exp\left(-\frac{E_g}{RT}\right)}{1 + \frac{k_1}{10^{-pH}} + \frac{1}{k_2}} \right) \frac{S}{K_{sp} + S} X \quad (5.53)$$

$$\frac{dS}{dt} = \left(1 + \frac{k_1}{10^{-pH}} + \frac{1}{k_2}\right) \left(\frac{-X k_g \exp\left(-\frac{E_g}{RT}\right)}{10^{-pH}} - \frac{\mu_{max} \exp\left(-\frac{E_g}{RT}\right) S}{Y_x (K_{sx} + S)} + \frac{q_{max} \exp\left(-\frac{E_g}{RT}\right) S}{Y_p (K_{sp} + S)} \right) - X(G_s + M_s)$$

$$\frac{dX}{dt} = \left(\frac{\mu_{max} (1 - K_{isx} S) \exp\left(-\frac{E_g}{RT}\right) k_g \exp\left(-\frac{E_g}{RT}\right)}{1 + \frac{k_1}{10^{-pH}} + \frac{1}{k_2}} \right) \frac{S}{K_{sx} + S} X$$

$$\frac{dP}{dt} = \left(\frac{q_{max} (1 - K_{isp} S) \exp\left(-\frac{E_g}{RT}\right) k_g \exp\left(-\frac{E_g}{RT}\right)}{1 + \frac{k_1}{10^{-pH}} + \frac{1}{k_2}} \right) \frac{S}{K_{sp} + S} X \quad (5.54)$$

$$\frac{dS}{dt} = \left(\frac{-X k_g \exp\left(-\frac{E_g}{RT}\right)}{1 + \frac{k_1}{10^{-pH}} + \frac{1}{k_2}} \right) \left(\frac{\mu_{max} (1 - K_{isx} S) S}{Y_x (K_{sx} + S) \exp(K_{ix} P)} + \frac{q_{max} (1 - K_{isp} S) S}{Y_p (K_{sp} + S) \exp(K_{ip} P)} \right) - X(G_s + M_s)$$

$$\frac{dP}{dt} = \left(\frac{q_{max} \exp(-K_{ip}P) \exp(-K_{isp}S) k_g \exp\left(-\frac{E_g}{RT}\right)}{1 + \frac{k_1}{10^{-pH}} + \frac{10^{-pH}}{k_2}} \right) \frac{S}{K_{sp} + S} X \quad (5.55)$$

$$\frac{dX}{dt} = \left(\frac{\mu_{max} \exp(-K_{ix}P) \exp(-K_{isx}S) k_g \exp\left(-\frac{E_g}{RT}\right)}{1 + \frac{k_1}{10^{-pH}} + \frac{10^{-pH}}{k_2}} \right) \frac{S}{K_{sx} + S} X$$

$$\frac{dS}{dt} = \left(\frac{-X k_g \exp\left(-\frac{E_g}{RT}\right)}{1 + \frac{k_1}{10^{-pH}} + \frac{10^{-pH}}{k_2}} \right) \left(\frac{\mu_{max} \exp(-K_{isx}S) S}{Y_x (K_{sx} + S) \exp(K_{ix}P)} + \frac{q_{max} \exp(-K_{isp}S) S}{Y_p (K_{sp} + S) \exp(K_{ip}P)} \right) - X(G_s + M_s)$$

5.6 Optimal Control Problem Formulation

An optimal control problem is posed formally as follows: Determine the state (equivalently, the trajectory or path) $\mathbf{X}(t) \in \mathbb{R}^n$, the control $(t) \in \mathbb{R}^m$, the vector of static parameters $\mathbf{p} \in \mathbb{R}^q$, the initial time $t_0 \in \mathbb{R}$ and terminal time, $t_f \in \mathbb{R}$ (where $t \in [t_0 \ t_f]$ is the independent variable) that optimizes the performance index

$$J = \phi[\mathbf{x}(t_0), t_0, \mathbf{x}(t_f), t_f; \mathbf{p}] + \int_{t_0}^{t_f} \mathcal{L}[\mathbf{x}(t), \mathbf{u}(t), t; \mathbf{p}] dt \quad (5.61)$$

$$f = (1 - K_{ip}P) \quad (5.72)$$

$$\mu(S) = \frac{\mu_{max}S}{K_{sx}+S} \quad (5.73)$$

$$q_p(S) = \frac{q_{max}S}{K_{sp} + S} (1 - K_{ip}P)$$

The dynamic equations describing the cell growth, product formation and substrate utilization were developed by applying the principle of conservation of mass, resulting in the systems of first order ordinary differential equations presented in equation (5.74).

$$\frac{dX}{dt} = \mu X - k_d X$$

$$\frac{dP}{dt} = q_p X + M_p X$$

$$\frac{dS}{dt} = -Y_x \frac{dX}{dt} - Y_p \frac{dP}{dt} - G_s X - M_s X$$

The expressions for μ and q from equation (5.73), equation (5.74) becomes

$$\frac{dX}{dt} = \frac{\mu_{max}S}{K_{sx}+S} X - k_d X$$

$$\frac{dP}{dt} = (1 - K_{ip}P) \frac{q_{max}S}{K_{sp} + S} X + M_p X$$

$$\frac{dS}{dt} = -Y_x \frac{dX}{dt} - Y_p \frac{dP}{dt} - G_s X - M_s X$$

The optimal control problem to be maximized is then formulated with equation (5.75) as follows;

$$\begin{aligned}
 J &= \int_0^{t_f} \left[AP^2 + B \exp\left(-\frac{E_g}{RT}\right) + C \left(\frac{k_1}{10^{-pH}} + \frac{10^{-pH}}{k_2} \right) \right] dt \\
 &\text{s.t.} \\
 \frac{dX}{dt} &= \frac{\mu_{max} \exp\left(-\frac{E_g}{RT}\right)}{1 + \frac{k_1}{10^{-pH}} + \frac{10^{-pH}}{k_2}} \frac{S}{K_{sx} + S} X - k_d \exp\left(-\frac{E_g}{RT}\right) X \\
 \frac{dP}{dt} &= q_{max} (1 - K_{ip} P) \frac{S}{K_{sp} + S} X + M_p X \\
 \frac{dS}{dt} &= \frac{-\mu_{max} \exp\left(-\frac{E_g}{RT}\right)}{1 + \frac{k_1}{10^{-pH}} + \frac{10^{-pH}}{k_2}} \frac{SX}{Y_x (K_{sx} + S)} - X(G_s + M_s) \\
 T_{min} &\leq T(t) \leq T_{max} \\
 pH_{min} &\leq pH(t) \leq pH_{max}
 \end{aligned} \tag{5.76}$$

Together with this, the reduced state and control signals (x_i and u_i) are defined:

$$\begin{aligned}
 x_1 &= X, \quad x_2 = P, \quad x_3 = S \quad p_1 = \mu_{max}, \quad p_2 = q_{max} \quad p_3 = K_{sx}, \quad p_4 = K_{sp}, \\
 p_5 &= Y_x, \quad p_6 = k_d \quad p_7 = G_s, \quad p_8 = M_s, \quad p_9 = M_p, \quad p_{10} = K_{ip} \\
 u_1 &= \exp\left(-\frac{E_g}{RT}\right), \quad u_2 = \frac{k_1}{10^{-pH}} + \frac{10^{-pH}}{k_2}
 \end{aligned}$$

Replacing these variables into equation (5.76)

$$\begin{aligned}
 \text{Max } J &= \int_0^{t_f} [Ax_2(t)^2 + Bu_1(t)^2 + Cu_2(t)^2] dt \\
 \text{s.t.} \\
 \frac{dx_1}{dt} &= \frac{p_1}{1 + u_2 p_3 + x_3} x_1 - p_6 u_1 x_1 \\
 \frac{dx_2}{dt} &= (1 - p_{10} x_2) \frac{p_2 x_3}{p_4 + x_3} x_1 + p_9 x_1 \\
 \frac{dx_3}{dt} &= \frac{-p_1 u_1}{1 + u_2 p_5 (p_3 + x_3)} x_3 x_1 - x_1 (p_7 + p_8) \\
 u_{1\min} &\leq u_1(t) \leq u_{1\max}
 \end{aligned} \tag{5.77}$$

$$u_{2\min} \leq u_2(t) \leq u_{2\max}$$

If the state, control, and static parameter can each be written in component form as

$$\mathbf{x}(t) = \begin{bmatrix} x_1(t) \\ \vdots \\ x_3(t) \end{bmatrix}; \mathbf{u}(t) = \begin{bmatrix} u_1(t) \\ \vdots \\ u_2(t) \end{bmatrix}; \mathbf{p}(t) = \begin{bmatrix} p_1(t) \\ \vdots \\ p_{10}(t) \end{bmatrix};$$

$$\mathbf{f}[\mathbf{x}(t), \mathbf{u}(t), t; \mathbf{p}] = \begin{bmatrix} \mathbf{f}_1[\mathbf{x}(t), \mathbf{u}(t), t; \mathbf{p}] \\ \vdots \\ \mathbf{f}_3[\mathbf{x}(t), \mathbf{u}(t), t; \mathbf{p}] \end{bmatrix}$$

where,

$$\mathbf{f}_1[\mathbf{x}(t), \mathbf{u}(t), t; \mathbf{p}] = \frac{p_1}{1 + u_2 p_3 + x_3} x_1 - p_6 u_1 x_1$$

$$\mathbf{f}_2[\mathbf{x}(t), \mathbf{u}(t), t; \mathbf{p}] = (1 - p_{10} x_2) \frac{p_2 x_3}{p_4 + x_3} x_1 + p_9 x_1$$

$$\mathbf{f}_3[\mathbf{x}(t), \mathbf{u}(t), t; \mathbf{p}] = \frac{-p_1 u_1 p_5^{-1} x_3 x_1}{1 + u_2 (p_3 + x_3)} - x_1 (p_7 + p_8)$$

Then optimal control problem can be simply written as equation (5.78):

$$\begin{aligned}
 & \text{Max } J(\mathbf{u}) = \int_{t_0}^{t_f} \mathcal{L}[\mathbf{x}(t), \mathbf{u}(t), t; \mathbf{p}] dt \\
 & \text{Subject to } \dot{\mathbf{x}}(t) = \mathbf{f}[\mathbf{x}(t), \mathbf{u}(t), t; \mathbf{p}] \\
 & (5.78) \\
 & \mathbf{u}_{min} \leq \mathbf{u}(t) \leq \mathbf{u}_{max}
 \end{aligned}$$

This is referred to as the Lagrangean form of an optimal control problem

5.8 Solution Technique by Calculus of Variations

In an indirect method, calculus of variations is applied to determine the first-order optimality conditions first-order necessary conditions for an optimal trajectory is obtained, derived using the augmented Hamiltonian, H defined as

$$H(\mathbf{x}, \boldsymbol{\lambda}, \mathbf{u}, t; \mathbf{p}) = \mathcal{L} + \boldsymbol{\lambda}^T \mathbf{f} \quad (5.81)$$

Where $\boldsymbol{\lambda}(t) \in \mathbb{R}^n$ is the costate or adjoint. In the case of a single phase optimal control problem with no static parameters, the first-order optimality conditions of the continuous-time problem are given as follows:

$$\dot{\mathbf{x}} = \left[\frac{\partial H}{\partial \boldsymbol{\lambda}} \right]^T, \quad \dot{\boldsymbol{\lambda}} = - \left[\frac{\partial H}{\partial \mathbf{x}} \right]^T \quad (5.82)$$

$$\mathbf{u}^* = \underset{\mathbf{u} \in U}{\text{arg min}} H \quad (5.83)$$

where, U is the feasible control set

The systems of differential equations presented in equation (5.82) is referred to as the Hamiltonian system, derived from the differentiation of a Hamiltonian (Athans and Falb, 2006; Leitman, 1981). Furthermore, the optimal control profile to the system is determined from the application of the Pontryagin's Minimum Principle (PMP) resulting in equation (5.84) and this is the classical method of determining the control (Pontryagin, 1962). The

Hamiltonian system, together with the boundary, transversality, is referred to as a Hamiltonian boundary-value problem (HBVP) (Athans and Falb, 2006; Ascher et al., 1996) and the solution to such a system is called an extremal.

Now applying calculus of variations to equation (5.77), the Hamiltonian becomes

$$\begin{aligned}
 H = & Ax_2(t)^2 + Bu_1(t)^2 + Cu_2(t)^2 + \lambda_1 \left(\frac{p_1}{1+u_2} \frac{u_1 x_3}{p_3+x_3} x_1 - p_6 u_1 x_1 \right) \\
 & + \lambda_2 \left((1 - p_{10} x_2) \frac{p_2 x_3}{p_4+x_3} x_1 + p_9 x_1 \right) + \lambda_3 \left(\frac{-p_1 u_1}{1+u_2} \frac{x_3 x_1}{p_5(p_3+x_3)} - x_1 (p_7 + p_8) \right)
 \end{aligned} \tag{5.84}$$

5.8.1 State Equations

This is obtained by applying equation (5.82) to the equation (5.81)

$$\dot{x} = \left[\frac{\partial H}{\partial \lambda} \right]^T,$$

becomes

$$\begin{aligned}
 \frac{dx_1}{dt} &= \frac{p_1}{1+u_2} \frac{u_1 x_3}{p_3+x_3} x_1 - p_6 u_1 x_1 \\
 \frac{dx_2}{dt} &= (1 - p_{10} x_2) \frac{p_2 x_3}{p_4+x_3} x_1 + p_9 x_1 \\
 \frac{dx_3}{dt} &= \frac{-p_1 u_1}{1+u_2} \frac{x_3 x_1}{p_5(p_3+x_3)} - x_1 (p_7 + p_8)
 \end{aligned} \tag{5.85}$$

5.8.2 Costate Equations

This is obtained by differentiating the Hamiltonian with respect to the states,

$$\lambda = - \left[\frac{\partial H}{\partial x} \right]^T$$

$$\left. \begin{aligned} \frac{d\lambda_1}{dt} &= \lambda_1 \left(p_6 u_1 - \frac{p_1 x_3 u_1 (1 + u_2)}{p_3 + x_3} \right) - \lambda_2 \left(p_9 - \frac{p_2 x_3 (p_{10} x_2 - 1)}{p_4 + x_3} \right) + \lambda_3 \left(p_7 + p_8 + \frac{p_1 x_3 (p_3 + x_3)}{p_5} \right) \\ \frac{d\lambda_2}{dt} &= \frac{p_2 p_{10} \lambda_2 x_1 x_3}{p_4 + x_3} - 2A x_2 \frac{dt}{3} \frac{-1}{3} \end{aligned} \right\} (5.86)$$

$$\begin{aligned} \frac{d\lambda_3}{dt} &= -\lambda_1 \left(\frac{p_1 x_1 u_1 (1 + u_2)}{p_3 + x_3} - \frac{p_1 x_1 x_3 u_1 (1 + u_2)}{p_3 + x_3^2} \right) + \lambda_2 \left(\frac{p_2 x_1 (p_{10} x_2 - 1)}{p_4 + x_3} - \frac{p_2 x_1 x_3 (p_{10} x_2 - 1)}{p_4 + x_3^2} \right) \\ &\quad + \lambda_3 \left(\frac{p_1 x_1 (p_3 + x_3)}{p_5} - \frac{p_1 x_1 x_3}{p_5} \right) \end{aligned}$$

5.8.3 Optimal Control Equations

These are obtained by apply the Pontryagin's Minimum Principle, equation (14) to equation (12). The Hamiltonian gradient can be represented by differentiating the Hamiltonian with respect to the controls as follows:

$$\left. \begin{aligned} \frac{dH}{du_1} &= 2B u_1 - \lambda_1 \left(p_6 x_1 - \frac{p_1 x_1 p x_{33} + (x_{13} + u_2)}{p_3 + x_3} \right) \\ \frac{dH}{du_2} &= 2C u_2 + \frac{p_1 u_1 \lambda_1 x_1 x_3}{p_3 + x_3} \end{aligned} \right\} (5.87)$$

The necessary optimality conditions for a local maximizer is that this gradient should be equal to zero, so that:

$$u_1^* = \frac{2\lambda_1 x_1 (C p_3 + C x_3) (p_6 p_3 + p_6 x_3 - p_1 x_3)}{-(p_1 \lambda_1 x_1 x_3)^2 + 4BC p_3^2 + 8BC p_3 x_3 + 4BC x_3^2} \quad (5.88)$$

$$u_2^* = \frac{-p_1 (\lambda_1 x_1)^2 x_3 (p_6 p_3 + p_6 x_3 - p_1 x_3)}{-(p_1 \lambda_1 x_1 x_3)^2 + 4BC p_3^2 + 8BC p_3 x_3 + 4BC x_3^2} \quad (5.89)$$

The expressions for temperature and pH can then be written as follows

$$T = \frac{1}{R} \ln \frac{k_g}{u_1^*} \quad (5.90)$$

$$pH = \frac{1}{\ln 10} \ln \left(\frac{k_2 u_2^* + \sqrt{(k_2 u_2^*)^2 - 4k_1 k_2}}{2k_1 k_2} \right) \quad (5.91)$$

Applying the Pontryagin's Minimum Principle (PMP) of

$$\mathbf{u}^* = \mathit{arg} \min_{\mathbf{u} \in U} H$$

The optimal control Trajectory becomes

$$T^* = \min(T_{max}, \max(T_{min}, T)) \quad (5.92)$$

$$pH^* = \min(pH_{max}, \max(pH_{min}, pH)) \quad (5.93)$$

5.8.4 Numerical Simulations and Control Validation

The states, costate and optimal control equations are referred to as the Hamiltonian Boundary Value Problem (HBVP) with boundary conditions

$$\lambda(t_f) = \begin{bmatrix} 0 \\ 0 \\ 0 \end{bmatrix} \quad \mathbf{x}(t_0) = \begin{bmatrix} 0.1 \\ 0.7 \\ 16.8 \end{bmatrix}$$

A collocation method based on the Labatto IIIA formula was used to simulate the HBVP and a Matlab code was written to implement this algorithm using the Matlab routine 'bvp4c'. The collocation polynomial provides a continuous solution that is fourth order accurate uniformly in [a b]. Mesh selection and error control are based on the residual of the continuous solution. In validating the controls, the alcohol fermentation model described in section III was implemented in the SIMULINK environment. This implemented model includes the objective function to be maximized.

5.8.5 Results and Discussion

Figure 5.84 presents the fitting for the model taking into consideration the death rate while and Table 5.81 the parameter values. Figure 5.81 and 5.82 presents the optimal temperature and pH profiles optimizes the fermentation process. Simulation using the Simulink model, figure 5.83 shows that the optimal temperature and pH profiles obtained an increment in cell growth of 71.96%, product formation by 14.18% and substrate utilization by 84.77% compared to using the conventional temperature and pH values used by the industry. This improvement in process performance observed can be explained by the fact that due to the dynamic nature of the culture medium, yeast cells often suffer from various stresses resulting from both the environmental conditions, and from both product and or substrate inhibition as the fermentation proceeds. Optimal profiles (and not constant values) of temperature and pH are important in the control these stresses, and ensure that the culture medium conditions stays constant, hence maximizing yield (Saerens et al., 2008). The increase in substrate utilization didn't balance up with product formation because some of the substrate was utilized for cell growth and maintenance. Table 5.82 presents the values of the final states and cost functional for both the Optimal and the conventional operation conditions. Figures 5.85 to 5.87 compares the optimal and conventional operating strategies, clearly depicting increase in process performance.

Table 5.81: Estimated Parameters for dynamic model used in optimal control, equation 3

	K_{ip}	K_{sx}	K_{sp}	Y_x	m_s	G_s
Value	2.2004	0.4358	0.0721	0.6857	0.3353	246.2663
Model Error	0.8940					

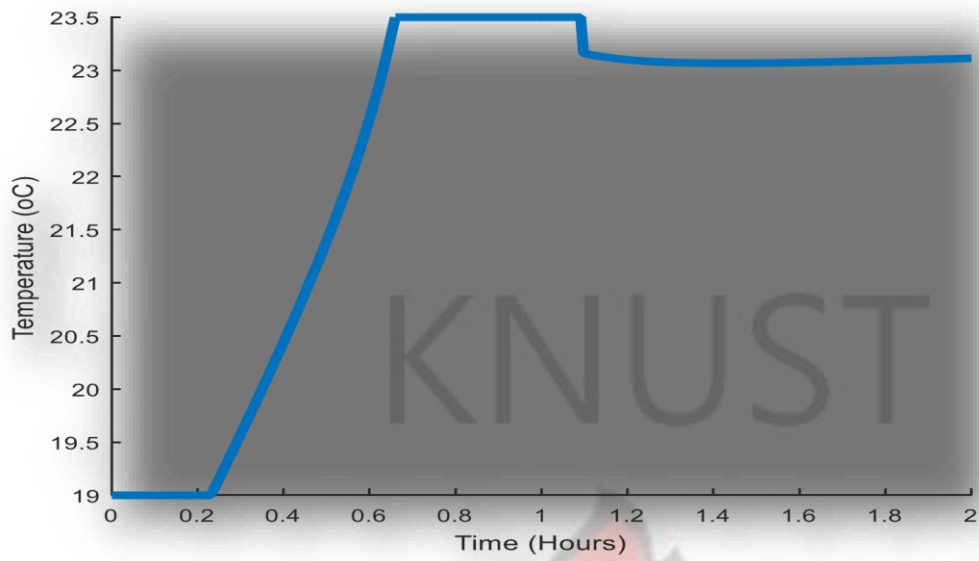


Figure 5.83: Optimal temperature profile obtained from numerical simulation of the necessary optimality conditions

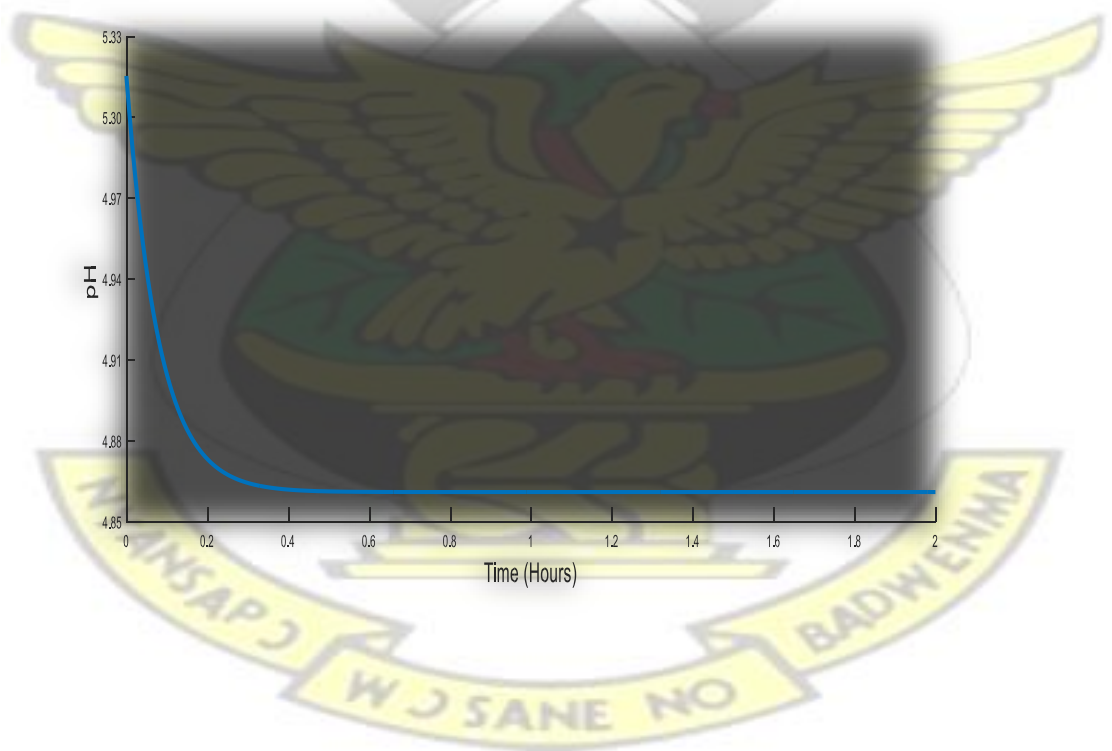


Figure 5.82: optimal pH profile obtained from numerical simulation of the necessary optimality conditions

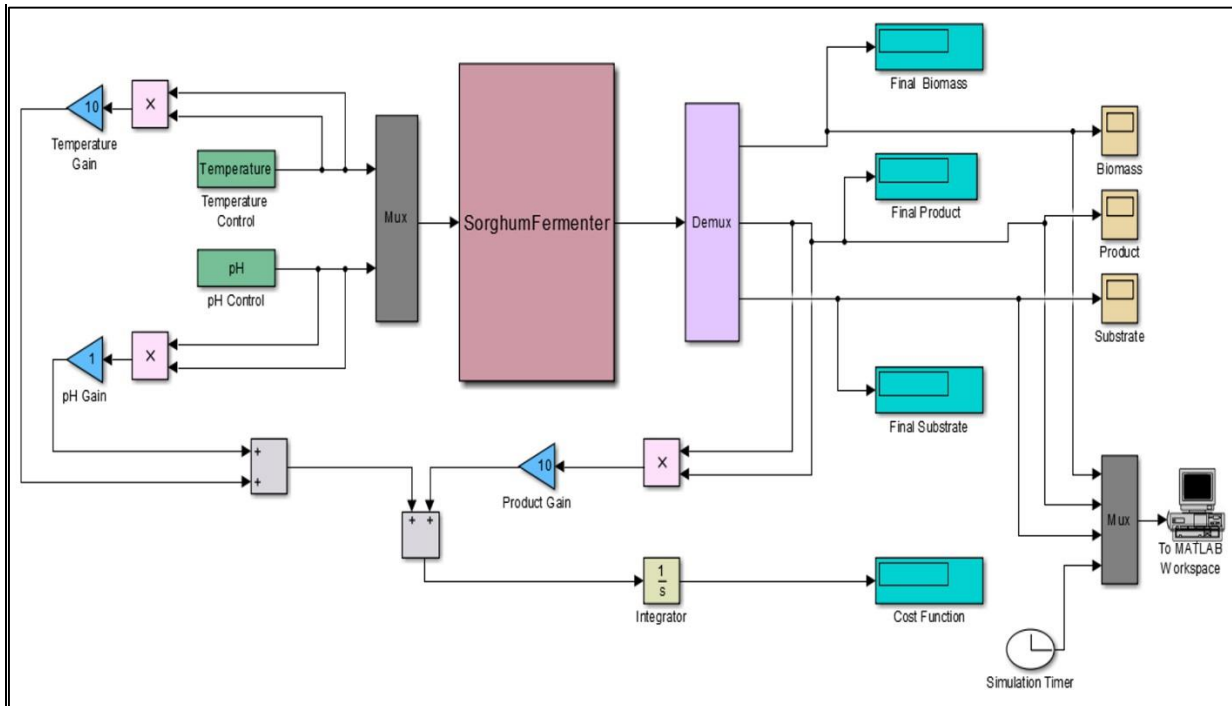


Figure 5.83: Simulink Model designed for the alcoholic fermentation of sorghum extracts.

Table 5.82: Obtainable concentrations for both the optimal and conventional operating conditions

Final State	Optimal	Conventional
Biomass (Mcells/0.1ml)	0.3219	0.1872
Product (g/100g)	7.748	6.785
Substrate (g/100g)	5.872	10.85
Performance Index	5.593e+05	5.455e+05

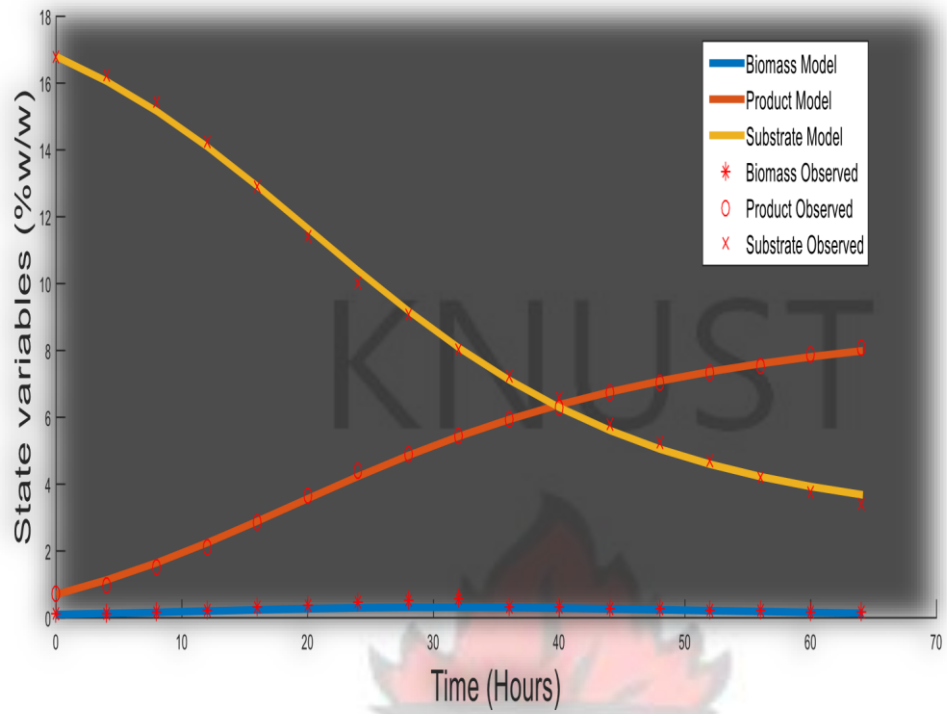


Figure 5.84: Experimental results and model fitting

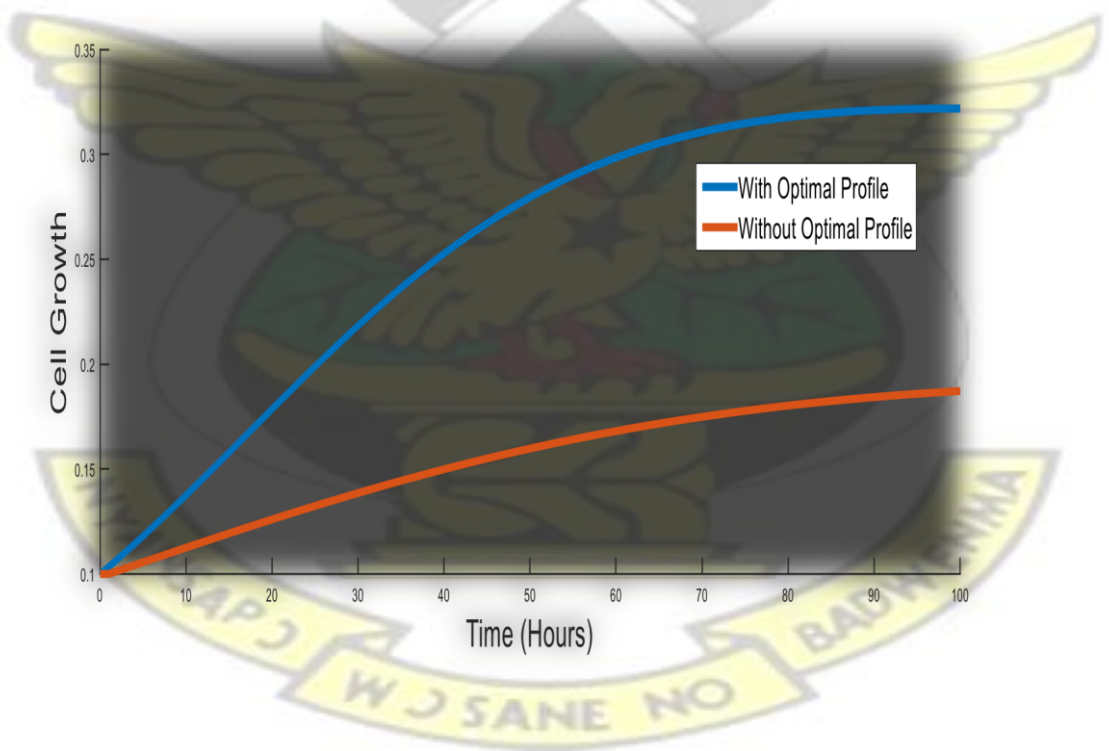


Figure 5.85: Dynamics of cell growth with optimal and conventional controls

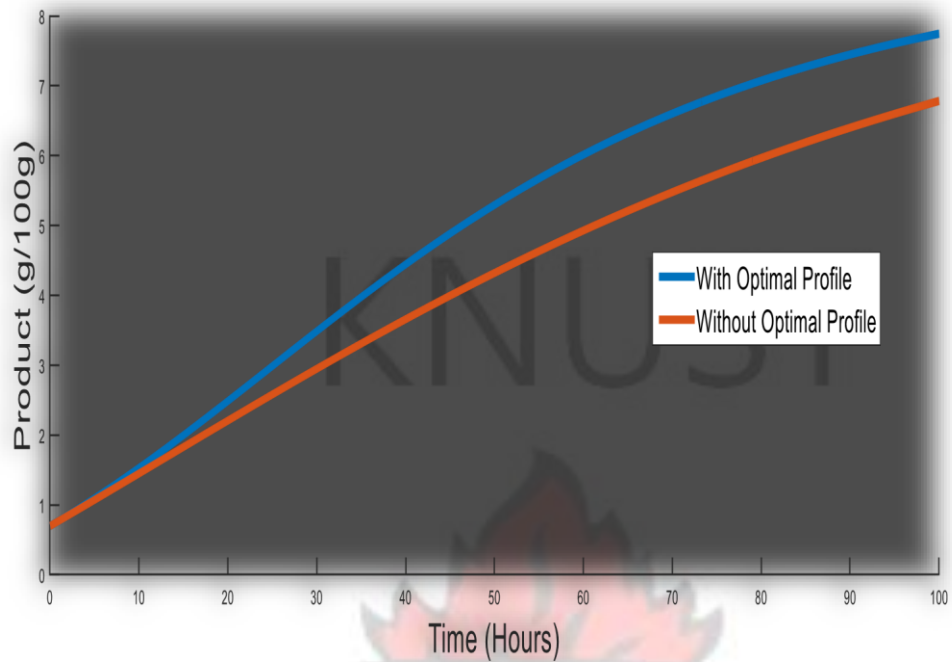


Figure 5.86: Dynamics of product formation with optimal and conventional controls

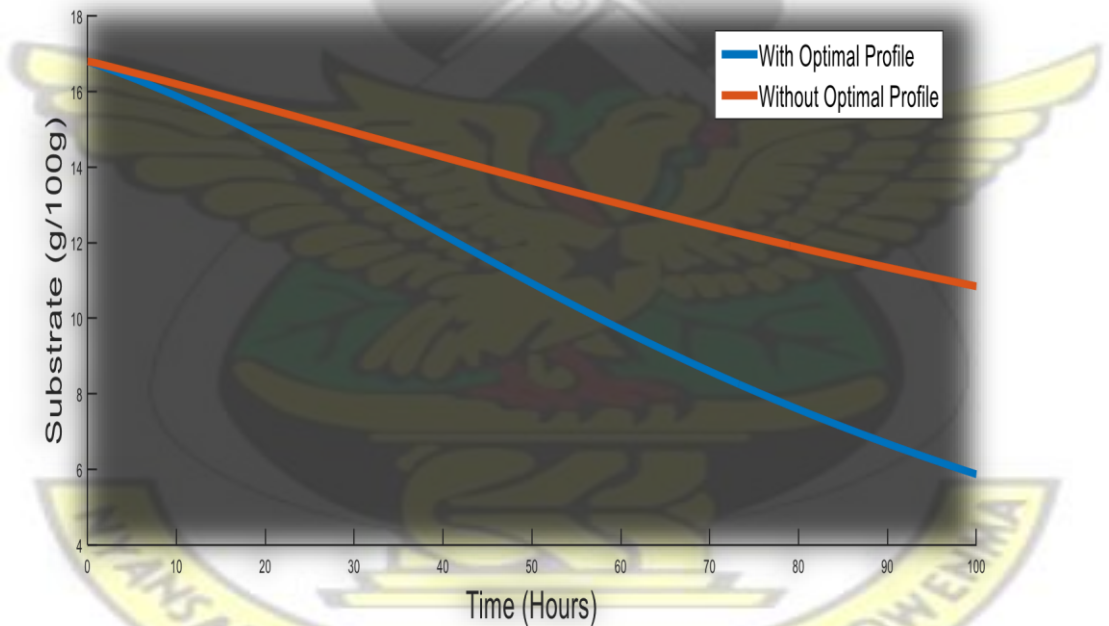


Figure 5.87: Dynamics of substrate utilization with optimal and conventional controls

5.9 Conclusion

This chapter presented the modeling of a batch alcoholic fermentation process using sorghum extracts, followed by the application of optimal control to determine the

optimal temperature and pH profiles that maximizes yield. Since the model was developed using industrial scale fermentation data, the results obtained in the simulations can satisfactorily represent a real operation unit. From the comparative results presented in the simulations it is concluded that the proposed strategy can be used in practice to improve the performance of industrial scale alcoholic fermentation using sorghum.

CHAPTER SIX

CONCLUSIONS AND RECOMMENDATIONS FOR FUTURE WORK

6.1 Conclusions

The overall objective of this research was achieved by the successful investigation of the dynamics of ethanol fermentation in three different fermentation worts and maximizing ethanol yield through the application of mathematical modeling and optimal control. This will greatly help in the development of various automatic tools such as: simulators able to reproduce system behavior and, software sensors which allow to obtain an estimation of an unmeasured signal or controllers to maintain optimal conditions. All these tools rely on a representation of the considered system, a mathematical model (Carrillo-Ureta, 2002). Substrate and product inhibition kinetics during alcoholic fermentation has been modelled using three different substrates. Substrates considered were sorghum, maize and cassava and the results show that there exist both ethanol inhibition in the alcoholic fermentation of sorghum and maize extracts while cassava extracts show both ethanol and substrate inhibition. At a 99% confidence interval the pattern of these inhibitions can be described as being a linear or an exponential decrease on ethanol concentration in the case of sorghum, linear and

sudden growth stop in the case of maize, linear substrate exponential product, and exponential substrate exponential product in the case of cassava.

Optimal control has been applied to minimize the effects of such inhibitions in the case sorghum extracts, using the linear product inhibition model and Calculus of variation has been introduced as a valuable tool to derive and solve the necessary conditions for optimality and the obtained results show the optimal temperature and pH profiles for the fermentation of sorghum extracts. A Simulink model has been developed to describe the fermentation process and correspondingly validate the controls. The performance of ethanol fermentation using sorghum extracts has been optimized using the proposed control strategy and ethanol yield increased by 14.18%, cell growth by 71.96% and residual sugar concentration decreased by 84.77%. Since the model was developed using industrial scale fermentation data, the results obtained in the simulations can satisfactorily represent a real operation unit. From the comparative results presented in the simulations it is concluded that the proposed strategy can be used in practice to improve the performance of industrial scale alcoholic fermentation.

6.2 Recommendations

6.2.1 Optimal Control and Dynamic Stability Using the Other Inhibition Models

Various inhibition patterns were modeled in this study and the application of optimal control to maximize ethanol yield was based on the linear product inhibition model using sorghum extracts. The other inhibition patterns (sudden growth stop, exponential, LS-EP and ES-EP) and substrates (cassava and maize) should also be used to determine the optimality conditions, followed by dynamic stability to determine which of the models will be more reliable in process control, in the various substrates.

6.2.2 Model Based Control of CO₂ during Alcohol Fermentation

One of the primary and well-known challenges of ethanol fermentation process is CO₂ management and pH control. CO₂ affects the bubble dynamics which play an important role in gas transport and cell viability during fermentation (Meier et al., 1999; Wang et al., 2001; Ma et al., 2006). Therefore optimum CO₂ levels are highly important and this optimum since CO₂ level depends on cell growth which in turn depends on the type of substrate used, and optimal control should also be applied to maintain CO₂ production and evolution rates at optimal levels throughout the fermentation.

6.2.3 Modeling the Effect of Temperature and pH on Cell Growth

The temperature dependency of the cellular activity was modeled using the Arrhenius-like equation, the Arrhenius constants used were values from previous research. In addition, the simple model used to model pH dependence on cell growth was not specific for the yeasts strains used for the fermentation but was rather used because literature shows it gives an adequate fit for many microorganisms (Nielsen & Villadsen, 1994). However, the model constants used in the models need to be estimated with data from temperature and pH measurements, using the various substrates considered, since the growth dynamics of the yeast strains varied with substrates and so will their temperature and pH dependence vary.

6.2.4 Development of and Optimal Simulator for Alcohol fermentation

Profit maximization by operating the most efficient process is the primary goal of all industrial fermentation operations. To help create efficient operations companies use process simulation, involving the application of a range of software tools to analyze the predict patterns in fermentation. These simulators are based on mathematical model and were recommend to develop a GUI (Graphical User Interface) which will use the

Matlab codes to develop a computer simulator for ethanol fermentation that is easily adaptable for any yeast strain and fermentation substrate.

REFERENCES

- Aiba S, Shoda M, Nagatani M (1968), Kinetics of product inhibition in alcohol fermentation. *Biotechnol Bioeng*, 10: 845-864.
- Alford, J. S. (2006), Bioprocess control: Advances and challenges, *Computers and chemical engineering*, 30: 1464-1475.
- Ali, M.M., Storey, C. and Torn, A. (1997). Application of stochastic global optimization algorithms to practical problems. *J. Optim. Theory Appl.*, 95: 545– 563,
- Anderson, B. D. O and Moore, J. B. (1990), *Optimal Control: Linear Quadratic Methods*. Englewood Cliffs, NJ: Prentice-Hall
- Ascher, U. M. Mattheij, R. M. and Russell, R. D. (1996). *Numerical Solution of Boundary-Value Problems in Ordinary Differential Equations*. Philadelphia SIAM Press.
- Assidjo, N. E, Akaki, D., Yao, K. B., Eboi, T. Y. (2009), A Hybrid Neural Network Approach for Batch Fermentation Simulation, *Australian Journal of Basic and Applied Sciences* 3(4): 3930-3936.
- Atala, D. I. P., Costa, A. C., Maciel, R. and Maugeril, F. (2001). Kinetics of ethanol fermentation with high biomass concentration considering the effect of temperature. *Applied Biochemistry and Biotechnology*, 91(93): 353–365.
- Athans, M. A. and Falb, P. L. (2006). *Optimal Control: An Introduction to the Theory and Its Applications*. Mineola, New York Dover Publications.
- Bastin, G. and Dochain, D. (1990) *On-line estimation and adaptive control of bioreactors*, Amsterdam, Elsevier, pp. 20-230
- Beers, K. J. (2007), *Numerical Methods for Chemical Engineering*. Cambridge, MA: Cambridge University Press,
- Bellgardt, K. H. (1991) “*Biotechnology*”, Ed. H.-J. Rehm, and G. Reed, VCH, Weinheim, 4: 267-298
- Bellgardt, K.H. (2000) “*Bioreaction Engineering*”, Ed. K. Schugerl, and K. H.

- Bellgardt, Springer Verlag, Berlin, pp. 1-18; 56-72; 391-412
- Betts, J. T. (1998). "Survey of Numerical Methods for Trajectory Optimization," *Journal of Guidance, Control, and Dynamics*, 21: 193–207.
- Beuse, M. R. B., Kopmann, A. H. D., Thoma, M. (1998). Effect of dilution rate on the mode of oscillation in continuous culture of *Saccharomyces cerevisiae*. *J. Biotechnol.*, 61: 15- 31.
- Biegler, L. T., Cervantes, A. M., Wachter, A. (2002). Advances in simultaneous strategies for dynamic process optimization. *Chemical Engineering Science*, 57(4): 575–593,
- Box, George E.P., William G. Hunter and J. Stuart Hunter. (2002). *Statistics for Experimenters: An Introduction to Design, Data Analysis and Model Building*. New York, NY: John Wiley & Sons,
- Brenner, S. (2010), Sequences and consequences. *Philos T Roy Soc B* 365 : 207-212
- Bryson Jr. A. E. 1996 *Optimal control 1950 to 1985*. IEEE Control Systems Magazine, pp. 26–33,
- Cacik, F., Dondo, R. G. and Marques, D. (2001). Optimal control of a batch bioreactor for the production of xanthan gum. *Computers and Chemical Engineering*, 25: 409– 418.
- Carrillo-Ureta, G.E. (2002). *Optimal Control of Fermentation Processes*, unpublished PhD Thesis, City University, London, U.K.
- Chachuat, B. (2007) *Nonlinear and Dynamic Optimization: From Theory to Practice*. Automatic Control Laboratory, EPFL, Switzerland.
- Chen, C.I. and McDonald, K.A. (1990a), Oscillatory behavior of *Saccharomyces cerevisiae* in continuous culture: I. Effects of pH and nitrogen levels. *Biotechnol. Bioeng*, 36: 19-27.
- Chen, C.I. and McDonald, K.A. (1990b), Oscillatory behavior of *Saccharomyces cerevisiae* in continuous culture: II. Analysis of cell synchronization and metabolism. *Biotechnol. Bioeng*, 36: 28-38.
- Chhatre, S., Bracewell, D.G. and Titchener-Hooker, N.J. (2009). A microscale approach for predicting the performance of chromatography columns used to recover therapeutic polyclonal antibodies. *J Chromatogra A*. 12(16): 7806-7815.
- Constantinides, Alkis and Navid M. (1999). *Numerical Methods for Chemical Engineers with MATLAB Applications*. Upper Saddle River, NJ: Prentice Hall PTR,

- Datta AK, Sabiani SS. (2007). Mathematical modelling techniques in food and bioprocesses: an overview. In: Sabiani SS, editor. Handbook of food and bioprocess modelling techniques. Boca Raton, FL: Taylor & Francis Group, pp. 2-11.
- Doran, P. M. (1995). *Bioprocess Engineering Principles*, Elsevier, Science & Technology Books
- Engasser, J.M., Marc, I., Moll, M. and Duteurtre, B., (1981). Kinetic modeling of beer fermentation. *Proceedings of the European Brewing Convention Congress, Copenhagen IRL Press: Oxford*, pp. 579–586.
- Fengwu, B. (2007), Process Oscillations in Continuous Ethanol Fermentation with *Saccharomyces cerevisiae*. Unpublished PhD thesis University of Waterloo, Ontario, Canada.
- Fischer, C.R, Klein-Marcuschamer, D., Stephanopoulos, G. (2008), Selection and optimization of microbial hosts for biofuel production. *Metab Eng.* 10: 295-304
- Franz Hamilton (2011). Parameter Estimation in Differential Equations: A Numerical Study of Shooting Methods
- Galvanauskas, V., Simutis R, Lubbert A. (2004). Hybrid process models for process optimisation, monitoring and control. *Bioproc Biosyst Eng.* 26: 393-400.
- Garcia, A.I., Garcia, L.A. and Diaz, M., (1994), Fusel alcohols production in beer fermentation. *Proc. Biochem.*, 29: 303–309.
- Garcia, L.A., Argueso, F., Garcia, A.I. and Diaz, M., (1995), Application of neural networks for controlling and predicting quality parameters in beer fermentation. *J. Ind. Microbiol.*, 15: 401–406.
- Gee, D.A. and Ramirez, W. F., (1994), A flavour model for beer fermentation. *J. Inst. Brew.* 100: 321–329.
- Ghana Renewable Energy Act, (2011). Act 832, Ghana Publishing Company Ltd, Assembly Press, Accra.
- Gill, P. E. Murray, W. and Wright, M. H. (1981). Practical Optimization. London: Academic Press,
- Goh, C. J. and. Teo, K. L. (1988) “Control Parameterization: A Unified Approach to Optimal Control Problems with General Constraints,” *Automatica*, 24: 3–18.
- Grossmann, I.E. (1996). *Global Optimization in engineering design*. Kluwer Academic Publishers, Dordrecht, the Netherlands,

- Holland, J.H. (1992). *'Adaption in natural and artificial systems'* MIT Press, Cambridge, MA
- Horst R. and Tuy. H. (1990). *Global Optimization: Deterministic approaches*. Springer-Verlag, Berlin,
- Ji, Y. (2012). Model based process design for bioprocess optimization: case studies on precipitation with its applications in antibody purification. Unpublished PhD thesis, University College London, U.K.
- Kemausuor, F., Kamp, A., Thomsen, S.T., Bensah, E.C., Østergård, H., (2014). Assessment of biomass residue availability and sustainable bioenergy yields in Ghana, *Resources, and Conservation & Recycling* 86: 28-37
- Komives, C. and Parker, R. S. (2003) *Current Opinion Biotech*, 14: 468-474
- Kouame, K. B., Koko Anauma, C. Diomande, M. (2015), Batch Fermentation Process of Sorghum Wort Modeling By Artificial Neural Network, *European Scientific Journal* 11(3):297-300
- Koutinas, M., Kiparissides, A., Efstratios, N. P., Athanasios, M. (2012). Bioprocess systems engineering: transferring traditional process engineering principles to industrial biotechnology. *Computational and structural biotechnology journal* 3(4): 2045-2098
- Leitman, G. (1981). *The Calculus of Variations and Optimal Control*. Springer, New York
- Logsdon, J. S., Biegler, L. T. (1989) .Accurate solution of differential-algebraic optimization problem. *Industrial and Engineering Chemistry Research*, 28: 1628–1639,
- Lübbert, A. and Jørgensen S. B. (2001): “Bioreactor Performance: A More Scientific Approach for Practice.” *Journal of Biotechnology* 85: 187-212.
- Luus, R. (1990). Application of dynamic programming to high-dimensional nonlinear optimal control problems. *International Journal of Control*, 52(1):239– 250,
- Ma, N., Mollet, M. And Chalmers, J. J. (2006). Aeration, Mixing and Hydrodynamics in Bioreactors. in *Cell Culture Technology for Pharmaceutical and Cell-Based Therapies*. Taylor & Francis, New York, NY pp. 225-248.
- Mandenius CF, Brundin A. 2008. Bioprocess optimization using design of experiments methodology. *Biotechnol Prog*. 24: 1191-1203.
- Mantovanelli, I.C., Rivera, E.C., da Costa, A.C., Maciel, F. R. (2007), Hybrid neural network model of an industrial ethanol fermentation process considering the effect of temperature, *Appl Biochem Biotechnol*. 137-140(1-12):817-33

- Marcus V. Normey-Rico, J. E (2011), Modeling, Control and Optimization of Ethanol Fermentation Process, Preprints of the 18th IFAC World Congress Milano
- Massimo, C.D., Willis, M.J., Montague, G.A, Tham, M.T., Morris, A.J. (1991). Bioprocess model building using artificial neural networks. *Bioprocess Eng.* 7: 77-82.
- Meier, S. J., Hatton, A. T. and Wang, D. I.C. (1999). Cell Death from Bursting Bubbles: Role of Cell Attachment to Rising Bubbles in Sparged Reactors. *Biotechnology and Bioengineering* 62: 468-478.
- Michaelis, L. and Menten M.L. (1913). Kinetk der Invertinwirkung. *Biochem Z.* Vol. 49: 333-369
- Mishra, J., Kumar, D., Samanta, S. and Vishwakarma, M.K. (2011). comparative study of ethanol production from various agro residues by using *Saccharomyces cerevisiae* & *Candida albicans*. *Journal of Yeast & Fungal Research* 3(2):12 17,
- Modak, J. M., Lim, H. C. and Tayeb, Y. J. (1986). General characteristics of optimal feed rate profiles for various fed-batch fermentation processes. *Biotechnology and Bioengineering* 28: 1396-1407.
- Montague, G. and Morris J. (1994). Neural-network contributions in biotechnology. *Trends Biotechnol.* 12: 312-324.
- Naydenova, V. Iliev, Kaneva, V.M., Kostov, G. (2013), Modeling of alcohol fermentation in brewing – Carbonyl compounds synthesis and reduction, Proceedings of the European Conference on Modelling and Simulation, 28: 434-440
- Nelson, D. L. Cox, M. M. (2001). *Lehninger principles of biochemistry*, Fourth Edition, University of Wisconsin Press.
- Nielsen, J. & Villadsen, J. (1994). *Bioreaction Engineering Principles*. New York: Plenum Press.
- Olivier, B. (2001). *Mass balance modelling of bioprocesses* Comore, Inria, France
- Osei, G., Arthur, R., Afrane, G., Agyemang, E.O., 2013. Potential feedstocks for bioethanol production as a substitute for gasoline in Ghana, *Renewable Energy.* 55: 12-20.
- Palsson, B.O., Papin, J.A. (2009), Applications of genome-scale metabolic reconstructions. *Mol Syst Biol* 5: 320-350.
- Parcunev, I., Naydenova, V., Kostov, G., Yanakiev, Y., Popova Z., Kaneva, M., Ignatov, I. (2012), Modelling of alcoholic fermentation in brewing – some practical approaches, Proceeding of the European Conference on Modelling and Simulation, 26: 434-440.

- Peifer M. and Timmer J. (2007) Parameter estimation in ordinary differential equations for biochemical processes using the method of multiple shooting. *IET Syst. Biol.*, 1(2): pp. 78–88
- Pontryagin, L. S., (1962) *Mathematical Theory of Optimal Processes*. John Wiley & Sons .New York:
- Qiangshan, J., Hui L., Liuye, M., Xiaoming, Z. (2006). Comparative study between fluidized bed and fixed bed reactors in methane reforming with CO₂ and O₂ to produce syngas, *Energy Conversion and Management*, 47(4): 459–469
- Ramirez, F. W. and Maciejowski, J. (2007). Optimal beer fermentation, *J. Inst. Brew.* 113(3): 325–333.
- Renge, V. C. Khedkar S. V. And Nikita R. N. (2012). Enzyme Synthesis By Fermentation Method: A Review *Sci. Revs. Chem. Commun.* 2(4): 585-590.
- Renge, V. C. Khedkar S. V. And Nikita R. N. (2012). Enzyme Synthesis By Fermentation Method: A Review *Sci. Revs. Chem. Commun.* 2(4): 585-590
- Rinnooy-Kan, A.H.G., and Timmer, G.T. (1987). ‘Stochastic global optimization methods. Part I: Clustering methods’, *Math. Prog.* 39: 27–56
- Russell, A. D. (2003), Similarities and differences in the responses of microorganisms to biocides, *Journal of Antimicrobial Chemotherapy*, 52: 750–765.
- Saerens, S.M.G. Verbeln, P.J. Vanbeneden, N. Thevelein J.M. and Delvaux F.R. (2008). Monitoring the influence of high-gravity brewing and fermentation temperature on flavour formation by analysis of gene expression levels in brewing yeast, *Applied Microbiology and Biotechnology* 80(6): 760-780
- Santos, d. K. G., Lobato, F. S. and Murata, V. V. (2006). Mathematical modeling and optimization of a fed batch reactor for alcoholic using agro-industrial wastes. *Horizonte Cientifico*, 1: 1–24
- Schugerl, K. (1991) “Biotechnology”, vol. 4, Ed. H.-J. Rehm, and G. Reed, VCH, Weinheim, pp. 6-28
- Shuler, M. & Kargi, F. (2002). *Bioprocess Engineering Basic Concepts* (2nd ed. Saddle River, NJ: Prentice Hall.
- Shuler, Michael L. and Fikret Kargi. (1992). *Bioprocess Engineering: Basic Concepts*. Englewood Cliffs, NJ: Prentice Hall,

- Stanbury, P. F. Whitaker A. and Hall, S. J. (1995). 'Principles of Fermentation Technology', Pergamon Press, 2nd Edn, Oxford,
- Subramaniam, R. and Vimala, R. (2012). Solid state and submerged fermentation for the production of bioactive substances: a comparative stud. *International journal of science and nature*. 3(3): 480-493
- Sussmann H. J. and Willems J. C., (1997). 300 years of optimal control: from the Brachystochrone to the Maximum Principle. *IEEE Control Systems Magazine*, pp. 32–44,
- Sutton, K.B. (2011). Fermentation Inhibitors, Novozyme report. 18600
- Thilakavathi, M., Basak, T., Panda, T. (2007), Modeling of enzyme production kinetics. *Appl Microbiol Biotechnol* 73: 991-1007
- Titchener-Hooker NJ, Dunnill P, Hoare M. (2008), Micro biochemical engineering to accelerate the design of industrial-scale downstream processes for biopharmaceutical proteins. *Biotechnol Bioeng*. 100: 473-487.
- Titica, M., Dochain, D. and Guay, M. (2004). Adaptive extremum seeking control of enzyme production in filamentous fungal fermentation. 9th International Symposium on Computer Applications in Biotechnology, pp. 28 - 31
- Torn, M. A. and Viitanen, S. (1999). Stochastic global optimization: problems classes and solution techniques. *J. Glob. Optim.*, 14: 437-458.
- Velayudhan A, Menon MK. 2007. Modeling of purification operations in biotechnology: enabling process development, optimization and scale-up. *Biotechnol Progr*. 23: 68-73.
- Verbelen, P.J. Sacerens, S.M.G., Mulders, V. S.E. Delvaux, F. and Delvaux, F. R. (2009). The role of oxygen in yeast metabolism during high cell density brewery fermentations, *Applied Microbiology and Biotechnology* 82: 760-789
- Vidyalakshmi, R., Paranthaman R. and Indhumathi, J. (2009), Amylase Production on Submerged Fermentation by *Bacillus* spp. *World Journal of Chemistry* 4(1): 89-91
- Wang, B. (2012), Parameter Estimation for ODEs using a Cross-Entropy Approach. Unpublished Master's thesis, Graduate Department of Computer Science University of Toronto

- Wang, F. S., Su, T. L. and Jang, H. J. (2001). Hybrid differential evolution for problems of kinetic parameter estimation and dynamic optimization of an ethanol fermentation process. *Industrial & Engineering Chemistry Research*, 40: 2876–2885.
- Wang, F., Jianchun, Z., Limin, H., Shiru, J., Jianming, B. and Shuang, N. (2012). Optimization of Submerged Culture Conditions for Mycelial Growth and Extracellular Polysaccharide Production by *Coriolus versicolor*. *Bioprocessing & Biotechnique* 2(4):299-345
- Willaert R. (2007), The Beer Brewing Process: Wort Production and Beer Fermentation. In: Handbook of Food Products Manufacturing. Hui, Y.H. (ed.), John Wiley & Sons, Inc.
- Williams, J. A. (2002) Keys to Bioreactor Selections, EPS: Environmental & Production Solutions
- Yu, L., Wensel, P.C., Ma, J., Chen, S. (2013). Mathematical Modeling in Anaerobic Digestion (AD). *J Bioremed Biodeg* 10(3): 4172-4185
- Zabczyk, J. (2008). Mathematical control theory. Modern Birkhauser Classics. Birkhauser Boston Inc., Boston, MA,
- Zeng, An-Ping and Jing-Xiu Bi. (2006). *Cell Culture Kinetics and Modeling. in Cell Culture Technology for Pharmaceutical and Cell-Based Therapies*. Taylor & Francis, New York, NY, pp. 299-348.
- Zhi-Long, X. and An-Ping, Z. (2008), Present state and perspective of downstream processing of biologically produced 1,3-propanediol and 2,3-butanediol, *Appl. Microbiol. Biotechnol*, 78: 917–926

APPENDICES

Appendix 1. Matlab codes for Parameter Estimation

Appendix 1a sample of code used for Product inhibition

```
format short; clear all %clear all variables global y0 time
Xobs Pobs Sobs param Xpred Ppred Spred data
=xlsread('Sorghum.xlsx');
%initial conditions
y0=[0.1 0.7 16.8];
%initial guess
P1=0.4; P2=0.2; P3=90; P4=100; P5=0.1; P6=6; P7=0.09; P8=1;P9=0.3;P10=0.2;
param(1)=P1; param(2)=P2; param(3)=P3; param(4)=P4; param(5)=P5;
param(6)=P6;param(7)=P7;param(8)=P8;param(9)=P9;param(10)=P10;
%param=100*rand(1,10);
%Measured data
time=data(:,1); Xobs=data(:,2);
Pobs=data(:,3);
Sobs=data(:,4);

lb=[0.01,0.1,0.01,0.3,0.1,0.1,0.001,0.01,0.1,0.1];
ub=[5,250,250,200,1,7,1,0.5,10,10];
options=optimoptions('fmincon','MaxFunEval',3000);
[xval, fval] = fmincon(@LinInhKin,param,[],[],[],[],lb,ub,[],options);
disp('Estimated parameters param:'); disp(xval) disp('Smallest value
of the error E:'); disp(fval)

figure
hold on
```

```

%predicted values for state variables plot(time,
Xpred,'LineWidth',3.5) ; plot(time,
Ppred,'LineWidth',3.5); plot(time,
Spred,'LineWidth',3.5);

%Experimental/observed values for state variables
plot(time, Xobs, 'r*','MarkerSize',7); plot(time, Pobs,
'ro','MarkerSize',7); plot(time, Sobs, 'rx','MarkerSize',7);
xlabel('Time (Hours)') ylabel('State variables (%w/w)')

```

```

function E = LinInhKin(param)
%This function called LinInhKin (Linear Inhibition kinetics) calculates the
%error between experimental data and model prediction. It takes initial
%guess of model parameters and outputs the sum of the squared error

global y0 time Xobs Pobs Sobs Xpred Ppred Spred

%Numerical integration of the Model using the Runge-Kutta 4-5th order t0=0;
tf=ceil(max(time)); tspan=[t0 tf]; %we want y at every t
[t,x]=ode45(@ff,tspan,y0); %param(1) is y(0)

%This section presents the dynamic model for ethanol fermentation in the %case of
Linear inhibition

function dx = ff(t,x) %function that computes the dydt
dx(1)=param(1)*(1-
param(9)*x(2))*x(1)*x(3)/(param(3)+x(3)); %biomass
dx(2)= param(2)*(1-
param(10)*x(2))*x(1)*x(3)/(param(4)+x(3)); %product
dx(3)= -
1/param(5)*dx(1)-1/param(6)*dx(2)-x(1)*(param(7)+param(8));
%substrate
dx=dx';

```

```

end

%Calculation the model predicted values for Biomass (Xpred), Product(Ppred)
%and substrate(Spred)
Xpred = interp1(t,x(:,1),time);
Ppred = interp1(t,x(:,2),time);
Spred = interp1(t,x(:,3),time);

%Computes the sum of squared error between the model prediction and the
%observed or experimental data
E = 0;
for i = 1:length(time)
E = E + (Xpred(i)-Xobs(i))^2+(Ppred(i)-Pobs(i))^2+ (Spred(i)-Sobs(i))^2;
end display(E) end

```

Appendix 1b Substrate and Product Inhibition (Case of ES-EP)

```

aclear all %clear all variables
global y0 time Xobs Pobs Sobs param Xpred Ppred Spred data
=xlsread('Cassava.xlsx');
%initial conditions y0=[0.16
1.7 12.79];
%initial guess
P1=0.05; P2=10; P3=90; P4=91; P5=0.5; P6=0.1; P7=0.9;
P8=3;P9=0.3;P10=0.2; P11=0.05; P12=0.1; param(1)=P1; param(2)=P2;
param(3)=P3; param(4)=P4; param(5)=P5; param(6)=P6;
param(7)=P7;param(8)=P8;param(9)=P9;param(10)=P10;param(11)=P11;param(12)=
P12;

```

```

%Measured data time=data(:,1); Xobs=data(:,2);
Pobs=data(:,3);
Sobs=data(:,4);

lb=[0.01,0.1,0.01,0.3,0.1,0.1,0.0001,0.0001,0.1,0.1,0.0001,0.001];
ub=[3,250,250,200,3,5,1,0.5,5,2,1,1];
[xval, fval] = fmincon(@ExpSExpPIinhKin,param,[],[],[],[],lb,ub); disp('Estimated
parameters param:'); disp(xval) disp('Smallest value of the error E:'); disp(fval)

figure hold on
%predicted values for state variables plot(time,
Xpred,'LineWidth',3.5) ; plot(time, Ppred,'LineWidth',3.5);
plot(time, Spred,'LineWidth',3.5);

%Experimental/observed values for state variables plot(time, Xobs,
'r*','MarkerSize',7); plot(time, Pobs, 'ro','MarkerSize',7); plot(time,
Sobs, 'rx','MarkerSize',7); xlabel('Time (Hours)') ylabel('State
variables (%w/w)')

```

```

function E = ExpSExpPIinhKin(param)
%This function called LinInhKin (Linear Inhibition kinetics) calculates the
%error between experimental data and model prediction. It takes initial
%guess of model parameters and outputs the sum of the squared error

global y0 time Xobs Pobs Sobs Xpred Ppred Spred

%Numerical integration of the Model using the Runge-Kutta 4-5th order t0=0;
tf=ceil(max(time)); tspan=[t0 tf]; %we want y at every t
[t,x]=ode45(@ff,tspan,y0); %param(1) is y(0)

%This section presents the dynamic model for ethanol fermentation in the %case of
Linear inhibition

function dx = ff(t,x) %function that computes the dydt
dx(1)=param(1)*exp(-
param(9)*x(2))*exp(param(11)*x(3))*x(1)*x(3)/(param(3)+x(3));
%biomass dx(2)= param(2)*exp(-
param(10)*x(2))*exp(param(12)*x(3))*x(1)*x(3)/(param(4)+x(3));
%product
dx(3)= -1/param(5)*dx(1)-1/param(6)*dx(2)-x(1)*(param(7)+param(8));
%substrate
dx=dx'; end

%Calculation the model predicted values for Biomass (Xpred), Product(Ppred)
%and substrate(Spred)
Xpred = interp1(t,x(:,1),time);
Ppred = interp1(t,x(:,2),time);
Spred = interp1(t,x(:,3),time);

```

```

%Computes the sum of squared error between the model prediction and the
%observed or experimental data
E = 0;
for i = 1:length(time)
E = E + (Xpred(i)-Xobs(i))^2+(Ppred(i)-Pobs(i))^2+ (Spred(i)-Sobs(i))^2;
end display(E) end

```

Appendix 2. Matlab code for Optimality Conditions (Calculus of Variations)

```

clear all clc

%State Equations
syms x1 x2 x3 p1 p2 p3 p4 p5 p6 p7 p8 p9 p10 kg Eg kd k2 mp R u1 u2;
Dx1=p1*u1*x1*x3/(p3+x3)*(1+u2)-kd*u1*x1;
Dx2=p2*(1-p10*x2)*x1*x3/(p4+x3)+ mp*x1;
Dx3=(-x1*x3)*(p1/p5*(p3+x3))-x1*(p7+p8);

%Cost Function inside intergral syms g A B C

g=A*x2^2+B*u1^2+C*u2^2;

%Hamiltonian syms w1 w2 w3
H= g + w1*Dx1 + w2*Dx2 + w3*Dx3;

%Costate Equations

```

```

Dw1 = -diff(H,x1);
Dw2 = -diff(H,x2);
Dw3 = -diff(H,x3);

% solve for control u du1 =
diff(H,u1); du2 = diff(H,u2);
sol_u=solve(du1,du2,'u1','u2');

% % Substitute u to state equations
% Dx1 = subs(Dx1, [u1,u2], [sol_u.u1(1),sol_u.u2(1)]);
% Dw1 = subs(Dw1, [u1,u2], [sol_u.u1(1),sol_u.u2(1)]);
% Dx2 = subs(Dx2, [u1,u2], [sol_u.u1(1),sol_u.u2(1)]);
% Dw2 = subs(Dw2, [u1,u2], [sol_u.u1(1),sol_u.u2(1)]);
% Dx3 = subs(Dx3, [u1,u2], [sol_u.u1(1),sol_u.u2(1)]);
% Dw3 = subs(Dw3, [u1,u2], [sol_u.u1(1),sol_u.u2(1)]);
%
% %Simplification of equations
% Dx1=simplify(Dx1);
% Dx2=simplify(Dx2);
% Dx3=simplify(Dx3);
% Dw1=simplify(Dw1);
% Dw2=simplify(Dw2);
% Dw3=simplify(Dw3);

```

Appendix 3: Matlab Code to Simulate the Hamiltonian Boundary Value Problem

```
clear all clc
```

KNUST



KNUST



global p1 p2 p3 p4 p5 p6 p7 p8 p9 p10 A B C k1 k2 mp kd kg Eg R;

```

format long
% Model Parameter Values p1=0.9557; p2=2.2101; p3=129.433;
p4=29.213; p5=2; p6=0.8895; p7=0.502; p8=0.564; p9=0.1294;
p10=0.01004;
A=100; B=10; C=10; mp=0.01; kd=0.001; k1=10^(-5.4); k2=10^(-4.5);
R=8.314; kg=5000; Eg=5100; options = bvpset('RelTol',10^(-
6),'Nmax',5000,'Stats','off');

solinit = bvpinit(linspace(0,2),[0.7 1 0.05 0.1 10 1]); sol =
bvp4c(@HBVP2,@HBVPbc,solinit,options);
%% subplot(4,1,1)
%% plot(sol.x,sol.y(1,:), 'LineWidth',2)
%% subplot(4,1,2)
%% plot(sol.x,sol.y(2,:), 'LineWidth',2)
%% subplot(4,1,3)
%% plot(sol.x,sol.y(3,:), 'LineWidth',2)

x1=sol.y(1,:); x2=sol.y(2,:);
x3=sol.y(3,:);
w1=sol.y(4,:);
w2=sol.y(5,:);
w3=sol.y(6,:); hold on
%subplot(2,1,1) temp1=(2*w1.*x1.*(C*p3 + C*x3).*(kd*p3 + kd*x3 - p1*x3))./(-
p1^2*w1.^2.*x1.^2.*x3.^2 + 4*B*C*p3^2 + 8*B*C*p3*x3 + 4*B*C*x3.^2);
temp2=-(p1*w1.^2.*x1.^2.*x3.*(kd*p3 + kd*x3 - p1*x3))./(-

```

```

p1^2*w1.^2.*x1.^2.*x3.^2 + 4*B*C*p3^2 + 8*B*C*p3*x3 + 4*B*C*x3.^2);

%pH=log((k2*temp2 - k2 + (-k2*(- k2*temp2.^2 + 2*k2*temp2 + 4*k1 -
k2)).^(1/2))/(2*k1*k2))/log(10);
%pH=log(-(k2 - k2*temp2 + (-k2*(- k2*temp2.^2 + 2*k2*temp2 + 4*k1
k2)).^(1/2))/(2*k1*k2))/log(10);

pH=log((k2 + k2*temp2 + (k2*(k2*temp2.^2 + 2*k2*temp2 - 4*k1 +
k2)).^(1/2))/(2*k1*k2))/log(10);
%pH=log((k2*temp2 + (k2^2*temp2.^2 - 4*k1*k2).^(1/2))./(2*k1*k2))./log(10);
%pH=log((temp2 + (temp2.^2 ).^(1/2)));
% pH=log((temp2 - 1)/k1)/log(10);
T=1/R*log(kg./temp1); u1 =
min(23.5,max(19,10.5*T)); u2 =
min(14.5,max(0,1*pH));
%plot(sol.x,temp1,'LineWidth',2)
%plot(sol.x,temp2,'LineWidth',2)
hold on
plot(sol.x,u2,'LineWidth',4)
% subplot(2,1,2)
%
% plot(sol.x,u2,'LineWidth',2)

```

Appendix 4: Simulink S-function used to Design Fermenter

```
function [sys,x0,str,ts,simStateCompliance] = SorghumFermenter(t,x,u,flag)
%SFUNTMPL General MATLAB S-Function Template
% With MATLAB S-functions, you can define you own ordinary differential
% equations (ODEs), discrete system equations, and/or just about
% any type of algorithm to be used within a Simulink block diagram.
%
% The general form of an MATLAB S-function syntax is:
```



KNUST



% [SYS,X0,STR,TS,SIMSTATECOMPLIANCE] =

```

SFUNC(T,X,U,FLAG,P1,...,Pn)
%
% What is returned by SFUNC at a given point in time, T, depends on the
% value of the FLAG, the current state vector, X, and the current % input
vector, U.
%
% FLAG RESULT DESCRIPTION
% -----
% 0 [SIZES,X0,STR,TS] Initialization, return system sizes in SYS,
% initial state in X0, state ordering strings %
in STR, and sample times in TS.
% 1 DX Return continuous state derivatives in SYS.
% 2 DS Update discrete states SYS = X(n+1)
% 3 Y Return outputs in SYS.
% 4 TNEXT Return next time hit for variable step sample %
time in SYS.
% 5 Reserved for future (root finding).
% 9 [] Termination, perform any cleanup SYS=[].
%
% The state vectors, X and X0 consists of continuous states followed %
by discrete states.
%
% Optional parameters, P1,...,Pn can be provided to the S-function and %
used during any FLAG operation.
%
% When SFUNC is called with FLAG = 0, the following information %
should be returned:
%
%
% SYS(1) = Number of continuous states.
% SYS(2) = Number of discrete states.

```

- % SYS(3) = Number of outputs.
- % SYS(4) = Number of inputs.
- % Any of the first four elements in SYS can be specified



KNUST



% as -1 indicating that they are dynamically sized. The

GNUST



% actual length for all other flags will be equal to the %

KNUST



length of the input, U.

KNUST



% SYS(5) = Reserved for root finding. Must be zero.

KNUST



% SYS(6) = Direct feedthrough flag (1=yes, 0=no). The s-function

KNUST



% has direct feedthrough if U is used during the FLAG=3

KNUST



% call. Setting this to 0 is akin to making a promise that

KNUST



% U will not be used during FLAG=3. If you break the promise %

KNUST



then unpredictable results will occur.

KNUST



% SYS(7) = Number of sample times. This is the number of rows in TS.

KNUST



%

KNUST



%

KNUST



% X_0 = Initial state conditions or [] if no states.

KNUST



%

KNUST



% STR = State ordering strings which is generally specified as [].

KNUST



%

KNUST



% TS = An m-by-2 matrix containing the sample time

KNUST



% (period, offset) information. Where m = number of sample %

KNUST



times. The ordering of the sample times must be:

KNUST



%

KNUST



% $TS = [0 \quad 0, \quad]$: Continuous sample time.

KNUST



% 0 1, : Continuous, but fixed in minor step %

KNUST



sample time.

KNUST



%

PERIOD OFFSET, : Discrete sample time where %

KNUST



PERIOD > 0 & OFFSET < PERIOD.

KNUST



% -2 0]; : Variable step discrete sample time %

KNUST



where FLAG=4 is used to get time of %

KNUST



next hit.

KNUST



%

KNUST



% There can be more than one sample time providing

% they are ordered such that they are monotonically

KNUST



KNUST



% increasing. Only the needed sample times should be

KNUST



% specified in TS. When specifying more than one

KNUST



% sample time, you must check for sample hits explicitly by %

KNUST



seeing if

KNUST



% `abs(round((T-OFFSET)/PERIOD) - (T-OFFSET)/PERIOD)`

GNUST



% is within a specified tolerance, generally $1e-8$. This %

KNUST



tolerance is dependent upon your model's sampling times %

KNUST



and simulation time.

KNUST



%

KNUST



% You can also specify that the sample time of the S-function

KNUST



% is inherited from the driving block. For functions which

KNUST



% change during minor steps, this is done by

KNUST



% specifying $SYS(7) = 1$ and $TS = [-1 \ 0]$. For functions which

KNUST



% are held during minor steps, this is done by specifying %

KNUST



$\text{SYS}(7) = 1$ and $\text{TS} = [-1 \ 1]$.

KNUST



%

KNUST



% SIMSTATECOMPLIANCE = Specifies how to handle this block when saving

KNUST



and

KNUST



%

restoring the complete simulation state of the

KNUST



%

model. The allowed values are: 'DefaultSimState',

KNUST



%

'HasNoSimState' or 'DisallowSimState'. If this value

KNUST



%

is not specified, then the block's compliance with %

KNUST



simState feature is set to 'UknownSimState'.

KNUST



KNUST



KNUST



KNUST



KNUST



%

KNUST



% The following outlines the general structure of an S-function.

%

switch flag,

%%%%%%%%%KNUST

% Initialization %

%%%%%%%%%



KNUST



case 0,

KNUST



```
[sys,x0,str,ts,simStateCompliance]=mdlInitializeSizes;
```

KNUST



KNUST



%%%%%%%%%

KNUST



% Derivatives %

KNUST



%%%%%%%%%

KNUST



case 1,

KNUST



sys=mdlDerivatives(t,x,u);

KNUST



KNUST



%%%%%%%%%

KNUST



% Outputs %

KNUST



%%%%%%%%%

KNUST



case 3,

KNUST



```
sys=mdlOutputs(t,x,u);
```

KNUST



KNUST



%%%%%%%%%

KNUST



% Unhandled Flags %

KNUST



%%%%%%%%%

KNUST



case { 2, 4, 9 }, sys = [];

KNUST



KNUST



%%%%%%%%%

KNUST



% Unexpected flags %

KNUST



%%%%%%%%%

KNUST



otherwise

KNUST



DASudio.error('Simulink:blocks:unhandledFlag', num2str(flag));

KNUST



end

% end sfuntmpl

KNUST



%

%

=

KNUST



```

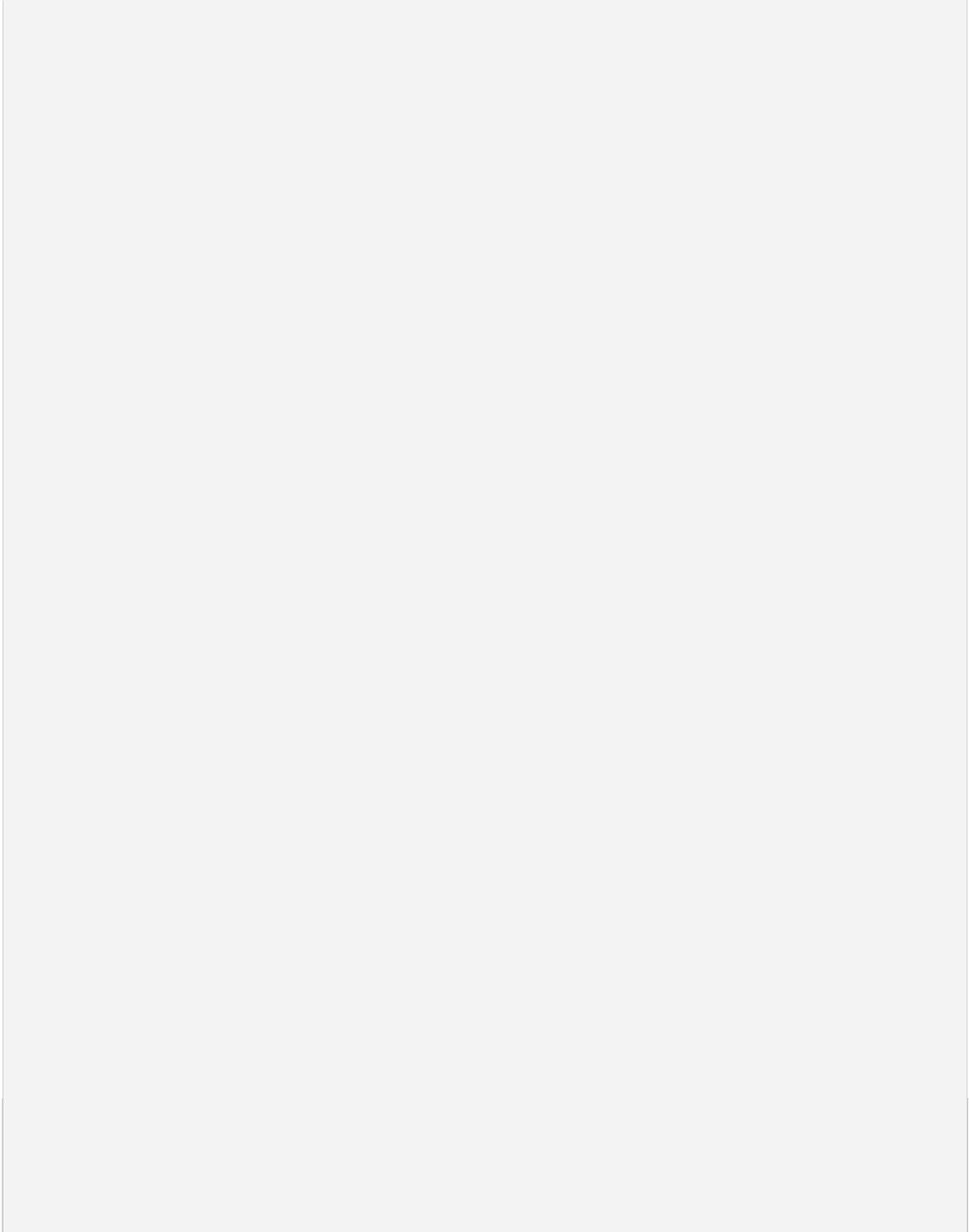
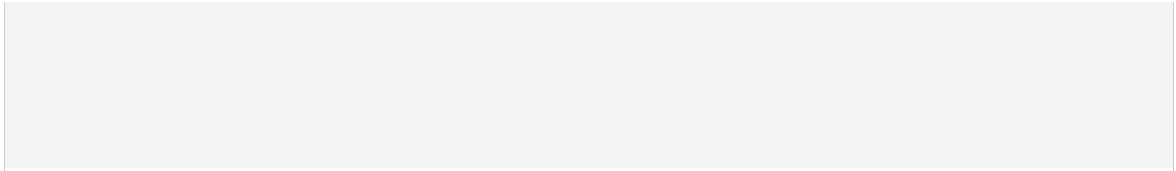
=====
% mdlInitializeSizes
% Return the sizes, initial conditions, and sample times for the S-function.
%=====
=====
%
function [sys,x0,str,ts,simStateCompliance]=mdlInitializeSizes

%
% call simsizes for a sizes structure, fill it in and convert it to a %
sizes array.
%
% Note that in this example, the values are hard coded. This is not a %
recommended practice as the characteristics of the block are typically
% defined by the S-function parameters.
%
sizes = simsizes;

sizes.NumContStates = 3; sizes.NumDiscStates = 0;
sizes.NumOutputs    = 3; sizes.NumInputs    = 2;
sizes.DirFeedthrough = 0; sizes.NumSampleTimes = 1; % at least
one sample time is needed

sys = simsizes(sizes);

```



```

%
% initialize the initial conditions
%
x0 = [0.1,0.7,16.8];

%
% str is always an empty matrix
%
str = [];

%
% initialize the array of sample times
%
ts = [0 0];

% Specify the block simStateCompliance. The allowed values are:
% 'UnknownSimState', < The default setting; warn and assume DefaultSimState
% 'DefaultSimState', < Same sim state as a built-in block
% 'HasNoSimState', < No sim state
% 'DisallowSimState' < Error out when saving or restoring the model sim state
simStateCompliance = 'UnknownSimState';

% end mdlInitializeSizes

```

```
%  
%=====
```

```
% mdlDerivatives  
% Return the derivatives for the continuous states.  
%=====
```

```
%  
function sys=mdlDerivatives(t,x,u)
```

```
X=x(1);  
P=x(2);  
S=x(3); T=u(1);  
pH=u(2);
```



```

% Modeling effects of controls on parameters
Eg=0.001; kg=7000; k1=10^(-5.4); k2=10^(-4.5);yp=1.8895;
R=8.314; kd0=10^33; Umax0=0.5557; kip=0.1004; mp=0.8900; yx=0.1086;
ms=0.0564; Gs=0.00502; ksx=125.433; ksp=29.213 ; Ed=50000; qmax=2.2101;
kix=0.1294;

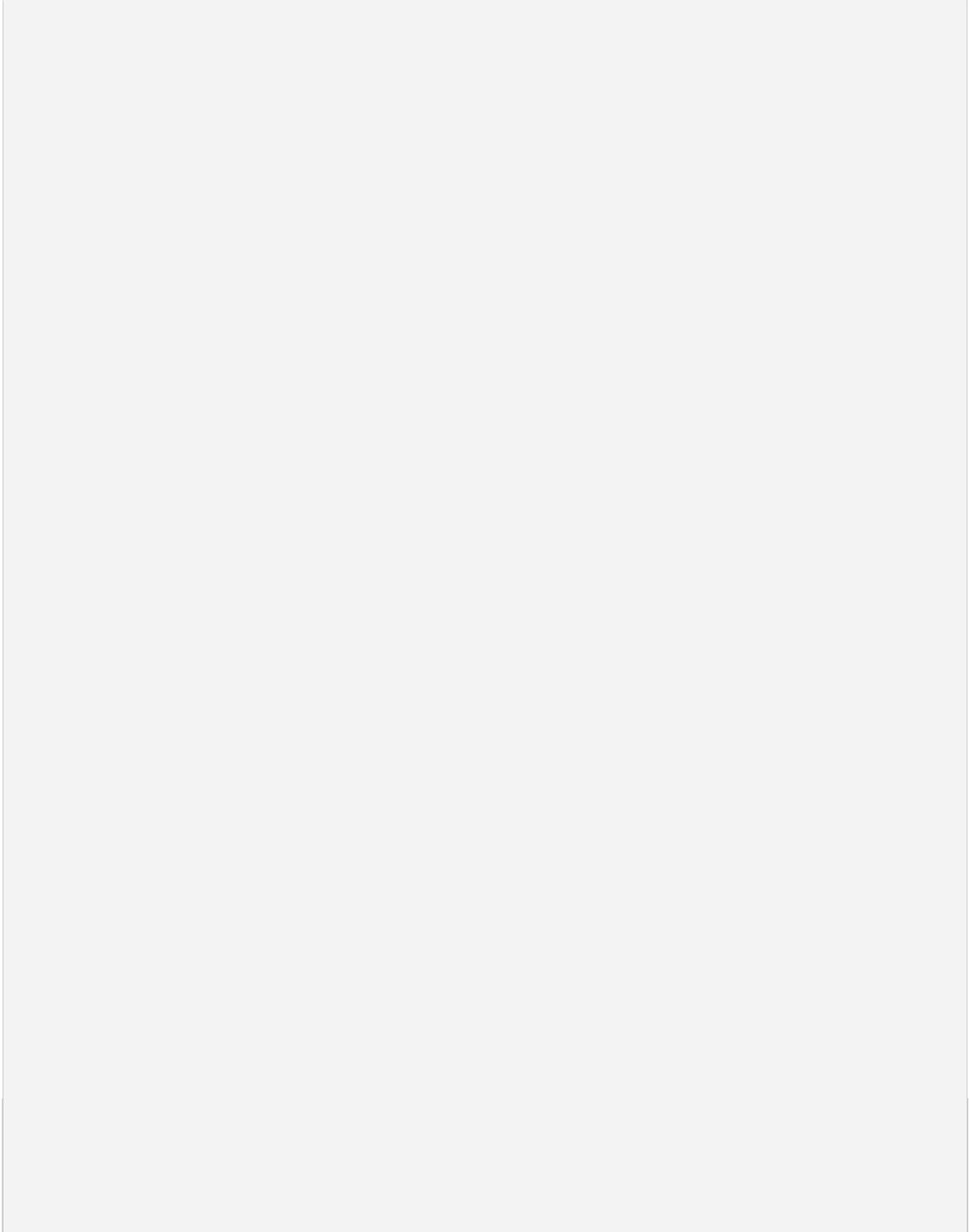
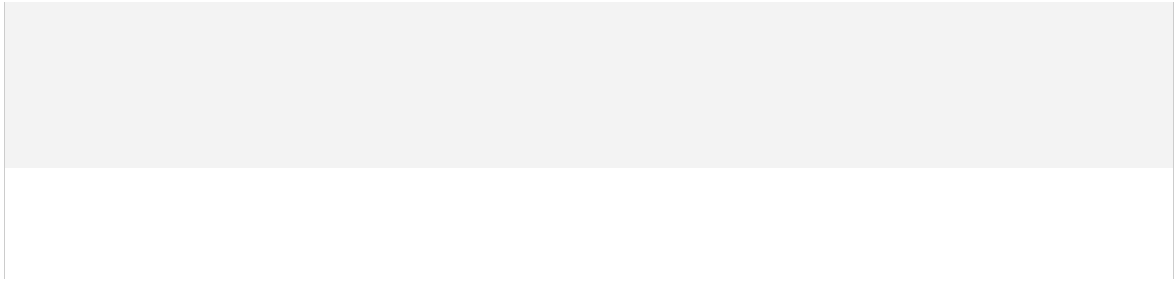
Umax=Umax0*exp(-Eg/R*T)/(1 + k1/10^(-pH)+ 10^(-pH)/k2);

%kd=kd0*exp(-Ed/R*T);
%Umax=exp(108.31-31934.09/(T+273.15));
%Factor Equations fp=(1-kip*P);
%product inhibition factor fx=(1-kix*P);
U=Umax*S/(ksx+S); %specific growth rate q=qmax*S/(ksp+S);
%specific rate of product formation

% Differential Equations

sys(1)=U*fx*X ; sys(2)=q*fp*X; sys(3)=-
U*X/yx -q*fp*X/yp-X*(ms+Gs);

```



% end mdlDerivatives

KNUST



```

%
%=====
%
% mdlOutputs
% Return the block outputs.
%=====
%
%
function sys=mdlOutputs(t,x,u)

sys = x;

% end mdlOutputs

```

Appendix 5: Tables for Model Statistical Validity for Cassava and Maize

Extracts

Appendix 5a: Table 5.1: Model Statistical Validity with kinetics Exponential Substrate and Exponential Product Inhibition, two sample F-test for variance (Cassava Extracts)

	Biomass		Product		Substrate	
	Experimental (Xobs)	Model (Xpred)	Experimental (Pobs)	Model (Ppred)	Experimental (Sobs)	Model (Spred)
Mean	2.093	2.113	5.881	5.886	5.275	5.280
Standard Error	0.245	0.228	0.403	0.397	0.722	0.727
Standard Deviation	0.979	0.913	1.613	1.588	2.889	2.909
Observations	16	16	16	16	16	16
Confidence Interval	0.990		0.990		0.990	
f	0.8695		0.9682		1.0143	

Pr(F < f)	0.7900	0.9509	0.9785
Two-tailed			

Appendix 5b Table 5.2: Model Statistical Validity with kinetics Linear Substrate and Exponential Product Inhibition, two sample F-test for variance (Cassava Extracts)

	Biomass		Product		Substrate	
	Experimental (Xobs)	Model (Xpred)	Experimental (Pobs)	Model (Ppred)	Experimental (Sobs)	Model (Spred)
Mean	2.093	2.112	5.881	5.886	5.275	5.280
Standard Error	0.245	0.228	0.403	0.397	0.722	0.727
Standard Deviation	0.979	0.914	1.613	1.588	2.889	2.910
Observations	16	16	16	16	16	16
Confidence Interval	0.990		0.990		0.990	
f	0.8719		0.9682		1.0144	
Pr(F < f) Two-tailed	0.7941		0.9508		0.9783	

Appendix 5c Table 5.3: Model Statistical Validity with kinetics of linear inhibition, two sample F-test for variance (maize extracts)

	Biomass		Product		Substrate	
	Experimental (Xobs)	Model (Xpred)	Experimental (Pobs)	Model (Ppred)	Experimental (Sobs)	Model (Spred)
Mean	0.673	0.670	5.580	5.592	5.644	5.641
Standard Error	0.054	0.052	0.566	0.556	1.023	1.017
Standard Deviation	0.218	0.206	2.263	2.223	4.091	4.069
Observations	16	16	16	16	16	16
Confidence Interval	0.990		0.990		0.990	
f	0.9002		0.9647		0.9890	

Pr(F < f) Two-tailed	0.8414	0.9455	0.9832
------------------------------------	--------	--------	--------

Appendix 5d Table 5.4: Model Statistical Validity with kinetics of Sudden Growth Stop inhibition, two sample F-test for variance (maize extracts)

	Biomass		Product		Substrate	
	Experimental (Xobs)	Model (Xpred)	Experimental (Pobs)	Model (Ppred)	Experimental (Sobs)	Model (Spred)
Mean	0.673	0.684	5.579	5.592	5.644	5.641
Standard Error	0.054	0.052	0.566	0.555	1.023	1.016
Standard Deviation	0.218	0.209	2.263	2.221	4.091	4.066
Observations	16	16	16	16	16	16
Confidence Interval	0.990		0.990		0.990	
f	0.9194		0.9630		0.9878	
Pr(F < f) Two-tailed	0.8728		0.9427		0.9814	

